

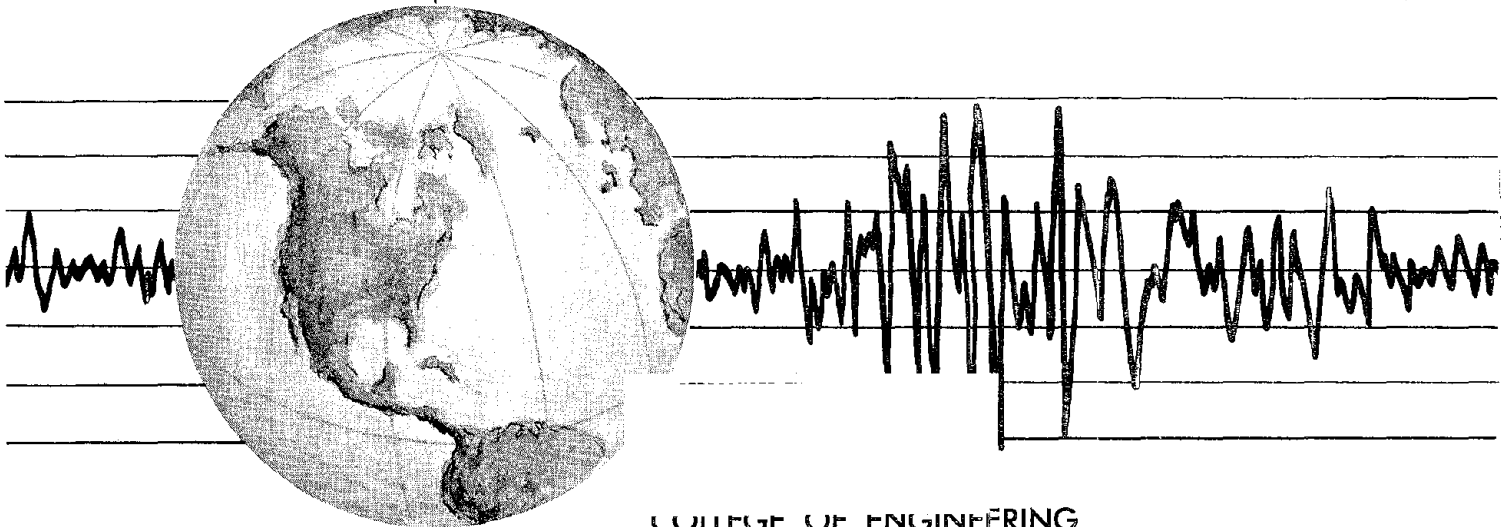
REPORT NO.
EERC 76-11
APRIL 1976

EARTHQUAKE ENGINEERING RESEARCH CENTER

**INFLUENCE OF ANALYSIS AND DESIGN
ASSUMPTIONS ON COMPUTED INELASTIC
RESPONSE OF MODERATELY TALL FRAMES**

by
GRAHAM H. POWELL
and
DENNIS G. ROW

Report to Sponsor:
National Science Foundation
Grant NSF-GI-36387



COLLEGE OF ENGINEERING
UNIVERSITY OF CALIFORNIA • Berkeley, California

See back of report for up to date listing of
EERC reports.

INFLUENCE OF DESIGN AND ANALYSIS ASSUMPTIONS
ON COMPUTED INELASTIC RESPONSE OF MODERATELY TALL FRAMES

by

Graham H. Powell
Professor of Civil Engineering

and

Dennis G. Row
Graduate Student

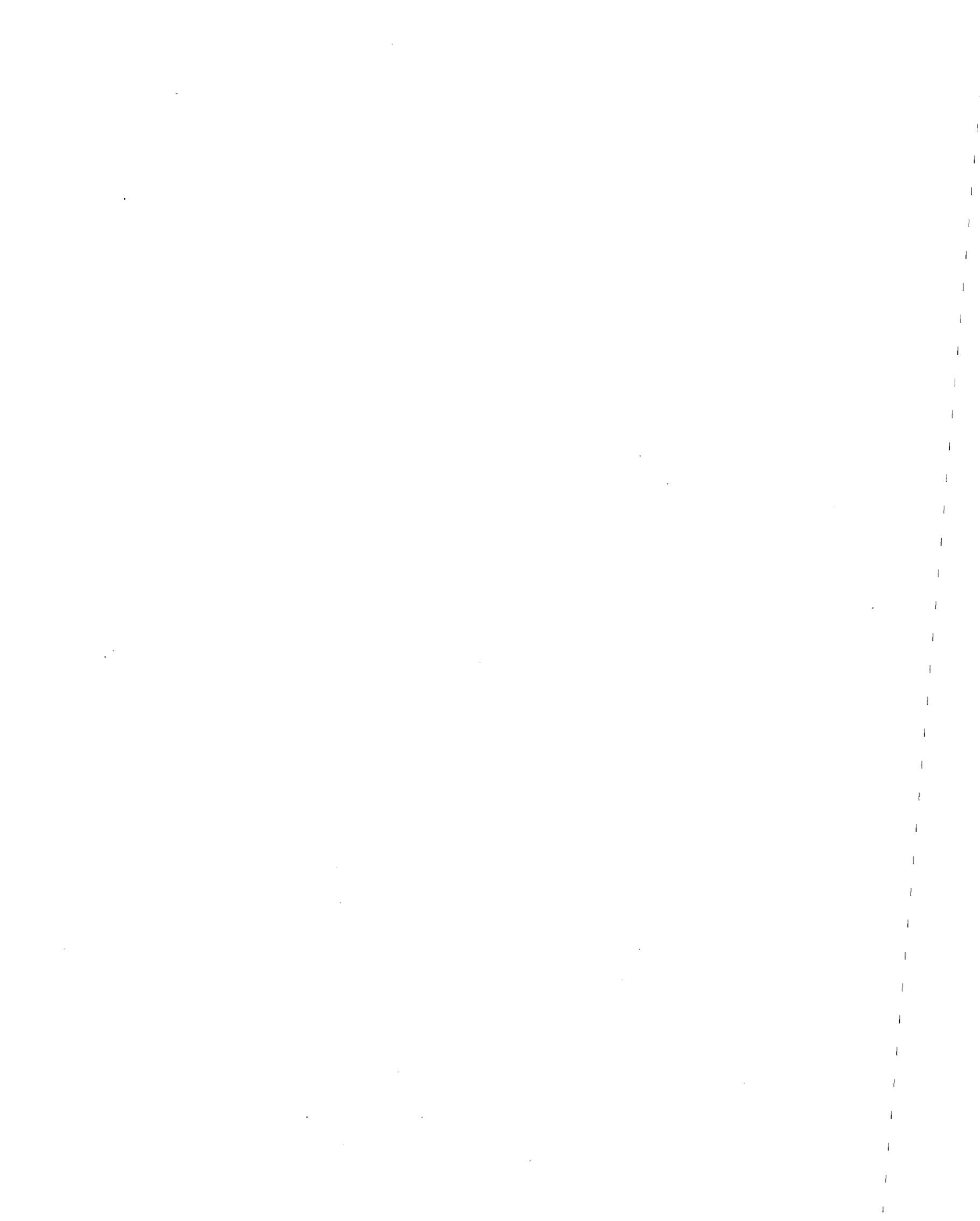
Prepared Under the Sponsorship of
the National Science Foundation

Report No. 76-11
Earthquake Engineering Research Center
College of Engineering
University of California
Berkeley, California

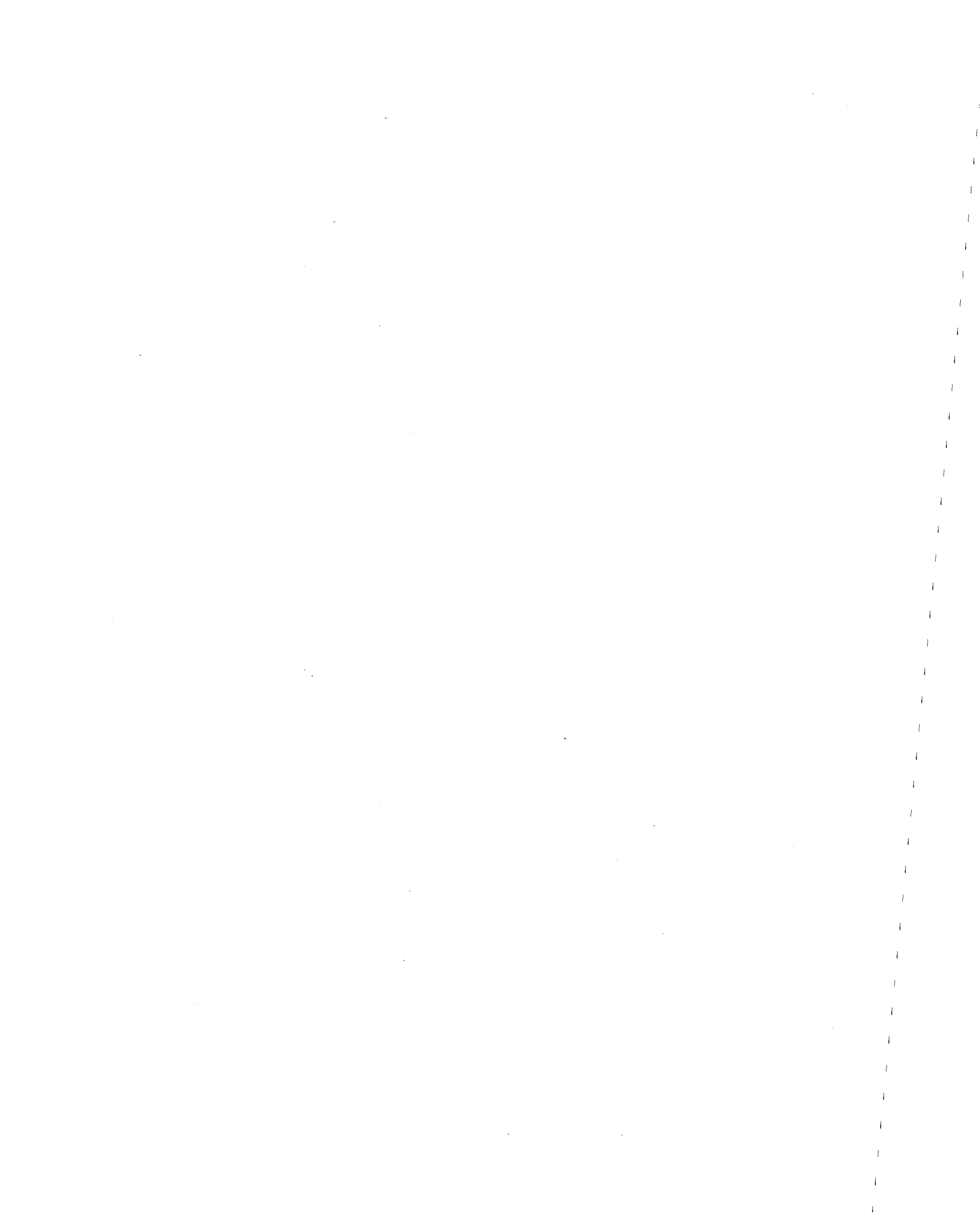
April 1976

TABLE OF CONTENTS

	<u>Page</u>
1. OBJECTIVE AND SCOPE	1
2. DESIGN OF EXAMPLE STRUCTURES	4
2.1 STRUCTURE TYPES	4
2.2 STIFFNESSES AND NATURAL PERIODS	4
2.3 GROUND MOTIONS	4
2.4 ELASTIC ANALYSIS	5
2.5 BEAM DESIGN	6
2.6 COLUMN DESIGN	8
3. INELASTIC ANALYSIS	12
3.1 BASIC IDEALIZATION	12
3.2 PARAMETERS VARIED	12
3.3 RESPONSE PARAMETERS	13
4. RESULTS	14
4.1 PRESENTATION OF RESULTS	14
4.2 ELASTIC RESPONSE	14
4.3 INFLUENCE OF BEAM STRENGTH ON DISPLACEMENTS	15
4.4 INFLUENCE OF COLUMN STRENGTH ON DISPLACEMENTS	16
4.5 INFLUENCE OF P-DELTA EFFECT ON DISPLACEMENTS	17
4.6 INFLUENCE OF DEGRADING STIFFNESS ON DISPLACEMENTS	17
4.7 TIME HISTORIES OF DISPLACEMENT	18
4.8 INFLUENCE OF BEAM AND COLUMN STRENGTH ON INTERSTORY DRIFTS	18
4.9 INFLUENCE OF P-DELTA EFFECT ON INTERSTORY DRIFTS	19
4.10 INFLUENCE OF DEGRADING STIFFNESS ON INTERSTORY DRIFTS	20
4.11 INFLUENCES OF BEAM AND COLUMN STRENGTH ON BEAM HINGE ROTATIONS	20



	<u>Page</u>
4.12 INFLUENCES OF DEGRADING STIFFNESS ON BEAM HINGE ROTATIONS	21
4.13 TIME HISTORIES OF BEAM HINGE ROTATIONS	21
4.14 COMPARISON OF MAXIMUM AND ACCUMULATED BEAM HINGE ROTATIONS: STRONGER COLUMN DESIGNS	22
4.15 COMPARISON OF MAXIMUM AND ACCUMULATED BEAM HINGE ROTATIONS: WEAKER COLUMN DESIGNS	22
4.16 INFLUENCE OF COLUMN STRENGTH ON COLUMN HINGE ROTATIONS . .	23
4.17 INFLUENCE OF DEGRADING BEAM STIFFNESS AND SPECIAL COLUMN DESIGN ON COLUMN HINGE ROTATIONS	24
4.18 COMPARISON OF MAXIMUM AND ACCUMULATED COLUMN HINGE ROTATIONS	25
4.19 EXPLANATION OF HINGE REVERSAL PHENOMENA	25
4.20 MAXIMUM COLUMN AXIAL FORCES	27
5. CONCLUSIONS AND RECOMMENDATIONS	28
REFERENCES	32



1. OBJECTIVE AND SCOPE

Procedures for the elastic dynamic analysis of frame structures under earthquake loading are well established, and are being used increasingly in design. It is commonly accepted that if the beams and columns are proportioned to resist the calculated forces, and if sound detailing practices are followed, then the performance of the structure in an actual earthquake will be satisfactory.

It is also commonly accepted, however, that it is economically unrealistic to design a structure with sufficient strength to remain elastic during a strong earthquake, and hence that inelastic behavior must occur. It does not necessarily follow, therefore, that elastic methods of analysis will lead to consistent designs. For example, if all beams are designed with the same load factor, it does not necessarily follow that all will experience the same inelastic deformations.

In order to estimate the actual inelastic response, it is necessary to carry out inelastic analyses. A large number of analytical techniques and computer programs have been developed for estimating inelastic dynamic response [3-50], several of which are applicable to practical frame structures. The modelling of inelastic behavior is usually rather simple, using plastic hinges with stable hysteresis loops. However, analyses incorporating such refinements as degrading stiffness have been reported. The results of several inelastic analyses of frame structures have been described in research reports. However, it is difficult to correlate the results of different investigators, and few general conclusions have been reached. Inelastic analyses are rarely used in building design, primarily because of cost.

The aim of the investigation described herein has been to develop general conclusions on the inelastic behavior of buildings designed by

elastic methods. The number of parameters which might be varied in a study of this type is large, and this study has been limited in scope. Hence, the conclusions which have been reached are only tentative. Nevertheless, it is believed that the investigation is more consistent and comprehensive than those which have previously been carried out. Similar procedures could be applied in future studies, considering a wider range of structures and design assumptions and hence drawing more definite conclusions. The procedure was as follows.

(1) Reinforced concrete building frames of three types were selected, namely a "typical" frame with slender members, a frame with stiff spandrel beams, and a coupled-wall frame. Each frame was of only ten stories with only a single bay, because of limited funds and the large number of analyses required. This is the most serious limitation of the study.

(2) A family of five ground motions was generated artificially. The major limitation here was that the earthquakes were of short duration. Response spectra were produced for these motions, and a smoothed envelope spectrum was constructed. Two design spectra were then produced by dividing this smoothed spectrum by 3 and 6, respectively.

(3) The forces in the beams and columns were calculated for combined gravity and earthquake loads, using the design spectra. The members were then designed for these forces.

(4) The frames were analyzed for each of the five ground motions, allowing plastic hinges to form at the member ends. The effects of column overdesign, stiffness degradation, and the P-delta effect were included in some of the analyses.

(5) The maximum values of story displacements, interstory drifts, beam hinge rotations, column hinge rotations and column axial forces

were determined for each analysis, and plotted in graphs for comparison.

(6) Trends were observed, and conclusions drawn.

The following chapters describe the procedures and results.

2. DESIGN OF EXAMPLE STRUCTURES

2.1 STRUCTURE TYPES

Three structures of different types were selected, namely (1) a "typical" frame, with slender beams and columns; (2) a "stiff beam" frame, with deep spandrel beams; and (3) a coupled-wall frame. The dimensions, masses and stiffness are shown in Figs. 2.1 and 2.2. The properties were selected as described in the following sections.

2.2 STIFFNESSES AND NATURAL PERIODS

First mode periods of 1.2, 0.9 and 0.6 seconds, respectively, were selected for the three frames. Each of these periods is a typical value for a frame of the corresponding type.

The stiffness ratios shown in Fig. 2.2 were chosen to provide reasonable ratios between the column and beam stiffnesses, and to provide reasonable stiffness variations over the frame heights. The values of EI_0 were then selected to give the required first mode periods. In each case the stiffness values correlate quite closely with the assumed column and girder dimensions. The floor masses correspond to frames at approximately 20 foot centers.

2.3 GROUND MOTIONS

A family of artificial ground motions was generated, using the procedure described by Ruiz and Penzien [4]. This procedure uses a linear stochastic model to generate records of filtered nonstationary shot noise, simulating ground motion accelerograms.

From consideration of several strong motion earthquake records obtained for similar soil conditions, epicentral distance and magnitude, Ruiz and Penzien suggested the use of a linear filter with a natural

frequency of 2.5 cycles/sec and 60% critical damping. The resulting accelerograms simulate strong motion earthquakes for firm soil at moderate epicentral distances.

Five records were created for the present study, using a single computer run of the Ruiz-Penzien program. Each record had a duration of 10 secs, made up of a 1.0 sec parabolic build-up, 6.0 secs at maximum intensity, and a 3.0 sec exponential decay. The ground motion records are shown in Figs. 2.3 through 2.7.

The peak ground accelerations are approximately 0.3g for each record. The peak ground velocities are approximately 20 ft/sec for records 1, 2 and 3, but substantially less for records 4 and 5. Records 1, 2 and 3 give comparable peak ground displacements of approximately 15 inches, with records 4 and 5 giving smaller displacements. Records 2 and 3 exhibit a tendency for the ground displacement to drift in one direction.

The response spectra for the five records are shown in Fig. 2.8. In this and subsequent figures, the solid line represents record 1, and the lines with successively shorter dashes represent records 2 through 5, respectively. The spectra indicate that records 4 and 5 represent generally weaker ground motions, although there is substantial overlap among all of the spectra.

2.4 ELASTIC ANALYSIS

Elastic analyses, using the TABS [1] program, were carried out to obtain member forces for design. The structures were idealized assuming rigid joint zones.

For gravity load effects, weights corresponding to the masses shown in Fig. 2.1 were applied as vertical loads, distributed over the

clear spans of the beams. For earthquake effects, the ground motion spectra were enveloped approximately, using engineering judgment, to give the smooth spectrum shown in Fig. 2.9. This spectrum was then used to define horizontal ground motion effects, vertical earthquake motions being ignored.

Two intensities of design spectrum were used to design the frames, namely a "higher" spectrum, obtained by dividing the smoothed spectrum ordinates by 3 (see Fig. 2.9), and a "lower" spectrum obtained by dividing these ordinates by 6. The TABS analysis was carried out considering 10 modes of vibration with 5% damping in each mode. The peak base shear coefficients obtained from the analyses are shown in Table 2.1, and compared with the design coefficients from the 1974 SEAOC recommendations [2] for ductile moment-resisting frames. For each frame, the SEAOC recommended base shear lies between the values obtained for the lower and higher spectra.

Member forces were calculated for the following two load conditions:

$$(1) \quad 1.4 (D + L) \pm E \quad (2.1)$$

$$(2) \quad 0.9D \pm E \quad (2.2)$$

where D = dead load, L = live load, and E = earthquake. The beams and columns were designed to have ultimate strengths equal to the member forces produced by these loads. For the calculation of gravity load effects, the vertical load was assumed to be 80% dead load and 20% live load.

2.5 BEAM DESIGN

At each end of each beam, the maximum positive and negative bending moments were determined from the elastic analyses, considering the

TABLE 2.1 BASE SHEAR COEFFICIENTS

	TYPICAL FRAME	STIFF BEAM FRAME	COUPLED WALLS
Higher Spectrum	0.1090	0.1240	0.1720
Lower Spectrum	0.0545	0.0622	0.0860
SEAOC*	0.0856	0.0989	0.1211

* coefficient = 1.4 KCS

where K = 0.67

$$C = \frac{1}{15\sqrt{T}}$$

and S = soil factor, assumed = 1.5

The factor 1.4 is to convert from working load to ultimate load values

two loading conditions of Eqs. 2.1 and 2.2. The maximum values are shown in Table 2.2 as the "required" moments. Note that because of the gravity loads, the negative moments are increased by less than 100% when the response spectrum ordinates are doubled, whereas the positive moments are increased by more than 100%.

The moment values for which the beams were proportioned (i.e. the yield moments for the beams) are also shown in Table 2.2. These moments were obtained by rounding the required values and smoothing over the building heights. Also a positive moment capacity equal to at least 50% of the corresponding negative moment capacity was provided at each point to conform to usual practice.

For the subsequent inelastic analyses, plastic hinges were allowed to form only at the ends of each beam. Hence, no consideration was given to the moment capacities at midspan of the beams.

2.6 COLUMN DESIGN

The column design was based on an assumed interaction relationship for column strength, as shown in Fig. 2.10. For any column width, h , this relationship is defined completely by the single parameter M_0 . Its shape was selected to be reasonable for a typical reinforced concrete column.

The column sections immediately above and below each floor were assumed to have the same strength, to be consistent with practical designs in which the column steel is changed between floors. For the two load conditions of Eqs. 2.1 and 2.2, combinations of gravity with positive and negative earthquake effects were extracted from the TABS printout for both the left and right columns above and below each floor. That combination of axial force and bending moment which required the largest value of

TABLE 2.2 BEAM DESIGN MOMENTS

LEVEL	LOWER SPECTRUM DESIGN				HIGHER SPECTRUM DESIGN			
	NEGATIVE		POSITIVE		NEGATIVE		POSITIVE	
	Required	Proportioned	Required	Proportioned	Required	Proportioned	Required	Proportioned
10	79.0	80.0	0	40.0	98.0	100.0	6.5	50.0
9	148.0	150.0	9.0	75.0	195.1	200.0	40.0	100.0
8	178.3	190.0	16.5	95.0	250.8	270.0	89.0	135.0
7	195.7	190.0	31.4	95.0	283.9	270.0	119.7	135.0
6	208.5	215.0	40.7	107.5	307.3	320.0	139.6	160.0
5	220.8	215.0	53.1	107.5	331.9	320.0	164.2	160.0
4	225.3	230.0	65.9	115.0	346.4	370.0	187.0	210.0
3	237.2	230.0	76.9	115.0	369.6	370.0	209.3	210.0
2	242.7	230.0	80.1	115.0	379.1	370.0	216.5	210.0
1	228.2	230.0	69.9	115.0	352.9	370.0	194.5	210.0
STIFF BEAM								
10	70.0	80.0	0	40.0	91.0	100.0	17.0	50.0
9	139.0	140.0	10.0	70.0	194.0	200.0	64.0	100.0
8	178.0	180.0	33.0	90.0	261.0	260.0	116.0	130.0
7	198.0	210.0	51.0	105.0	300.0	320.0	154.0	160.0
6	218.0	210.0	66.0	105.0	336.0	320.0	184.0	160.0
5	231.0	230.0	77.0	115.0	361.0	380.0	208.0	220.0
4	238.0	230.0	90.0	115.0	379.0	380.0	232.0	220.0
3	252.0	260.0	104.0	130.0	407.0	420.0	259.0	260.0
2	265.0	260.0	112.0	130.0	431.0	420.0	278.0	260.0
1	250.0	260.0	100.0	130.0	402.0	420.0	252.0	260.0
COUPLED WALLS								
10	90.0	90.0	5.0	45.0	131.0	140.0	56.0	70.0
9	128.0	140.0	12.0	70.0	180.0	200.0	64.0	100.0
8	144.0	140.0	27.0	70.0	211.0	200.0	95.0	100.0
7	160.0	160.0	43.0	80.0	243.0	250.0	127.0	125.0
6	173.0	180.0	57.0	90.0	271.0	290.0	154.0	170.0
5	183.0	180.0	66.0	90.0	290.0	290.0	173.0	170.0
4	186.0	180.0	69.0	90.0	296.0	290.0	179.0	170.0
3	181.0	180.0	65.0	90.0	286.0	290.0	169.0	170.0
2	162.0	160.0	46.0	80.0	248.0	250.0	132.0	125.0
1	132.0	130.0	16.0	65.0	189.0	200.0	72.0	100.0

unit of moment = kip-ft

M_o was then determined, to obtain the required column strength. The required strengths for all columns are shown in Table 2.3.

TABLE 2.3 REQUIRED COLUMN STRENGTHS

	LOWER SPECTRUM DESIGN		HIGHER SPECTRUM DESIGN		
	LEVEL	M _o * Kip-ft	P _o * Kips	M _o Kip-ft	P _o Kips
TYPICAL FRAME	10	70	262	86	324
	9	72	270	105	392
	8	83	312	126	471
	7	87	327	127	475
	6	101	379	131	490
	5	108	404	146	547
	4	122	459	147	551
	3	128	479	167	625
	2	136	510	180	675
	1	158	592	219	823
	G	166	621	274	1026
STIFF BEAM	10	50	187	64	241
	9	59	223	90	339
	8	72	270	109	410
	7	87	327	113	425
	6	93	349	122	459
	5	100	375	138	519
	4	111	418	149	557
	3	121	453	176	639
	2	129	485	187	700
	1	144	538	210	788
	G	176	660	271	1017
COUPLED WALLS	10	142	133	208	195
	9	155	145	254	238
	8	193	181	269	252
	7	217	203	306	287
	6	253	237	367	344
	5	322	302	417	391
	4	401	376	482	452
	3	440	412	625	586
	2	536	502	805	755
	1	688	645	1031	967
	G	824	772	1289	1209

* See Fig. 2.10

3. INELASTIC ANALYSIS

3.1 BASIC IDEALIZATION

The frames were analyzed inelastically by a step-by-step method, using the DRAIN-2D computer program [5,6]. The joint regions were considered to be rigid, and column axial deformations were permitted but beam axial deformations ignored. The masses were lumped at the floors, and only horizontal inertia effects were considered. Gravity load was first applied, followed by horizontal ground motion. These idealization assumptions are the same as those made for the TABS analyses.

Plastic hinges in the beams were permitted to form only at the beam and column ends. Interaction between axial force and bending moment was taken into account for hinge formation in the columns. Strain hardening following hinge formation was assumed to be zero (i.e. the yield and ultimate strengths were assumed to be equal).

The beam strengths for all inelastic analyses were the values shown in Table 2.2. The column strengths were varied, as explained in the following section, to investigate the effects of providing 'over-strength' columns.

3.2 PARAMETERS VARIED

In order to investigate the effects of idealization assumptions on the computed response, the following changes were made for some analyses.

- (1) The P-delta effect was included.

- (2) Degrading stiffness of Takeda type was assumed for the

beam hinges, using the beam element developed by Litton [3].

For the inelastic analyses, the case including the P-delta effect was used as the basic case, with only a few analyses repeated ignoring the effect.

In order to investigate the influence of column strength, three different column strength assumptions were made, as follows.

(1) Strengths equal to those shown in Table 2.3.

(2) Strengths equal to 1.4 times those shown in Table 2.3 (i.e. an overstrength provision of 40%).

(3) Infinite strengths (i.e. elastic columns).

3.3 RESPONSE PARAMETERS

The parameters used to characterize the inelastic response were as follows.

(1) Maximum horizontal displacements at floors (displacements relative to base).

(2) Maximum interstory drifts.

(3) Maximum and accumulated plastic hinge rotations in beams.

See Fig. 3.1 for definition of these quantities.

(4) Maximum and accumulated plastic hinge rotations in columns.

(5) Maximum axial forces in columns.

For a few cases, time histories of some of these parameters have been plotted, in order to obtain more detailed information on the response.

4. RESULTS

4.1 PRESENTATION OF RESULTS

The results of the study are presented graphically in the figures of Appendix A. The cases studied are identified by the following notations.

- (1) Frame type:
 - (a) Typical frame.
 - (b) Stiff beam frame.
 - (c) Coupled walls.
- (2) Response spectrum used for selecting member strengths:
 - (a) HI = higher spectrum.
 - (b) LO = lower spectrum.
- (3) Column strength:
 - (a) 1.0 = strengths as in Table 2.3.
 - (b) 1.4 = strengths 1.4 times those in Table 2.3.
 - (c) ∞ = elastic columns.

In addition, some fully elastic analyses with infinite strength assumed for both beams and columns were carried out.

For each case, results are presented for all five ground motions. A solid line is used for ground motion 1, and dashed lines with successively shorter dashes for motions 2 through 5.

In all cases, there are large variations in the response parameters from one earthquake to the next. Hence, the influences of changes in the design assumptions can be considered only in terms of qualitative trends.

4.2 ELASTIC RESPONSE

The computed story shear and floor displacement envelopes, obtained assuming infinitely strong beams and columns, are shown in Figs. A.1 and A.2, respectively. For any frame, the roof displacements produced

by the different ground motions differ substantially, and are essentially proportional to the spectral accelerations at the first mode period. This reflects the fact that the first mode response dominates. The story shears vary somewhat more erratically, indicating significant contributions from the higher modes. The story shears obtained from a response spectrum analysis using the smooth design spectra are also shown.

The results shown in Figs. A.1 and A.2 were obtained ignoring the P-delta effect. Results were also obtained including this effect, and were found to be negligibly different. This indicates that the P-delta effect produced only slight changes in the periods in the elastic range.

4.3 INFLUENCE OF BEAM STRENGTH ON DISPLACEMENTS

Displacement envelopes were computed assuming infinitely strong columns, with beams designed for (a) infinite strength, (b) the HI spectrum, and (c) the L0 spectrum. A comparison of the results indicates the influence of beam strength on the displacement response.

Figs. A.2 through A.4 show how the displacements vary from frame to frame, within each design. Figs. A.5 through A.7 show how the response varies from design to design, within each frame. The following points may be noted.

(1) As expected, the displacements decrease from the typical frame to the stiff beam frame to the coupled walls, for all three beam strengths (Figs. A.2 through A.4).

(2) The roof displacements for any frame remain of the same order of magnitude as the beam strengths are decreased (Fig. A.5 through A.7).

(3) For the typical and stiff beam frames, the displacements show greater variations from ground motion to ground motion as the beam strength is reduced (Figs. A.5 and A.6). However, there are marked variations in response even for the elastic case.

(4) For the typical and stiff beam frames, the shapes of the displacement envelopes change substantially as the beam strength decreases (Figs. A.5 and A.6). As the beams are made weaker, the displacements in the lower stories increase substantially, whereas the roof displacements remain generally of the same magnitude.

(5) For the coupled wall frame, there is no marked tendency for the displacement envelopes to change shape as the beam strengths decrease (Fig. A.7).

(6) For any frame, the ground motion which produces the largest roof displacement for the elastic structure does not necessarily produce the largest displacement for the inelastic structure. For example, for the stiff beam frame (Fig. A.6) the ground motions can be arranged in order of decreasing severity of effect as follows.

(a) Elastic: 3 - 4 - 5 - 1 - 2

(b) HI/ ∞ : 3 - 2 - 4 - 1 - 5

(c) LO/ ∞ : 1 - 4 - 3 - 2 - 5

4.4 INFLUENCE OF COLUMN STRENGTH ON DISPLACEMENTS

Displacement envelopes were computed for three different column strengths, namely with (a) elastic columns, (b) columns designed using an overstrength factor of 1.4, and (c) columns designed using an overstrength factor of 1.0 (i.e. no overstrength). The beams were inelastic in all cases, and designs using both the HI and LO spectra were analyzed. A comparison of the results indicates the effect of column strength on the displacement response.

Figs. A.8 through A.13 show how the responses vary as the column strengths are changed, for each of the three frames and for the HI and LO designs. The following points may be noted.

(1) As the column strength decreases, there is a marked tendency for the displacements in the lower stories to increase, for all three frames. This effect is more marked for the L0 designs (weaker beams and columns) than for the HI designs.

(2) As the column strengths are reduced, the different ground motions remain essentially the same in relative severity for each frame.

(3) The roof displacements again remain generally the same as the column strengths are reduced, although the different ground motions differ markedly in relative severity.

(4) Ground motion 3 has a much more severe effect on the coupled wall frame than the other ground motions (Figs. A.12 and A.13). This phenomenon is examined in a later section.

4.5 INFLUENCE OF P-DELTA EFFECT ON DISPLACEMENTS

It was noted in Section 4.1 that the influence of the P-delta effect was negligible for all three frames with elastic behavior. The maximum displacements computed considering and ignoring the P-delta effect are shown in Figs. A.14 and A.15 for the L0/1.0 designs of the typical frame and coupled wall frame. The L0/1.0 design of the typical frame is the most flexible structure, and the P-delta effect would be expected to be most significant for this case. Fig. A.14 indicates that the effect is noticeable, especially for the ground motions which produce the largest displacements, but that the changes in response are relatively small. Fig. A.15 indicates negligible changes in displacement response for the coupled wall frame.

4.6 INFLUENCE OF DEGRADING STIFFNESS ON DISPLACEMENTS

Analyses were carried out for the L0/1.4 designs of all three frames, firstly assuming simple elastic-plastic behavior for the beam hinges,

and secondly assuming degrading stiffness of Takeda type. The column hinges were assumed to have simple elastic-plastic behavior in all cases. The computed displacement envelopes are shown in Figs. A.16 through A.18. It can be seen that substantial differences in response resulted for some ground motions (for example, motion 2 in Fig. A.16 and motion 3 in Fig. A.18). Overall, however, there was no clear trend, and the displacements were generally similar for both idealizations.

4.7 TIME HISTORIES OF DISPLACEMENT

Time histories of displacement at the roof and fifth floor levels are shown in Figs. A.19 through A.21, for the LO/1.4 designs of each frame and for ground motions 1 and 3. The ground motion time histories are also shown. Note that the floor displacements are relative to the base.

For the typical frame, in Fig. A.19, it can be seen that ground motion 1 produces a distinctly biased displacement of the structure at about 5 seconds into the earthquake, and that the resulting displacements oscillate about a mean value (at the roof) of approximately 3 inches. Ground motion 3, on the other hand, produces no biased drift of the structure. A similar effect, but less marked, is produced by ground motion 1 for the stiff beam frame (Fig. A.20). For the coupled wall frame (Fig. A.21) a very marked bias is again produced, but this time by ground motion 3. It was noted earlier (see Figs. A.7, A.12 and A.13) that ground motion 3 produced more severe displacement responses for the coupled wall frame than the other motions. Fig. A.21 clearly illustrates the different nature of the response produced by ground motion 3 for that frame.

4.8 INFLUENCE OF BEAM AND COLUMN STRENGTH ON INTERSTORY DRIFTS

Envelopes of interstory drift were computed for the HI/1.4, HI/1.0, LO/1.4 and LO/1.0 designs for all three frames. Interstory drift is

likely to be of more value to a designer than floor displacement, because it gives a more direct indication of the amount of partition damage which is likely to be produced. The results are shown in Figs. A.22 through A.27. The following points may be noted.

(1) The interstory drifts decrease from the typical frame to the stiff beam frame to the coupled wall frame, as would be expected from the differing stiffnesses of the structures.

(2) As the design strengths are reduced from the HI to the LO values for the typical and stiff beam frames, there is a distinct tendency for the drifts to increase in the lower stories and decrease in the upper stories (compare Fig. A.22 with A.23, and Fig. A.24 with A.25). This tendency is not present, however, in the coupled wall frame (compare Fig. A.26 with A.27).

(3) As the column strength is reduced from a factor of 1.4 to 1.0 for the typical and stiff beam frames, there is again a distinct tendency for the drifts to increase in the lower stories (see Figs. A.22 through A.25). There appears to be some tendency, although less marked, for similar changes to occur for the coupled wall frame (see Figs. A.26 and A.27).

4.9 INFLUENCE OF P-DELTA EFFECT ON INTERSTORY DRIFTS

For the LO/1.0 design for the typical frame (i.e. the most flexible structure), the effect of ignoring the P-delta effect is shown in Fig. A.28. There is a tendency for the drift to increase when the P-delta effect is included, especially for those ground motions which produce the largest interstory drifts. However, the increases are small.

4.10 INFLUENCE OF DEGRADING STIFFNESS ON INTERSTORY DRIFTS

For the L0/1.4 designs of all three frames, the effects of assuming degrading stiffness for the beams are shown in Figs. A.29 through A.31. For the typical and stiff beam frames, the assumption of degrading stiffness produces a significant increase in drift for ground motion 1, but generally no significant changes for the other ground motions. For the coupled wall frame there are significant increases for ground motions 2 and 4, but a reduction for ground motion 3. Overall, degrading stiffness appears to have no substantial influence.

4.11 INFLUENCES OF BEAM AND COLUMN STRENGTH ON BEAM HINGE ROTATIONS

Maximum beam hinge rotations were computed for all three frames, for the HI and L0 designs, and for three different column strengths (elastic and factors of 1.4 and 1.0). Hinge rotations give a direct indication of local structural damage. The results are shown in Figs. A.32 through A.37. The following points may be noted.

(1) For the strong column designs (factor = 1.4), the maximum hinge rotations correlate very closely with the maximum interstory drifts, the rotations being somewhat less than the drift divided by the story height (compare, for example, Figs. A.22 and A.32). This is because there is little column yielding for the strong column designs (as shown subsequently), so that there is a simple geometrical relationship between the inelastic part of the drift and the hinge rotation.

(2) For the weaker column designs (factor = 1.0) there is an approximate correlation between drift and hinge rotation, but it is less direct (compare, for example, Figs. A.22 and A.32 again). The correlation is less close in these cases because of column hinging.

(3) As the design strengths are reduced from the HI to the L0 values for the typical and stiff beam frames, the beam hinge rotations increase substantially in the lower stories and decrease in the higher stories (compare Fig. A.32 with A.33 and Fig. A.34 with A.35). This tendency is not present to such a marked extent in the coupled wall frame (compare Fig. A.36 with A.37).

(4) As the column strength is reduced from a factor of 1.4 to 1.0 for the typical and stiff beam frames, the beam hinge rotations again increase in the lower stories and decrease in the higher stories (see Figs. A.32 through A.35). There is a similar tendency, although less marked, for the coupled wall frame (see Figs. A.36 and A.37).

4.12 INFLUENCES OF DEGRADING STIFFNESS ON BEAM HINGE ROTATIONS

The effects on hinge rotation of assuming degrading stiffnesses for the beams are shown for the L0/1.4 designs in Figs. A.38 through A.40. Because the hinge rotations correlate closely with the interstory drifts for these designs, the same point as in Section 4.9 may be noted.

4.13 TIME HISTORIES OF BEAM HINGE ROTATIONS

Time histories of bending moment and beam hinge rotation at the left ends of the fifth floor beams are shown in Figs. A.41 through A.43, for the L0/1.4 designs of each frame and ground motions 1 and 3. These time histories show the same tendencies for bias as was observed previously for the displacement time histories, especially for the coupled wall frame in Fig. A.43. The hinge rotations reverse several times for each frame, with a substantially larger number of reversals for the coupled wall frame. This reflects the higher frequency of vibration for this frame.

4.14 COMPARISON OF MAXIMUM AND ACCUMULATED BEAM HINGE ROTATIONS: STRONGER COLUMN DESIGNS

If a plastic hinge rotation undergoes reversal, then the maximum and accumulated rotations, as defined in Fig. 3.1, will differ. The difference provides some indication of the amount of reversal.

Maximum and accumulated beam hinge rotations are shown in Figs. A.44 through A.46, for the L0/1.4 designs of the three frames. The following points may be noted.

(1) There are substantial differences between the accumulated and maximum rotations for all three frames, indicating reversal of rotation in all cases.

(2) The ratio between accumulated and maximum rotation increases from the typical frame to the stiff beam frame to the coupled wall frame, being roughly 1.5, 3 and 6, respectively. This reflects the higher frequencies of vibration of the stiffer frames.

(3) The ratios between accumulated and maximum rotation decrease at the base of each frame, especially for the coupled wall frame. This is a consequence of column hinge formation, as explained subsequently.

(4) The products of yield moment and accumulated hinge rotation, summed over all beams, are of the same order of magnitude for all three frames. These products represent the amounts of inelastic energy absorbed by the beams.

4.15 COMPARISON OF MAXIMUM AND ACCUMULATED BEAM HINGE ROTATIONS: WEAKER COLUMN DESIGNS

Maximum and accumulated beam hinge rotations are shown in Figs. A.47 and A.48 for the L0/1.0 designs of the typical and coupled wall frames only. The following points may be noted.

(1) For the typical frame the ratio between the accumulated and maximum rotations is substantially less (approaching 1.0) than for the L0/1.4 design (compare Figs. A.44 and A.47). That is, the beam hinge rotations reversed less often for the weaker column design. The reason for this is presented in a later section.

(2) For the coupled wall frame there is still substantial reversal of beam hinge rotation, although the ratio of accumulated to maximum rotation is generally less than for the L0/1.4 design (compare Figs. A.46 and A.48).

(3) For the typical frame the maximum rotations increase significantly as the column strengths are decreased, particularly in the lower stories (compare Figs. A.44 and A.47). This result was unexpected, because it was felt that reduction in the column strength would allow hinging of the columns and hence require less hinging in the beams. The reason for this result is presented in a later section.

(4) For the coupled wall frame the maximum hinge rotations tend to increase in the lower stories and decrease in the upper stories as the column strength is reduced (compare Figs. A.46 and A.48). However, the increases are generally small.

(5) For the coupled wall frame there is a marked tendency for the accumulated hinge rotations, and the amount of hinge reversal, to decrease in the upper stories as the column strength is reduced. Again, this is explained in a later section.

4.16 INFLUENCE OF COLUMN STRENGTH ON COLUMN HINGE ROTATIONS

Maximum column hinge rotations were computed for all three frames, for the HI and L0 designs, and for column strength factors of 1.4 and 1.0. The results are shown in Figs. A.49 through A.54. In these figures, the

hinge rotation shown in any story is the larger of the rotations at the top and bottom of the column in that story. For story 1, the larger rotation is invariably at the foundation level. The following points may be noted

(1) The column hinge rotations are small for all designs with a column strength factor of 1.4. There is, however, a tendency for the rotations to be significant at the ground floor levels for these designs.

(2) For the typical and stiff beam frames, reduction of the column strength factor to 1.0 results in substantial increases in the column hinge rotations (see Figs. A.49 through A.52). The rotations are larger for the L0 design, especially in the lower stories, and reach values which would indicate severe column damage.

(3) For the coupled wall frame, reduction of the column strength factor again increases the column hinge rotations (see Figs. A.53 and A.54), especially for the L0 design. The rotation magnitudes are much less than for the typical and stiff beam frames, and exhibit interesting peaks in the middle stories.

4.17 INFLUENCE OF DEGRADING BEAM STIFFNESS AND SPECIAL COLUMN DESIGN ON COLUMN HINGE ROTATIONS

The influence of degrading beam stiffness on the column hinge rotations is shown in Figs. A.55 through A.57 for the L0/1.4 designs of all three frames. The column stiffnesses were assumed not to degrade in all cases. Again, the influence of degrading stiffness is not significant.

Results for "special" designs are also shown in Figs. A.55 through A.57. In these designs, the columns strengths were based on an overstrength factor of 1.4 at all points except at the foundation, where a factor of 1.0 was assumed. It was thought that allowing the column to hinge more freely at the base might eliminate the column hinging at other levels of the structure. The results indicate that this was not the case, the only

significant change being an increase in the column hinge rotations at the base.

4.18 COMPARISON OF MAXIMUM AND ACCUMULATED COLUMN HINGE ROTATIONS

For the typical frame only, and for the L0/1.4 and L0/1.0 designs, the maximum and accumulated column rotations are compared in Figs. A.58 and A.59. It can be seen that except at the base of the structure the maximum and accumulated rotations are identical, indication that there is no reversal of the column hinges except at the foundation level. This is explained in the following section.

4.19 EXPLANATION OF HINGE REVERSAL PHENOMENA

It has been noted in earlier sections that (1) the beam hinges exhibit larger maximum rotations but reduced reversal as the column strengths are decreased, and (2) the column hinges do not reverse, except at the base of the structure. The reasons for this are as follows.

For a simple single story frame, subjected to both gravity load and earthquake, the behavior is illustrated qualitatively in Fig. 4.1. Fig. 4.1a shows the elastic moment diagram for gravity load only, and Figs. 4.1b and 4.1c show these diagrams for gravity load plus lateral loads acting to the right and left, respectively. For an inelastic frame with strong columns, the moments at both the left and right ends may exceed the corresponding yield values. Hence, plastic hinges may form at both ends, as shown in Figs. 4.1d and 4.1e, and under earthquake loading there will be hinge reversal. Note that the required positive moment capacities at the beam ends are always less than the required negative moment capacities, because of the gravity loads. Note also that for the L0 spectrum designs, the required positive moments were all less than one half of the required negative moments (see Table 2.2), and hence additional capacities beyond

the required values were assumed for the design.

If the column strengths are reduced, there is an increasing tendency for hinges to form in the columns. This tendency is particularly marked on the compression side of the frame, firstly because the column moments are substantially larger on this side (the earthquake moments reinforce the gravity load moments) and secondly because the column compression reduces the moment capacity. On the tension side, however, the moments are smaller and the decreased compression tends to increase the moment capacity. Hence, column hinges tend to form on one side of the frame only, and hinges will form as shown in Figs. 4.1f and 4.1g. It is clear that for a single bay frame the column hinges will rotate in one direction only, without reversal. It can also be seen from Figs. 4.1d and 4.1f that the beam hinge rotation for the positive moment hinges will be related to the interstory drifts. As noted previously, because the interstory drifts occurring before yield are comparatively small, the beam hinge rotations are essentially equal to the story drifts divided by the story heights for both positive and negative beam hinges. For the strong column case the analyses generally showed comparable maximum hinge rotations for both positive and negative rotation (for example, see Fig. A.41). For the weaker column case, however, the negative hinge rotations were greatly reduced. Hence, the effect of reducing the column strength is to suppress negative hinge formation in the beams, without suppressing positive hinge formation. Further, because the column strength reduction leads to increased interstory drifts, the positive beam hinge rotations are generally increased above the values for a strong column design. Note, however, that this is not likely to be critical for the beam, because the positive "hinge" is less localized in an actual frame than the negative hinge.

4.20 MAXIMUM COLUMN AXIAL FORCES

An interesting question to explore is whether, at any time during the earthquake, it is possible for positive and negative hinges to form in all beams simultaneously. If this can happen, then the maximum possible column axial force in any story can be determined by statics from the gravity loads and the beam strengths. For selected designs of the typical and coupled wall frames, the maximum computed column compression forces are shown in Figs. A.60 through A.62, for four designs of the typical frame and two designs of the coupled wall frame.

Virtually identical results are produced by all ground motions for each frame. The lines of theoretical maximum compression (assuming hinges in all beams) are not shown in the figures, because they correspond very closely to the computed maximum compressions. Some computed values exceed the theoretical maximum by small amounts, but this results from overshoot of nominal yield values within the computer program. Clearly, for these example frames the situation with all beams hinging simultaneously is produced by all ground motions.

The maximum computed compressions for the HI/1.0 and LO/1.0 designs of the typical frames may be seen to be slightly less than for the HI/1.4 and LO/1.4 designs. This is because the hinges tend to form in the columns on the compression side of the frame for the weaker column designs, as explained in Section 4.19. The maximum compressions are reduced only slightly because the beam moments are close to their yield values when the column hinges form. This reduction is negligible for the coupled wall frame.

5. CONCLUSIONS AND RECOMMENDATIONS

The investigation described in this report has been limited in scope, and is essentially only a pilot study. In particular, it has been limited to single bay frames of modest height subjected to ground motions of short duration. The procedures used to conduct the study are believed to be sound, particularly with regard to the design of the example structures and the selection of the ground motions.

Certain conclusions can be drawn from the study, but a substantially broader range of structures will need to be investigated before definite conclusions and recommendations for design can be formulated. The conclusions which can be drawn from the study, and the areas in which further study is needed, are as follows.

(1) The computed inelastic response varied greatly from one ground motion to the next, even for motions having apparently similar characteristics. Hence, if inelastic analyses are to be carried out to estimate inelastic deformations, the computations should be repeated for several ground motions. It may be noted, however, that the earthquakes considered in this study were of short duration, with only a small number of cycles of ground displacement. It is possible that more consistent results would be obtained if earthquakes of longer duration were used. This aspect should be investigated.

(2) Although the computed elastic responses of the frames could be correlated with the elastic spectral accelerations for the first mode periods, there was no correlation between these spectral accelerations and the computed inelastic responses. Also, there was no obvious correlation between the maximum ground accelerations, velocities and displacements on the one hand and the computed inelastic responses on the other. It is possible that the computed response might correlate more closely with

inelastic response spectra. The possibility of such a correlation has not been considered in this study, but should definitely be investigated in future studies.

(3) The computed roof displacements were of essentially the same magnitude regardless of whether the structure yielded or remained elastic. This is a well known result. However, the pattern of story drift changed substantially as the frames were weakened, with large drifts in the lower stories and smaller drifts in the upper stories. The computed beam hinge rotations similarly were largest in the lower stories. This indicates that a more uniform distribution of inelastic deformation, and hence presumably a better structural design, would be produced if the members in the lower stories were proportioned using more conservative load factors than those in the upper stories. This aspect of design warrants further investigation.

(4) When the columns were designed using more conservative load factors than the beams, then inelastic behavior in the columns was reduced or eliminated. However, when similar load factors were used, the columns yielded substantially. The collapse of a structure during an earthquake will usually occur because the earthquake weakens the structure to such an extent that it can no longer support gravity loads, and it is generally accepted that the structure will be weakened more if the columns are damaged than if the beams are damaged. It would be sound practice, therefore, to design the columns using more conservative load factors than those used for the beams. An overstrength factor of 1.4 appears to be reasonable, although additional investigation of this point is desirable.

(5) If the yielding is limited to the beams, and if hinges form only at the beam ends, then the beam hinge rotations can be calculated from the story drifts. This indicates that it might be feasible to use a

simplified structural model (for example, an inelastic shear beam) for inelastic dynamic analyses. Provided the story drifts computed for the simplified model corresponded to those computed for a more elaborate model, the simplified analyses could be used to predict beam hinge rotations. A shear beam analysis using load-deflection relationships calculated for single story subassemblages of the actual frame is a possibility which warrants further study.

(6) For strong column designs in which hinges form only in the beams, reversal of hinge rotation can be expected to occur. For weaker column designs, however, a hinge may form, say, on the left side of the frame with a column hinge on the right side. When the direction of sway reverses then a beam hinge forms on the right and a column hinge on the left. That is, there is no reversal of rotation at the hinges. Because of the column hinging, however, this is not necessarily a desirable situation.

(7) For a column which is fixed at the foundation level, significant inelastic deformation is likely to occur at this level even though the column may be below yield at all other levels. Hence, the column should be detailed to provide substantial ductility at this point.

(8) The computed hinge rotations were smaller for the stiffer frames. The members of such frames might be inherently less ductile, so that smaller hinge rotations do not necessarily indicate less damage. Nevertheless, the smaller computed deflections, interstory drifts and hinge rotations for the stiffer frames appear to imply superior performance.

(9) For the frames considered in this study, the P-delta effect exerted only a small influence. This effect would be larger, however, for taller structures.

(10) The computed hinge rotations were not markedly increased if

beams with degrading stiffnesses were assumed. This confirms a conclusion reached by Chopra and Kan [7], and indicates that elaborate inelastic models of the structural members may not be needed for practical inelastic analysis. This aspect also warrants further investigation.

(11) For the structures studied, the maximum computed compression forces in the columns were equal to the theoretical maxima for all earthquakes. This might not be the case for taller frames or for multibay frames. However, if this were generally true, then it could be an important consideration for column design. Further investigation, particularly of tall multibay frames, is needed.

(12) Ground motion 3 exerted a markedly more severe effect on the coupled wall frame, producing a distinctly biased drift of the frame. There is no obvious feature of this ground motion which might indicate such a response. It might be of value to investigate this phenomenon in greater detail, to determine what combination of circumstances can produce this type of behavior.

REFERENCES

1. Wilson, E.L. and Dovey, H.H., "TABS-Three Dimensional Analysis of Building Systems," Report No. EERC 72-8, Earthquake Engineering Research Center, Univ. of California, Berkeley, Dec. 1972.
2. Seismology Committee, Recommended Lateral Force Requirements and Commentary, Structural Engineers Association of California, San Francisco, California, 1974.
3. Litton, R.W., "A Contribution to the Analysis of Concrete Structures Under Cyclic Loading," Ph.D. Dissertation, University of California, Berkeley, June 1975.
4. Ruiz, P. and Penzien, J., "Probabilistic Study of the Behavior of Structures During Earthquakes," Report No. EERC 69-3, Earthquake Engineering Research Center, Univ. of California, Berkeley, March 1969.
5. Powell, G.H., "DRAIN-2D Users Guide", Report No. EERC 73-22, Earthquake Engineering Research Center, Univ. of California, Berkeley, Oct. 1973.
6. Kanaan, A.E. and Powell, G.H., "General Purpose Computer Program for Inelastic Dynamic Response of Plane Structures," Report No. EERC 73-6, Earthquake Engineering Research Center, Univ. of California, Berkeley, April 1973.
7. Chopra, A.K. and Kan, C., "Effects of Stiffness Degradation on Earthquake Ductility Requirements for Multistory Buildings," International Journal of Earthquake Engineering and Structural Dynamics, Vol. 2, pp. 35-45, 1973
8. Jacobsen, L.S., "Dynamic Behavior of Simplified Structures up to the Point of Collapse," Proceedings, Symposium on Earthquake and Blast Effects on Structures, Los Angeles, 1952.
9. DiMaggio, F.L., "Dynamic Elastic-Plastic Response of Rigid Frames," Proceedings, ASCE, Journal of the Engineering Mechanics Division, Vol. 84, No. EM 3, July 1958.
10. Berg, G.V. and DaDeppo, D.A., "Dynamic Analysis of Elasto-Plastic Structures," Proceedings, ASCE, Journal of the Engineering Mechanics Division, Vol. 86, No. EM 2, April 1960.
11. Penzien, J., "Dynamic Response of Elasto-Plastic Frames," Proceedings, ASCE, Journal of the Structural Division, Vol. 86, No. ST 7, July 1960.
12. Veletsos, A.S. and Newmark, N.M., "Effects of Inelastic Behavior of Simple Systems to Earthquake Motions," Vol. II, Proceedings, Second World Conference on Earthquake Engineering, Tokyo, 1960.
13. Jennings, P.C., "Response of Simple Yielding Structures to Earthquake Excitation," Earthquake Engineering Research Laboratory, California Institute of Technology, Pasadena, June 1963.

14. Jennings, P.C. and Husid, R., "Collapse of Yielding Structures during Earthquakes," Proceedings, ASCE, Journal of the Engineering Mechanics Division, Vol. 94, No. EM 5, Oct. 1968.
15. Husid, R., "The Effect of Gravity on the Collapse of Yielding Structures with Earthquake Excitation," Vol. II, Proceedings, Fourth World Conference on Earthquake Engineering, Santiago, Chile, 1969.
16. Heidebrecht, A.C., Lee, S.L. and Flemming, J.F., "Dynamic Analysis of Elastic-Plastic Frames," Proceedings, ASCE, Journal of the Structural Division, Vol. 90, No. ST 2, April 1964.
17. Clough, R.W., Benuska, K.L. and Wilson, E.L., "Inelastic Earthquake Response of Tall Buildings," Proceedings, Third World Conference on Earthquake Engineering, Wellington, New Zealand, 1965.
18. Clough, R.W. and Benuska, K.L., "Nonlinear Earthquake Behavior of Tall Buildings," Proceedings, ASCE, Journal of the Engineering Mechanics Division, Vol. 93, No. EM 3, June 1967.
19. Goel, S., "Response of Multistory Steel Frames to Earthquake Forces," Bulletin No. 12, Steel Research for Construction, AISI, Nov. 1968.
20. Giberson, M.F., "The Response of Nonlinear Multistory Structures Subject to Earthquake Excitation," Earthquake Engineering Research Laboratory, California Institute of Technology, Pasadena, June 1967.
21. Goel, S.C. and Berg, G.V., "Inelastic Earthquake Response of Tall Steel Frames," Proceedings, ASCE, Journal of the Structural Division, Vol. 94, No. ST 8, Aug. 1968.
22. Guru, G.P. and Heidebrecht, "Factors Influencing the Inelastic Response of Multistory Frames Subject to Strong Earthquakes," Proceedings, Fourth World Conference on Earthquake Engineering, Santiago, Chile, 1969.
23. Hanson, R. and Fan, W., "The Effects of Minimum Cross Bracing on the Inelastic Response of Multistory Buildings," Proceedings, Fourth World Conference on Earthquake Engineering, Santiago, Chile, 1969.
24. Workman, G.H., "The Inelastic Behavior of Multistory Braced Frame Structures Subjected to Earthquake Excitation," Ph.D. Thesis, University of Michigan, Ann Arbor, Sept. 1969.
25. Anderson, J.C. and Bertero, V.V., "Seismic Behavior of Multistory Frames Designed by Different Philosophies," Report No. EERC 69-11, Earthquake Engineering Research Center, University of California, Berkeley, Oct. 1969.
26. Walpole, W.R. and Shepherd, "Elasto-Plastic Seismic Response of Reinforced Concrete Frames," Proceedings, ASCE, Journal of the Structural Division, Vol. 95, No. ST 10, October 1969.
27. Raj, G. and Goel, S.C., "Dynamic Analysis of Staggered Truss Framing System," paper presented at ASCE Structural Engineering Meeting, Baltimore, April 1971.

28. Suko, M. and Adams, P.F., "Dynamic Analysis of Multibay Multistory Frames," Proceedings, ASCE, Journal of the Structural Division, Vol. 97, No. ST 10, Oct. 1971.
29. Kamil, H., "Optimum Inelastic Design of Unbraced Multistory Frames Under Dynamic Loads," Ph.D. Thesis, University of California, Berkeley, June 1972.
30. Nigam, N.C., "Inelastic Interactions in the Dynamic Response of Structures," Earthquake Engineering Research Laboratory, California Institute of Technology, Pasadena, June 1967.
31. Nigam, N.C., "Yielding in Framed Structures Under Dynamic Loads," Proceedings, ASCE, Journal of the Engineering Mechanics Division, Vol. 96, No. EM 5, Oct. 1970.
32. Nigam, N.C. and Housner, G.W., "Elastic and Inelastic Response of Framed Structures During Earthquake," Proceedings, Fourth World Conference on Earthquake Engineering, Santiago, Chile, 1969.
33. Wen, R.K. and Farhoomand, F., "Dynamic Analysis of Inelastic Space Frames," Proceedings, ASCE, Journal of the Engineering Mechanics Division, Vol. 96, No. EM 5, Oct. 1970.
34. Farhoomand, F., Iverson, J.K. and Wen, R.K., "Dynamic Analysis of Nonlinear Space Frames," Meeting Preprint 1371, ASCE Structural Engineering Meeting, Baltimore, April 1971.
35. Porter, F.L. and Powell, G.H., "Static and Dynamic Analysis of Inelastic Frame Structures," Report No. EERC 71-3, Earthquake Engineering Research Center, University of California, Berkeley, June 1971.
36. Clough, R.W. and Johnston, S., "Effects of Stiffness Degradation on Earthquake Ductility Requirements," Report No. SEL-66-16, Department of Civil Engineering, University of California, Berkeley, 1966. NTIS accession No. PB 189 496.
37. Takeda, T., Sozen, M.A. and Nielsen, N.N., "Reinforced Concrete Response to Simulated Earthquakes," Proceedings, ASCE, Journal of the Structural Division, Vol. 96, No. ST 12, Dec. 1970.
38. Gulkan, P. and Sozen, M.A., "Response and Energy Dissipation of Reinforced Concrete Frames Subjected to Strong Base Motion," Structural Research Series No. 377, University of Illinois, Urbana, May 1971.
39. Scordelis, A.C., "Finite Element Analysis of Reinforced Concrete Structure: paper presented at Specialty Conference on the Finite Element Method in Civil Engineering, Montreal, Canada, June 1972.
40. Driscoll, G.C. and Armacost, J.O., "The Computer Analysis of Unbraced Multistory Frames," Fritz Engineering Laboratory Report No. 345.5, Lehigh University, May 1968.
41. Newmark, N.M., "A Method of Computation for Structural Dynamics," Proceedings, ASCE, Journal of the Engineering Mechanics Division, Vol. 85, No. EM 3, July 1959.

42. Wilson, E.L. and Clough, R.W., "Dynamic Response by Step-by-Step Matrix Analysis," Symposium on Use of Computers in Civil Engineering, Lisbon, Portugal, Oct. 1962.
43. Wilson, E.L., Farhoomand, I. and Bathe, K.J., "Nonlinear Dynamic Analysis of Complex Structures," to be published in International Journal for Earthquake Engineering and Structural Dynamics.
44. Powell, G.H., "Computer Evaluation of Automobile Barrier Systems," Report No. UC-SESM-70-17, Dept. of Civil Engineering, University of California, Berkeley, Aug. 1970.
45. Peyrot, A.H., "Probabilistic Response of Nonlinear Buildings During Earthquakes," Proceedings, ASCE, Journal of the Structural Division, Vol. 98, No. ST 11, Nov. 1972.
46. Anderson, J.C. and Gupta, R.P., "Earthquake Resistant Design of Unbraced Frames," Proceedings, ASCE, Journal of the Structural Division, Vol. 98, No. ST 11, Nov. 1972.
47. Goel, S.C. and Hanson, R.D., "Seismic Behavior of Multistory Braced Steel Frames," Proceedings, ASCE, Journal of the Structural Division, Vol. 100, No. ST 1, Jan. 1974.
48. Otani, S. and Sozen, M.A., "Simulated Earthquake Tests of R/C Frames," Proceedings, ASCE, Journal of the Structural Division, Vol. 100, No. ST 3, March 1974.
49. Mahin, S.A. and Bertero, V.V., "Nonlinear Seismic Response Evaluation - Charaima Building," Proceedings, ASCE, Journal of the Structural Division, Vol. 100, No. ST 6, June 1974.
50. Otani, S., "Inelastic Analysis of R/C Frame Structures," Proceedings, ASCE, Journal of the Structural Division, Vol. 100, No. ST 7, July 1974.

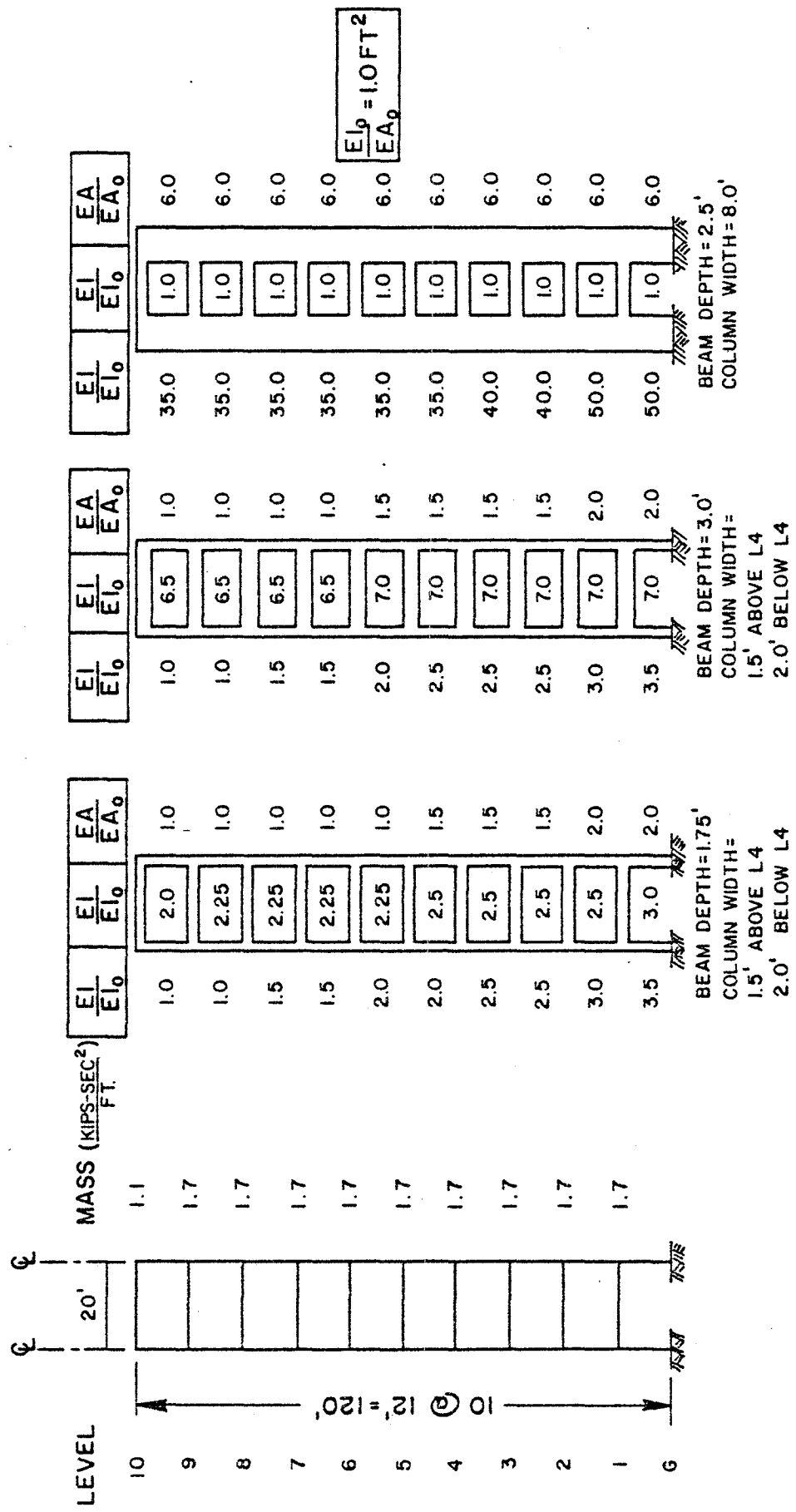


FIG. 2.1 BASIC STRUCTURE PROPERTIES

FIG. 2.2 FLEXURAL & AXIAL STIFFNESS RATIOS

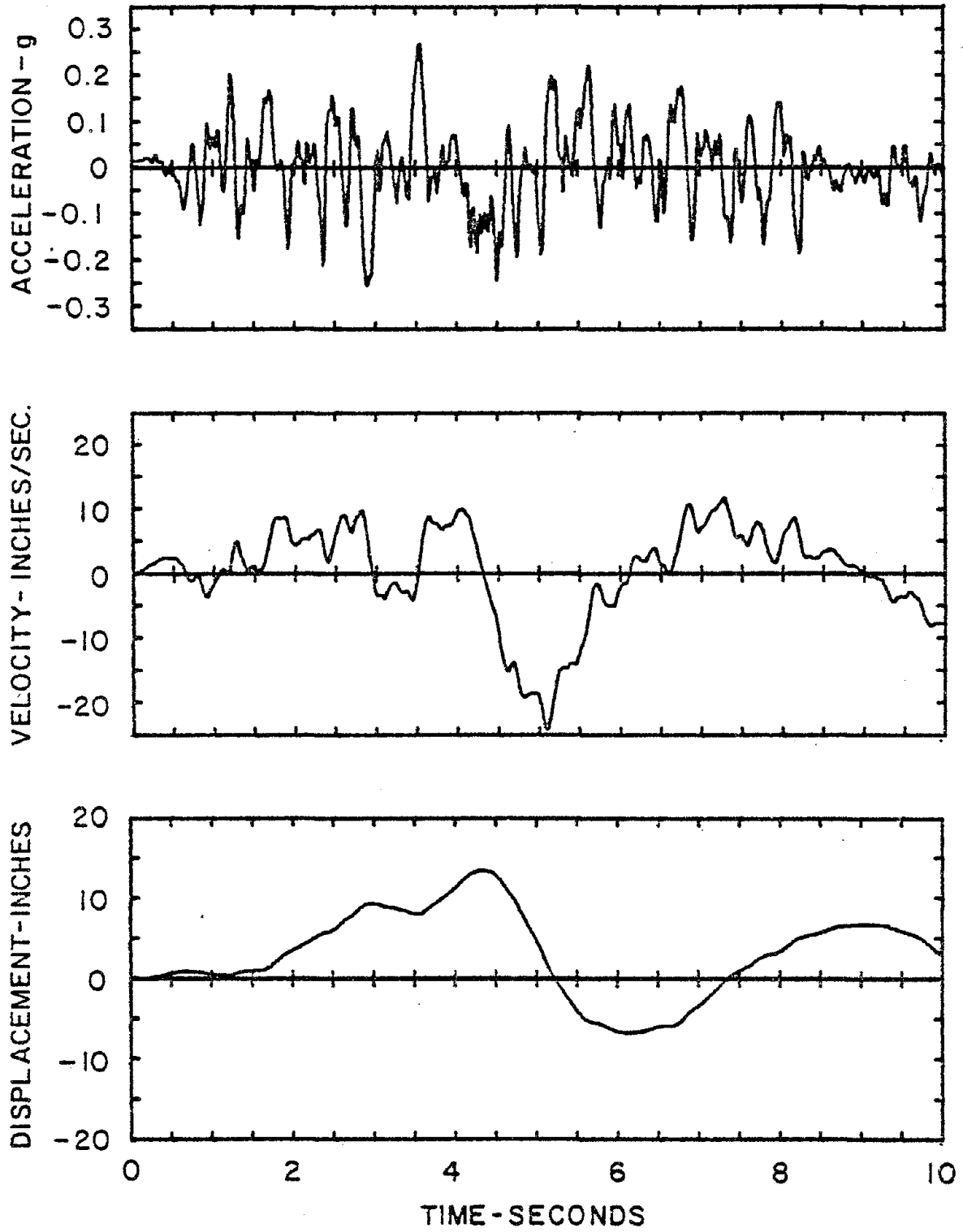


FIG. 2-3 SIMULATED GROUND MOTION I

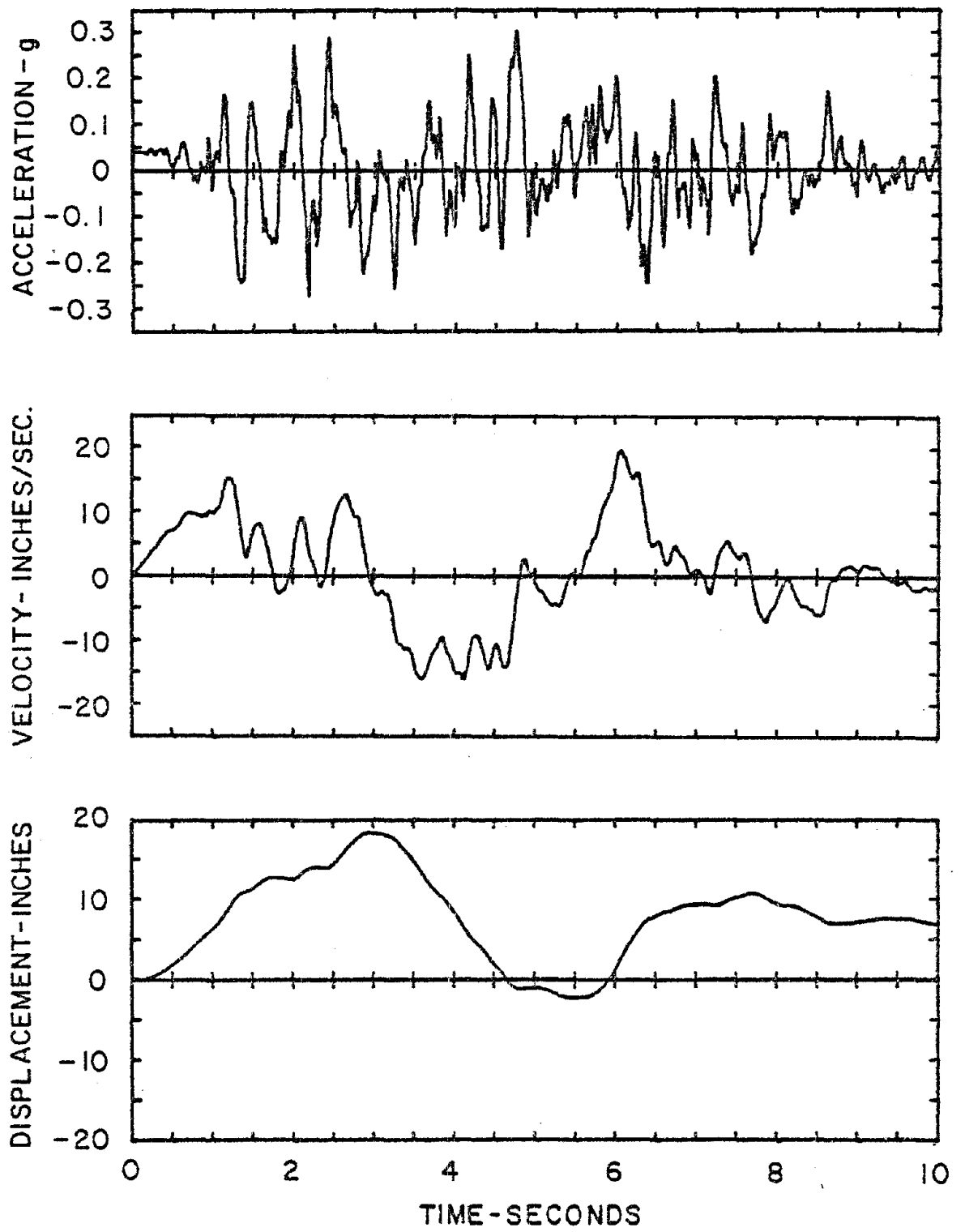


FIG. 2-4 SIMULATED GROUND MOTION 2

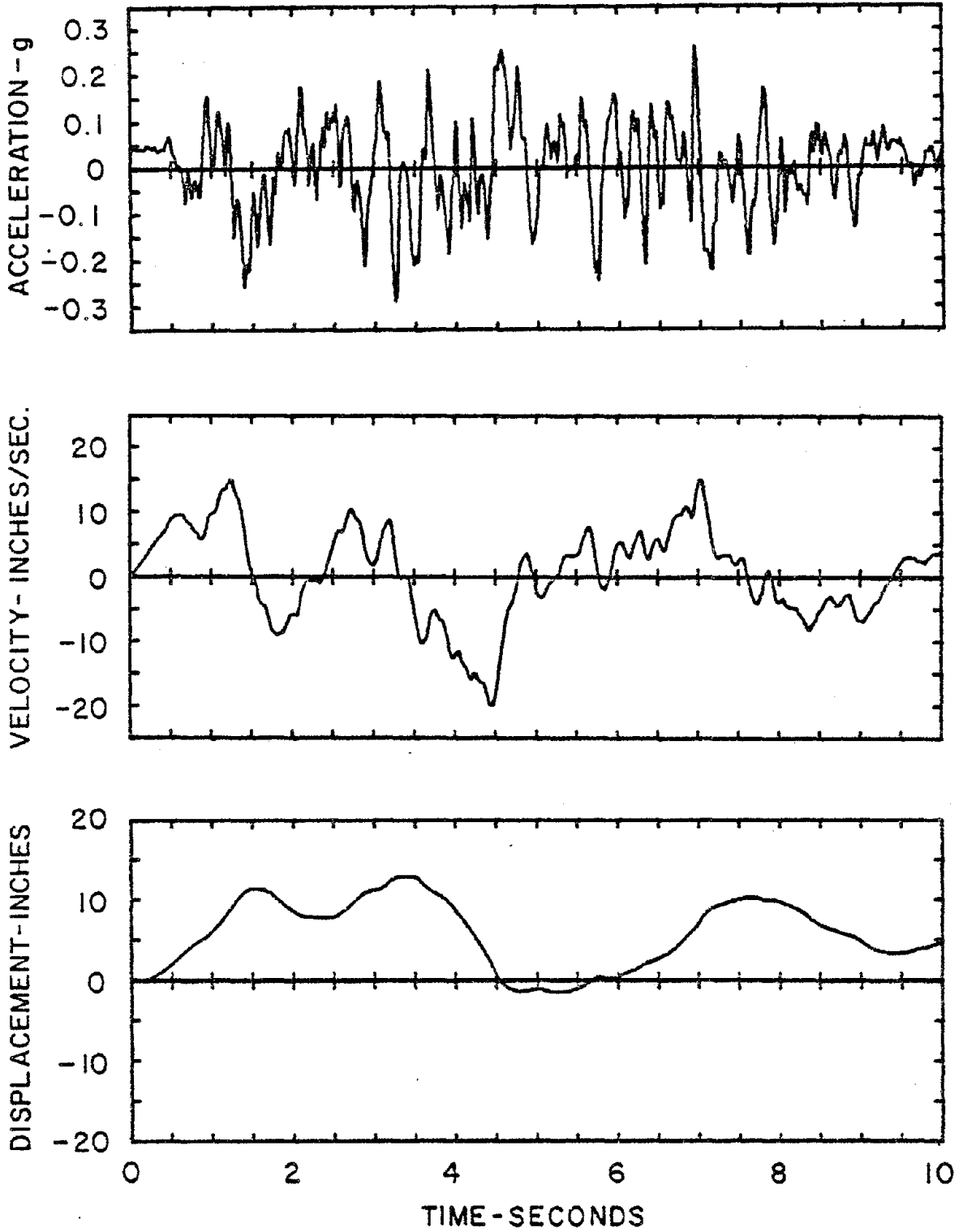


FIG. 2-5 SIMULATED GROUND MOTION 3

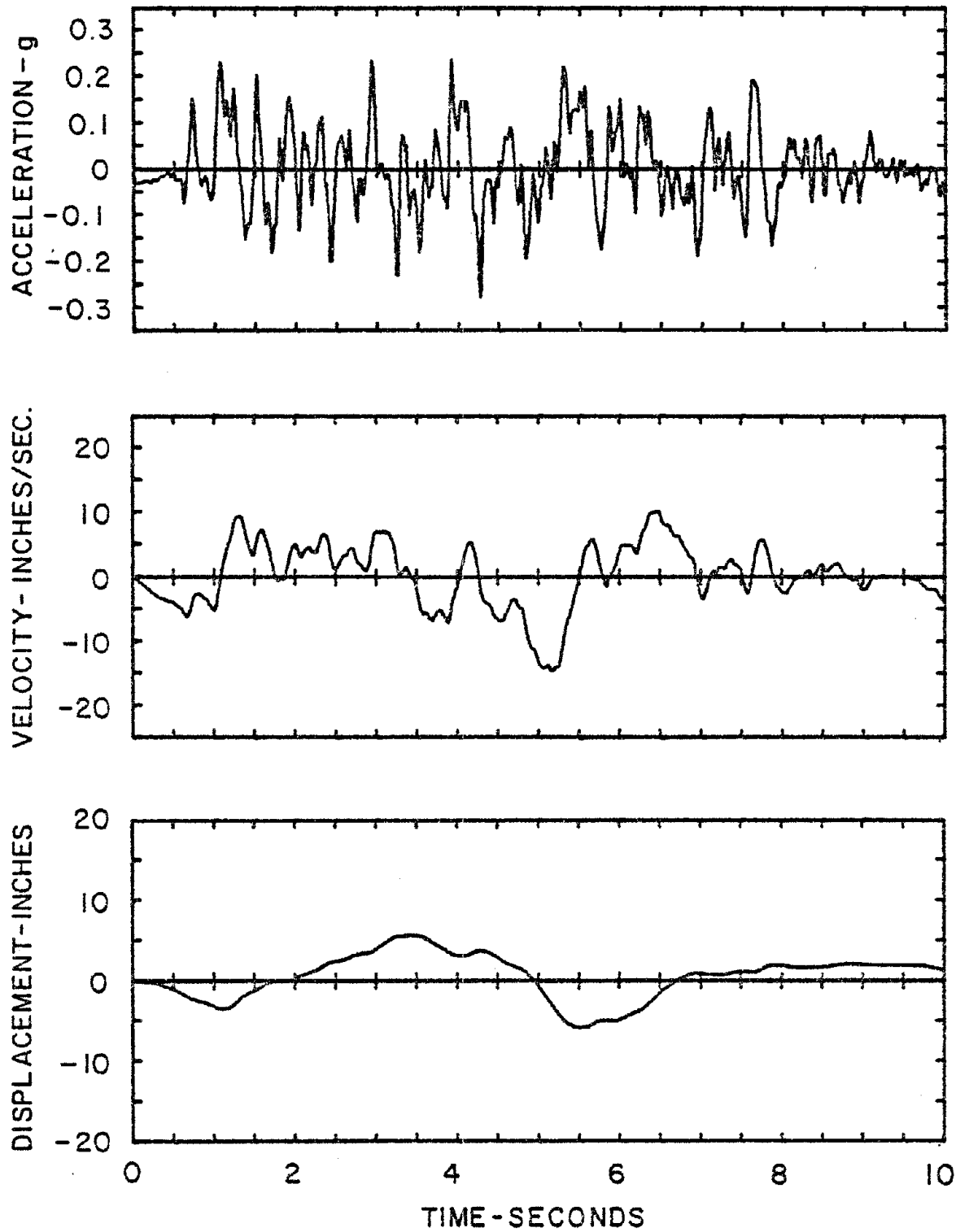


FIG. 2-6 SIMULATED GROUND MOTION 4

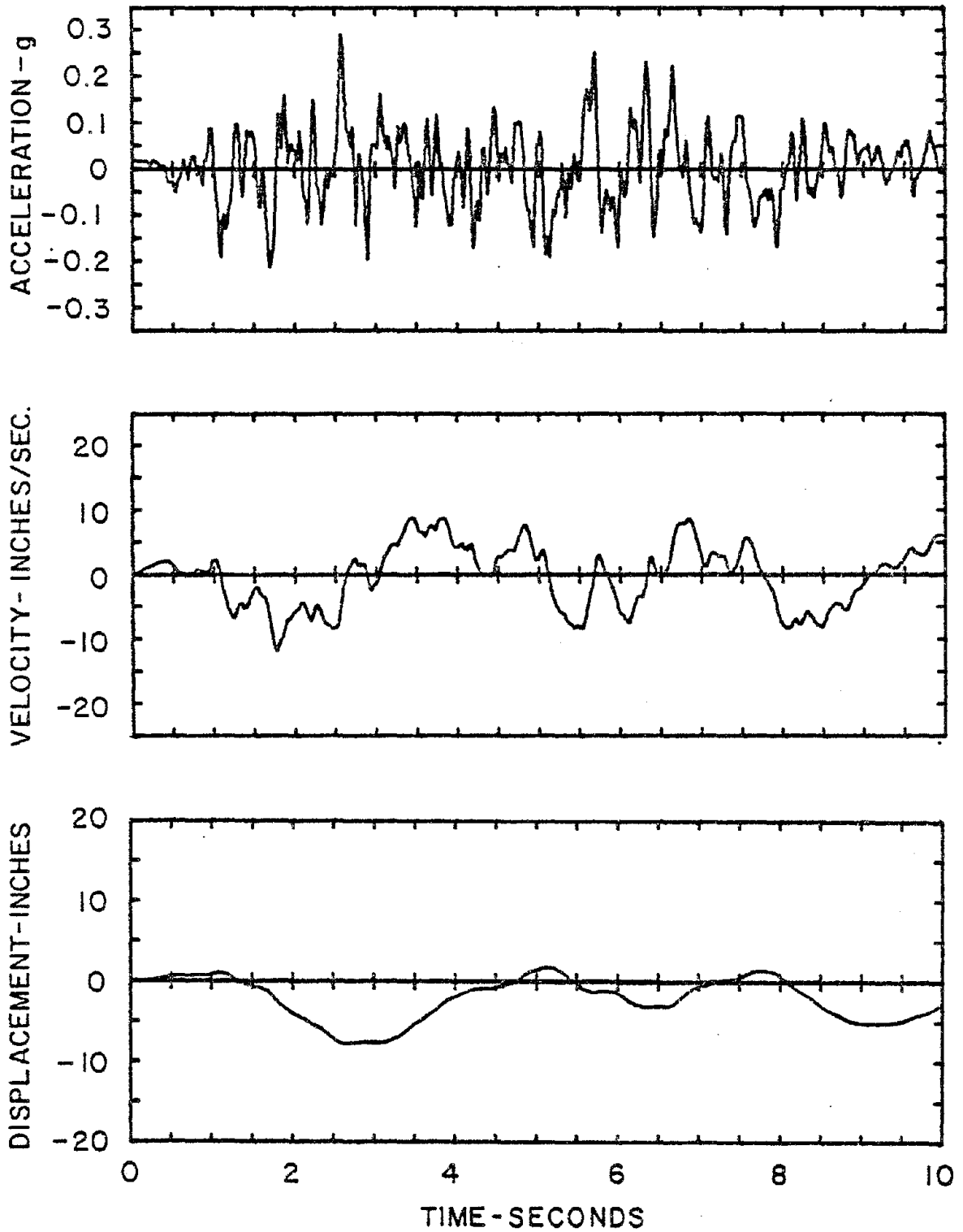


FIG. 2-7 SIMULATED GROUND MOTION 5

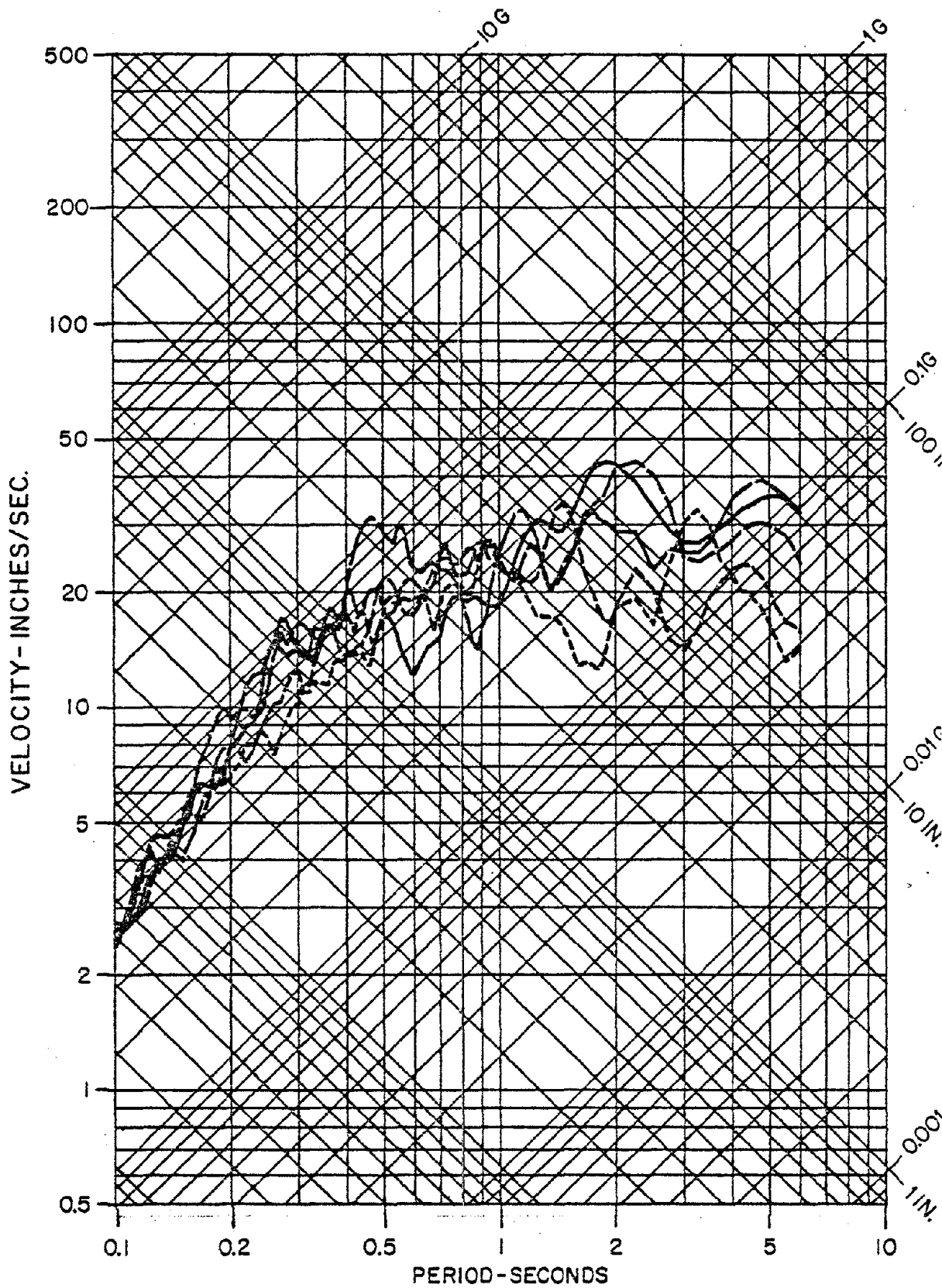


FIG. 2.8 RESPONSE SPECTRA OF SIMULATED GROUND MOTIONS FOR 5% VISCOUS DAMPING

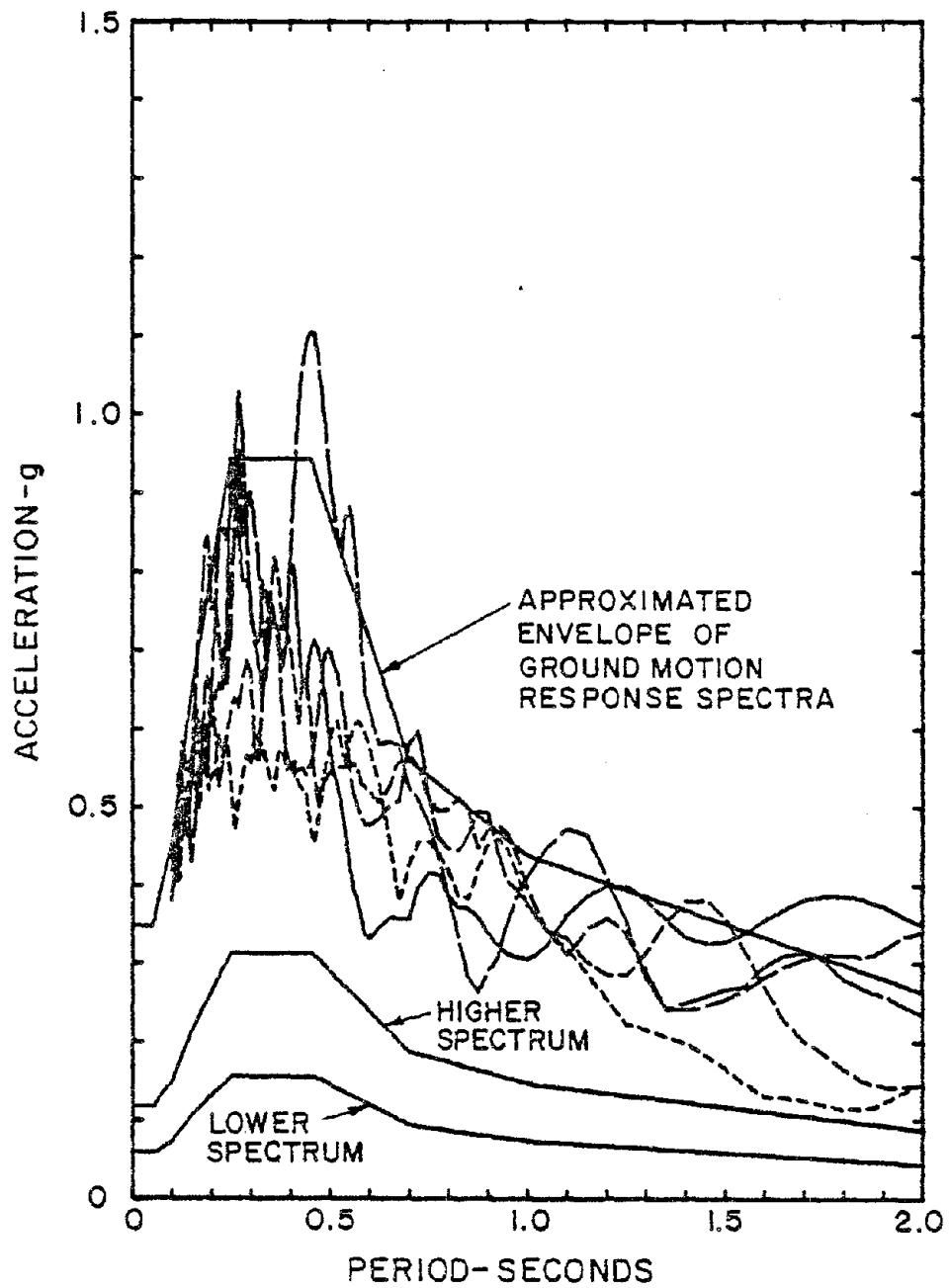


FIG. 2.9 GROUND MOTION RESPONSE SPECTRA AND DESIGN SPECTRA.

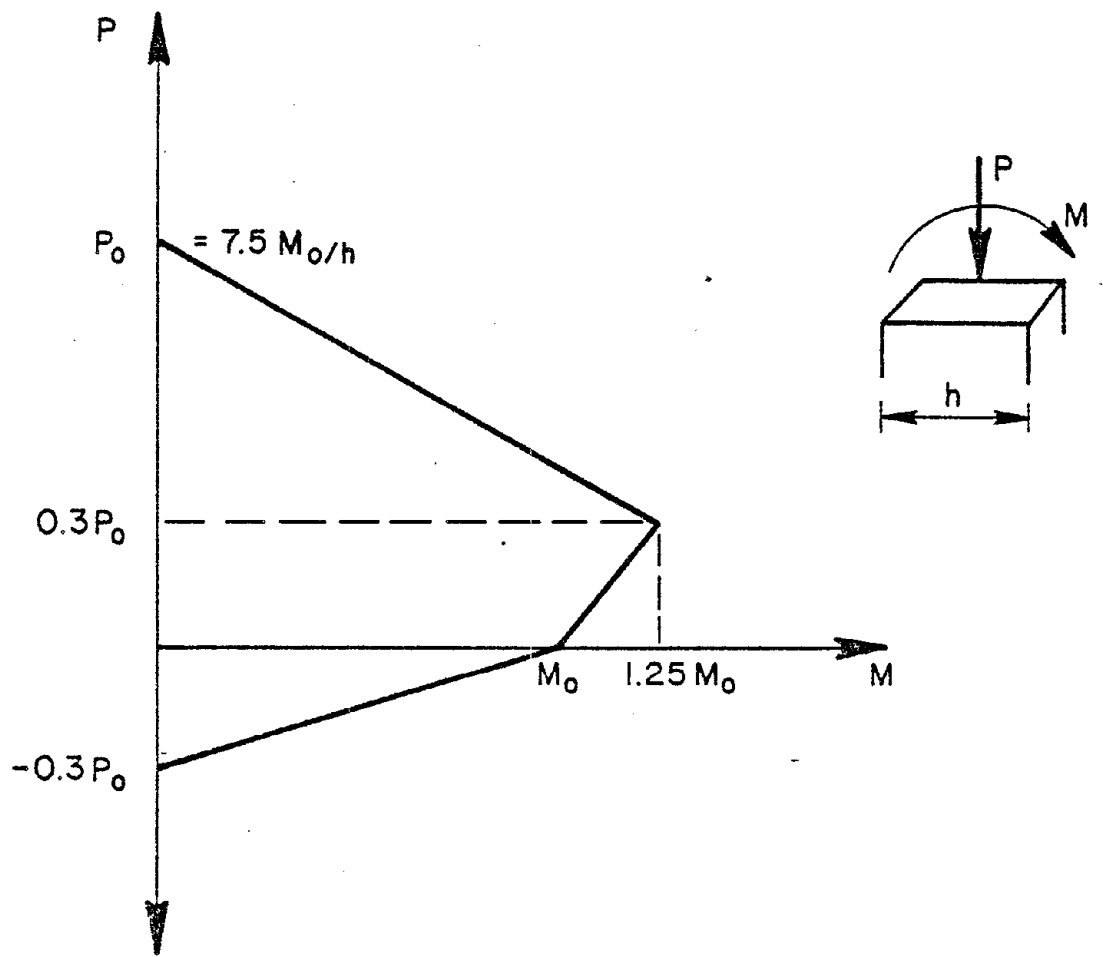


FIG. 2.10 ASSUMED INTERACTION RELATIONSHIP FOR COLUMNS.

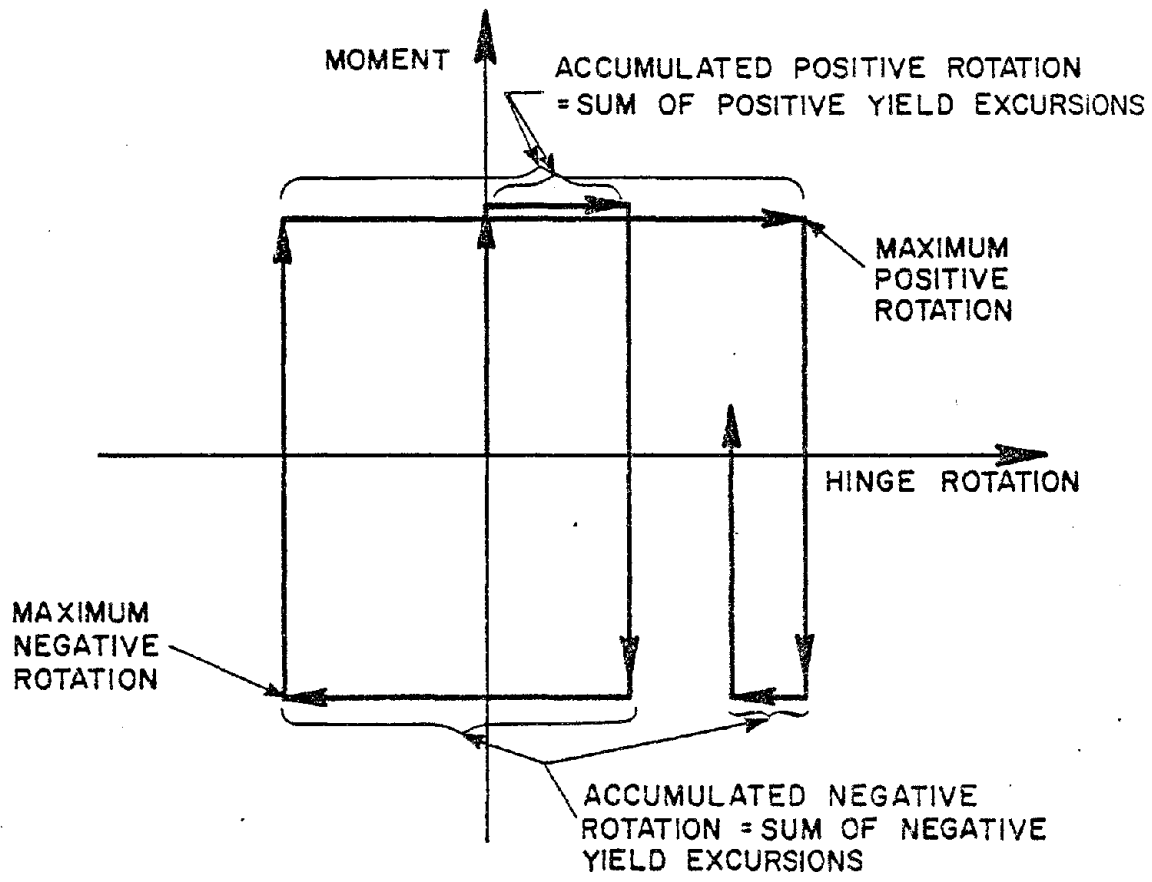
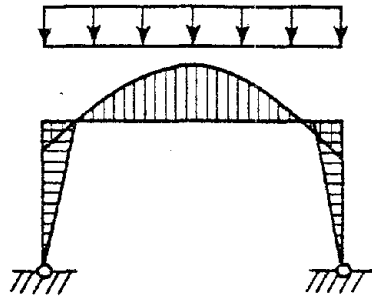
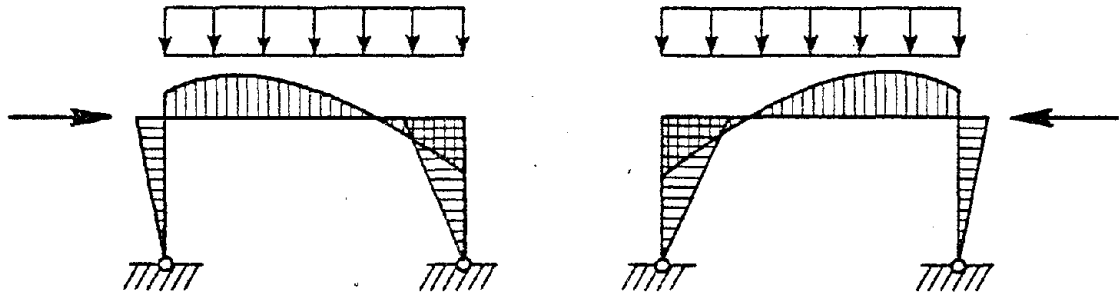


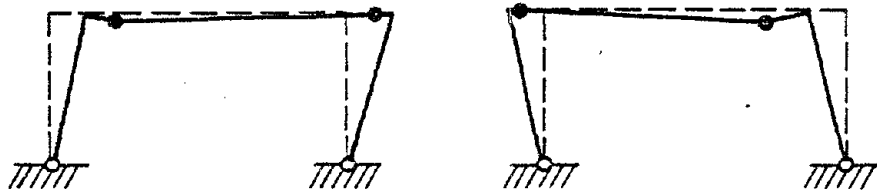
FIG. 3.1 DEFINITION OF HINGE ROTATION QUANTITIES



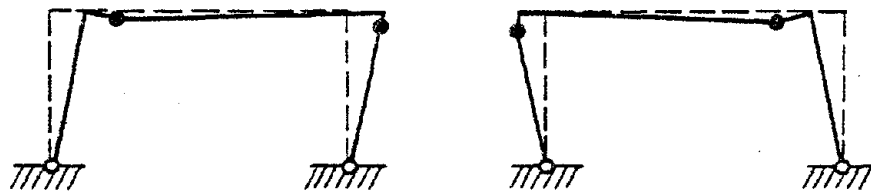
(a) GRAVITY LOAD MOMENTS



(b), (c): MOMENTS FOR GRAVITY PLUS LATERAL LOAD



(d), (e): HINGES WITH STRONG COLUMNS



(f), (g): HINGES WITH WEAKER COLUMNS

FIG. 4.1 HINGE REVERAL UNDER CYCLIC LOAD

APPENDIX A

GRAPHICAL PRESENTATIONS
OF RESULTS



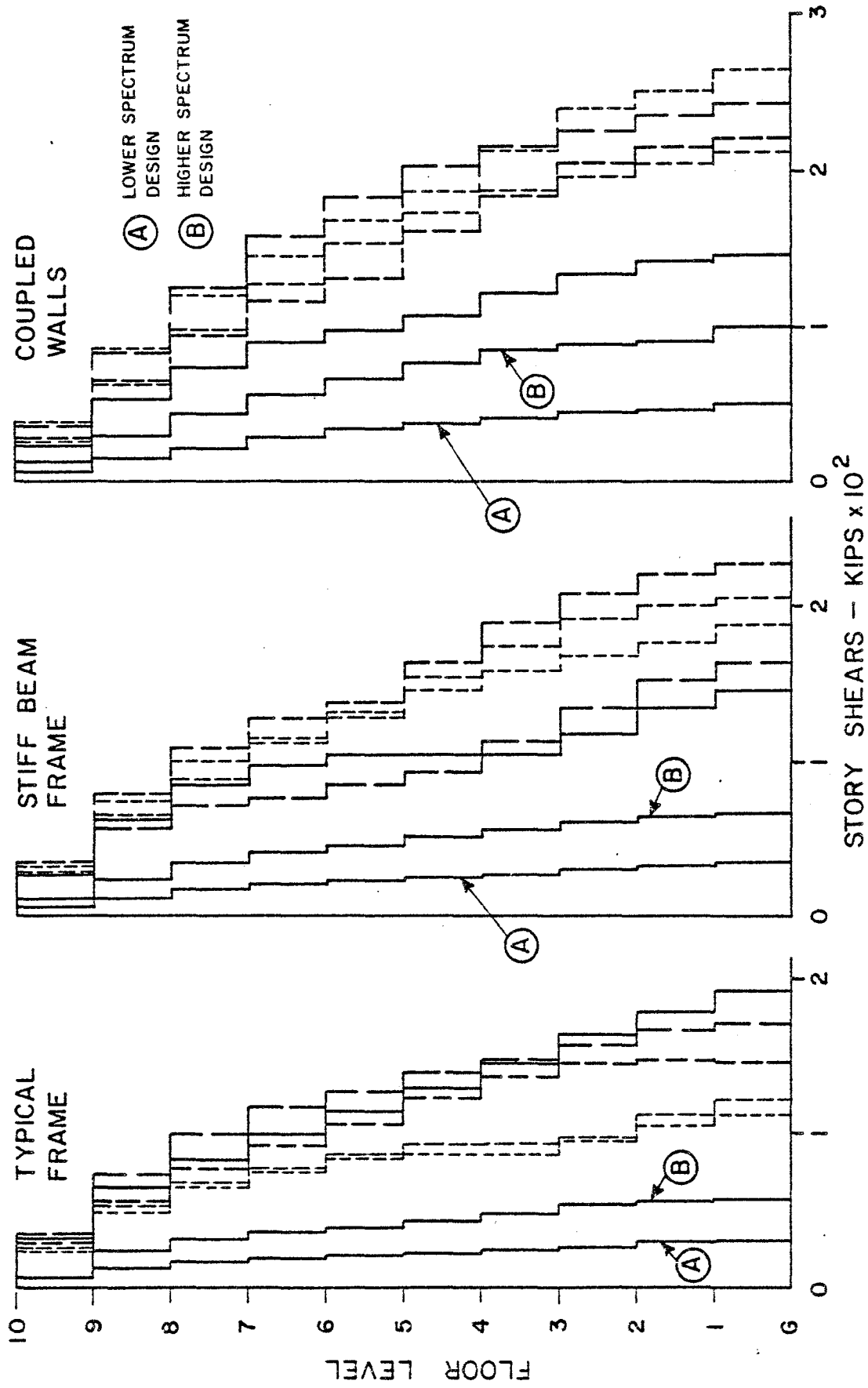


FIG. A.1: ELASTIC STORY SHEAR ENVELOPES AND DESIGN STORY SHEARS

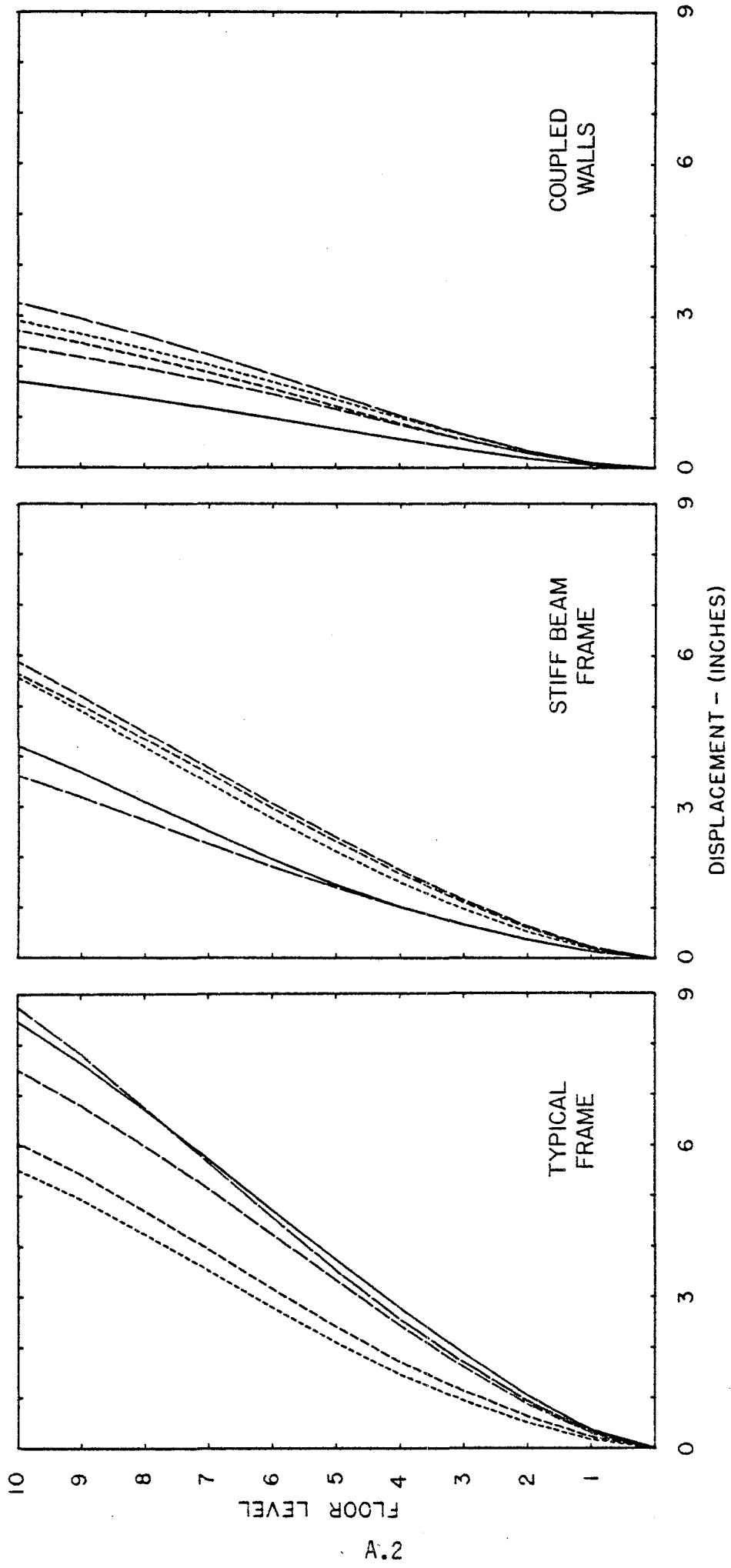


FIG. A-2 LATERAL DISPLACEMENT ENVELOPES
ELASTIC

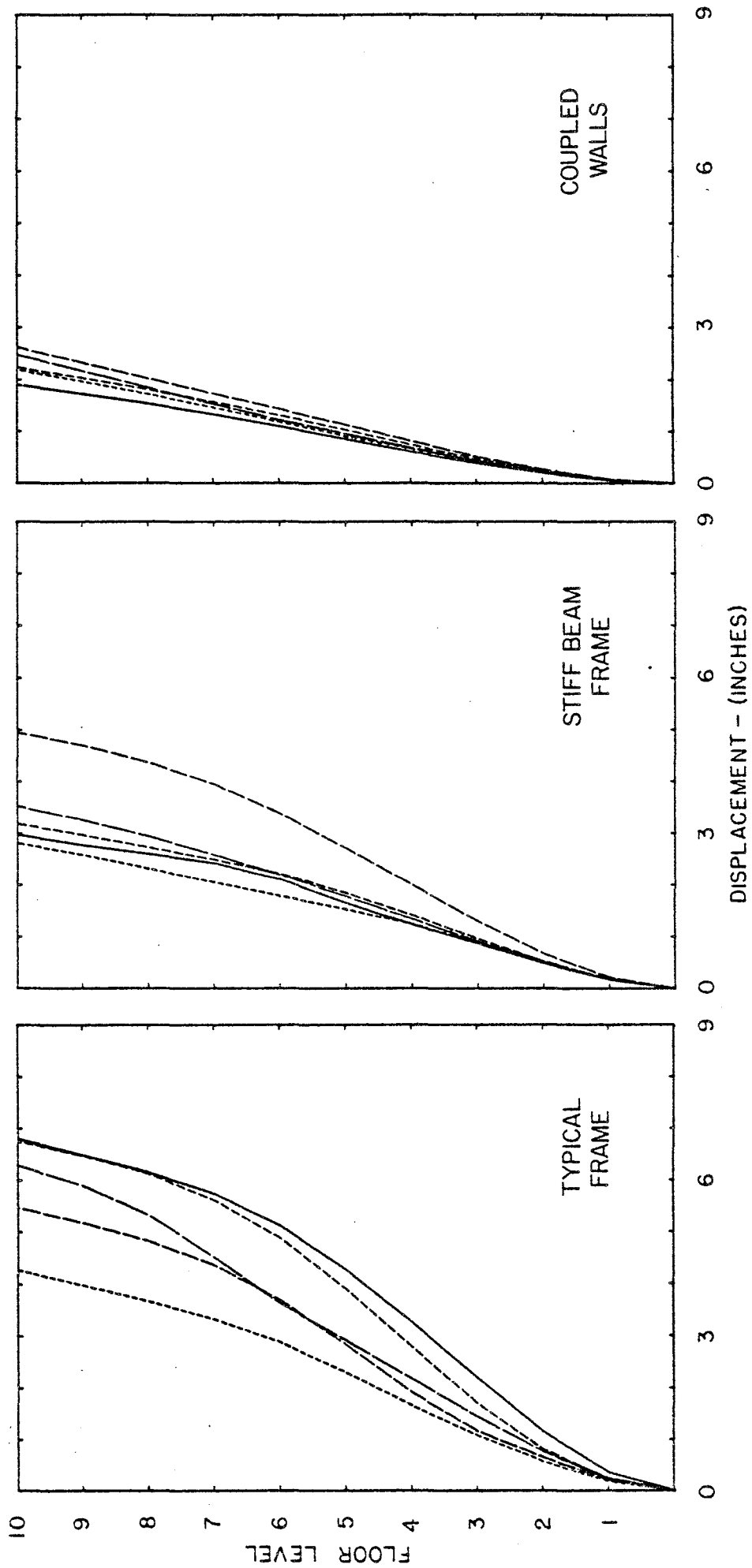


FIG. A-3 LATERAL DISPLACEMENT ENVELOPES
HI/∞ DESIGN

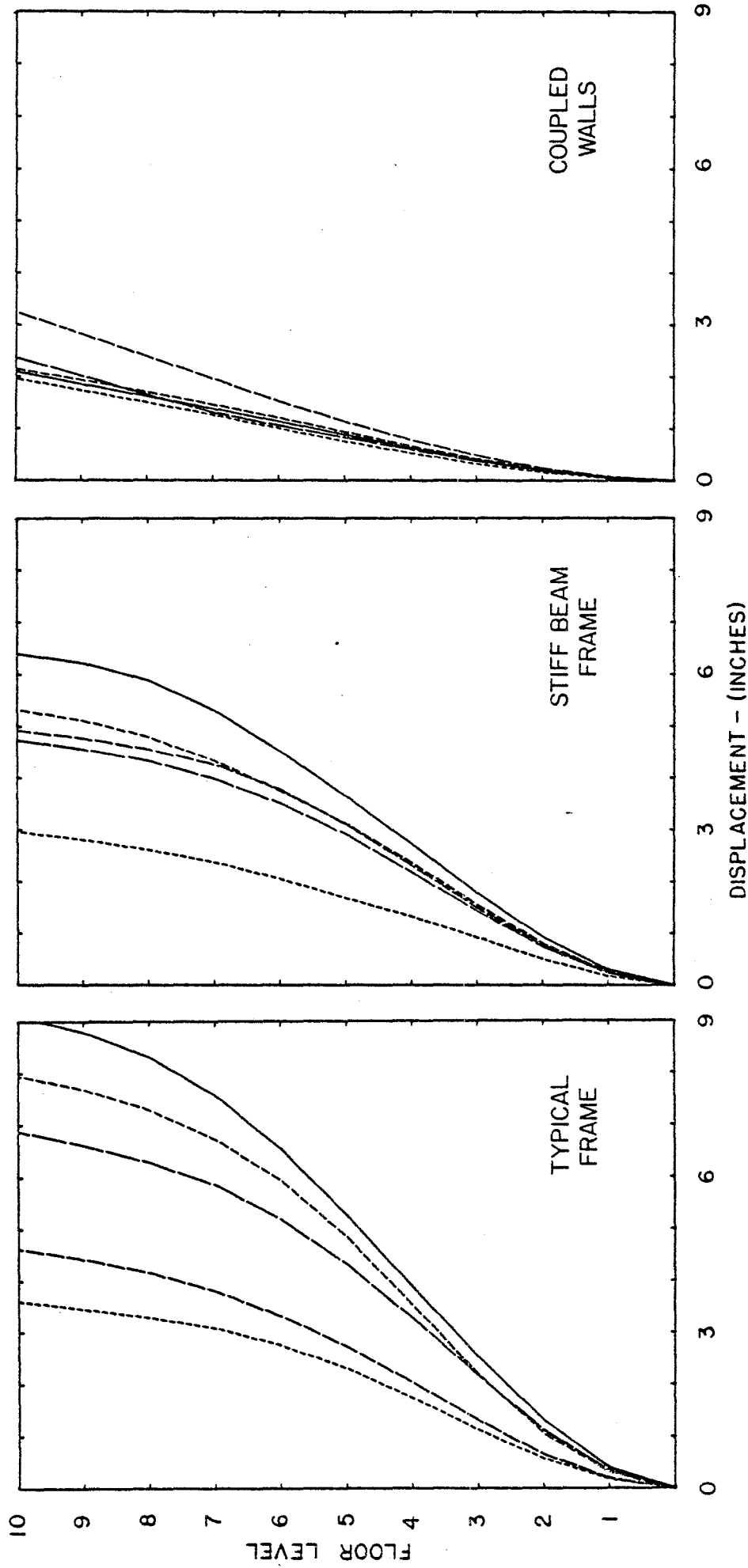


FIG. A-4 LATERAL DISPLACEMENT ENVELOPES
LO/100 DESIGN

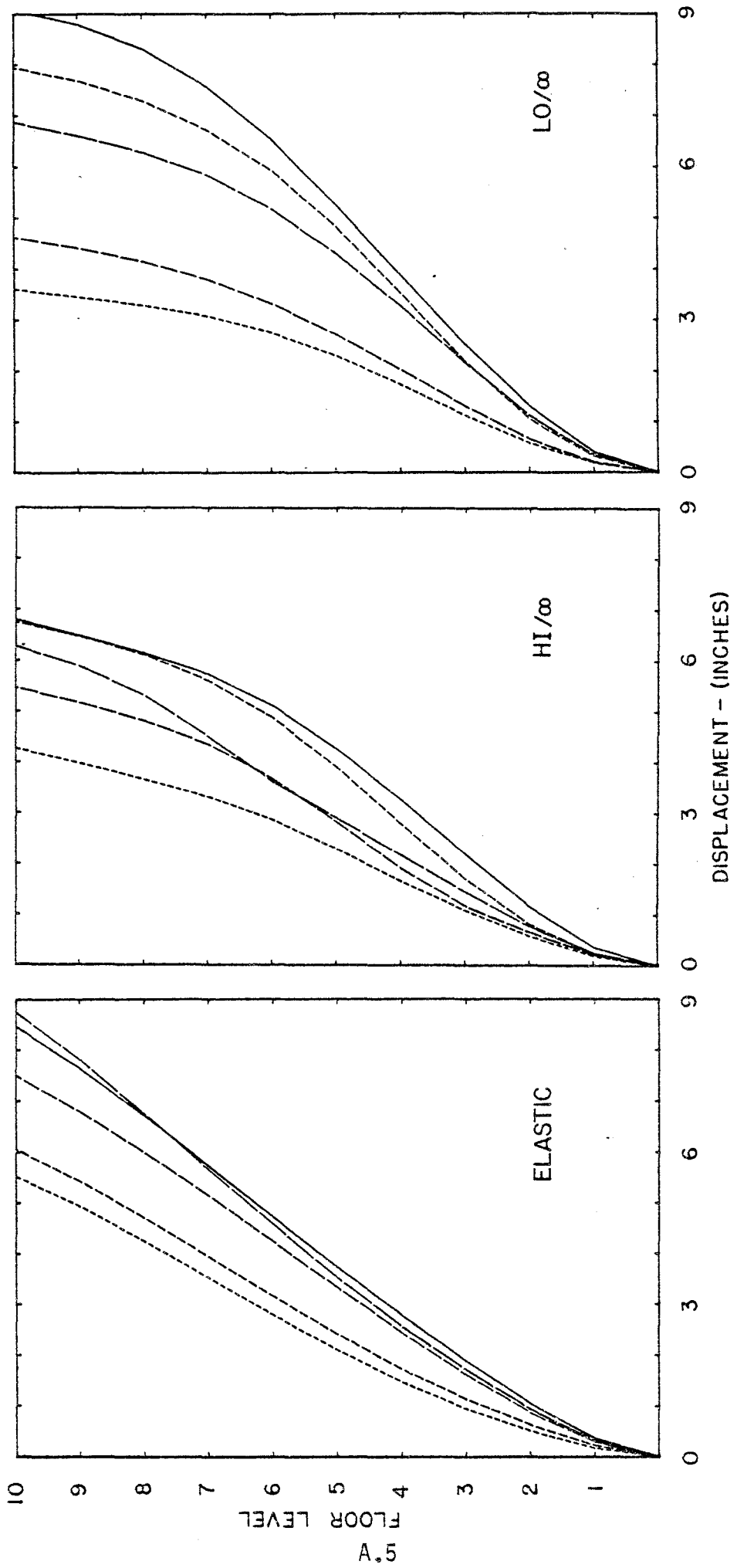


FIG. A-5 LATERAL DISPLACEMENT ENVELOPES
TYPICAL FRAME

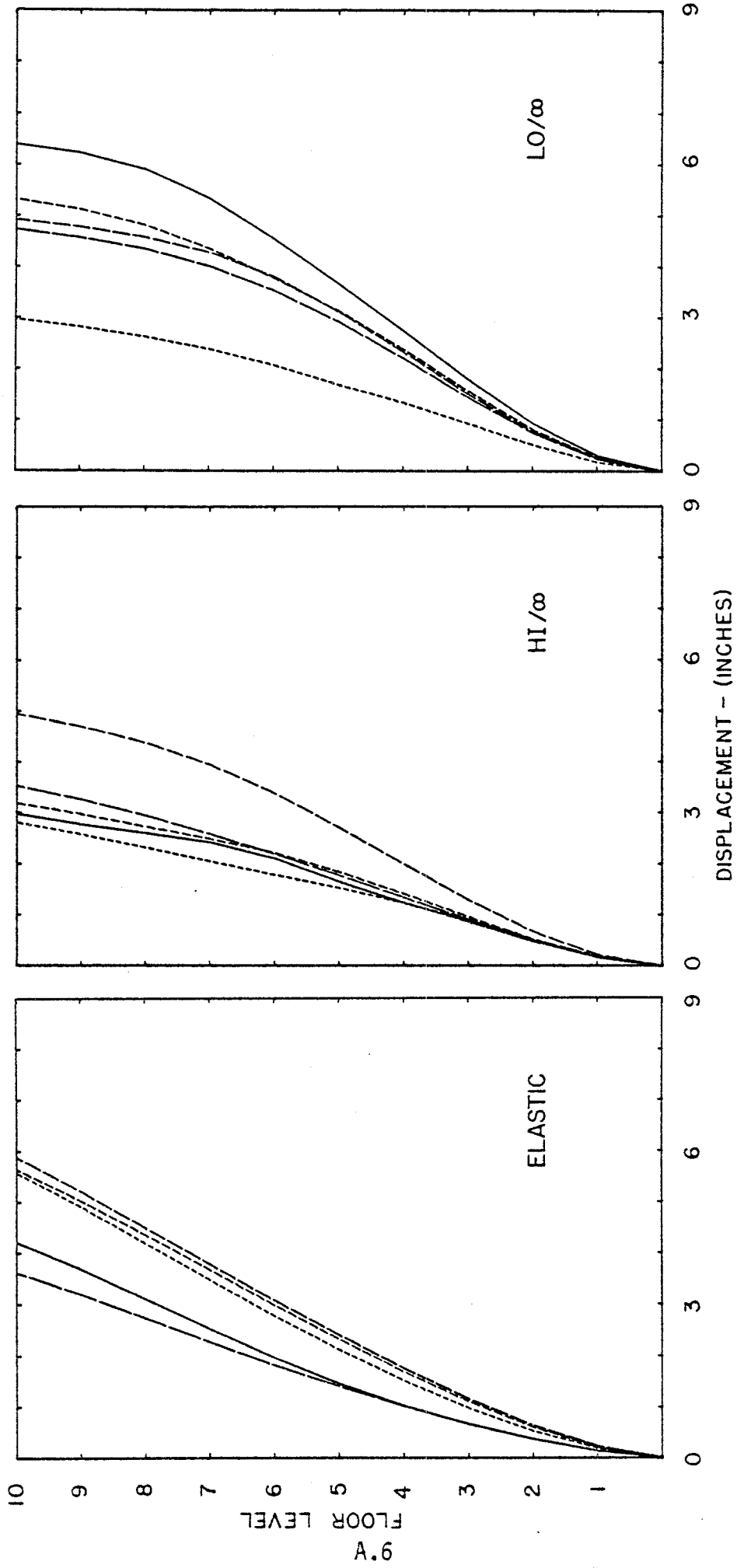


FIG. A-6 LATERAL DISPLACEMENT ENVELOPES
STIFF BEAM FRAME

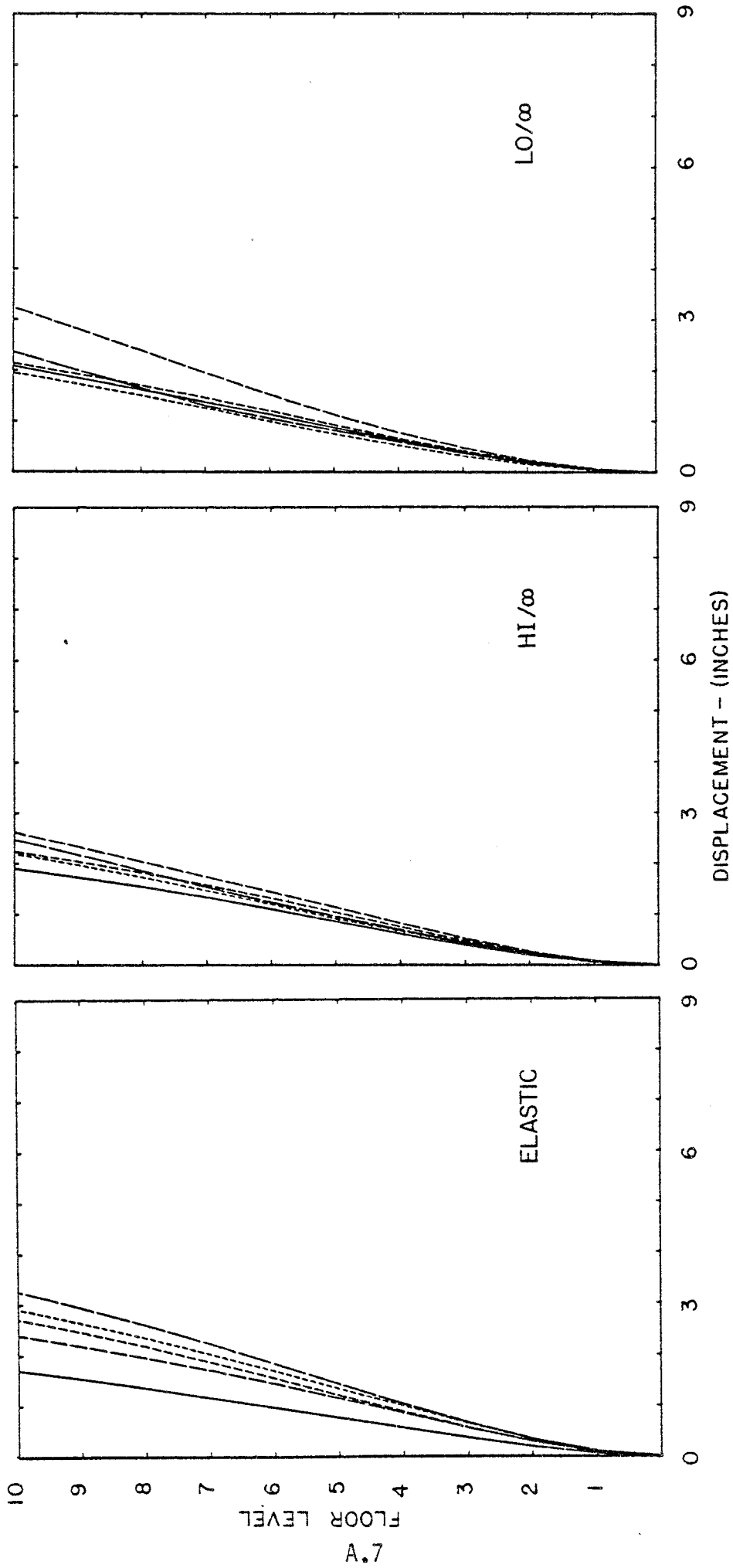


FIG. A-7 LATERAL DISPLACEMENT ENVELOPES
COUPLED WALLS

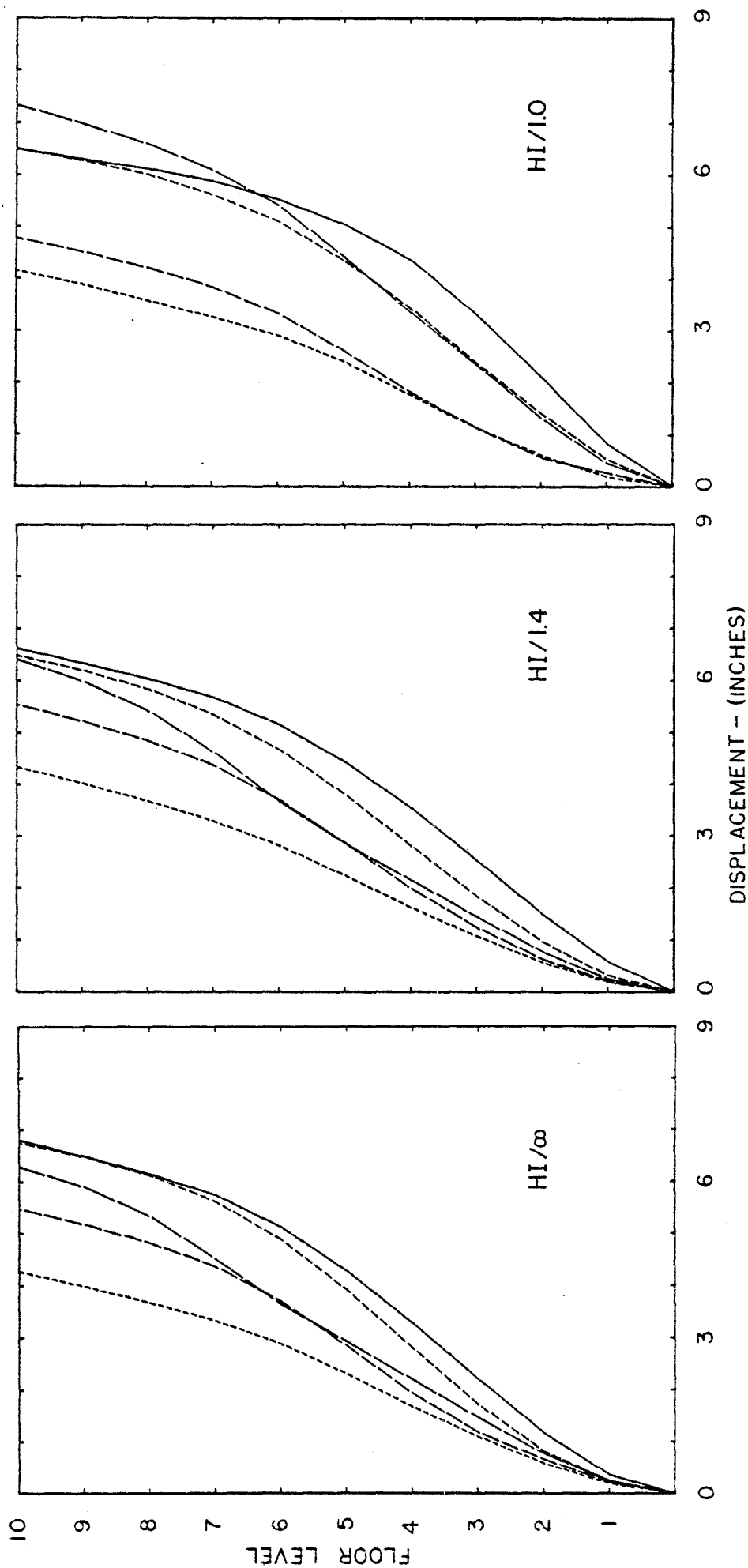


FIG. A-8 LATERAL DISPLACEMENT ENVELOPES
TYPICAL FRAME

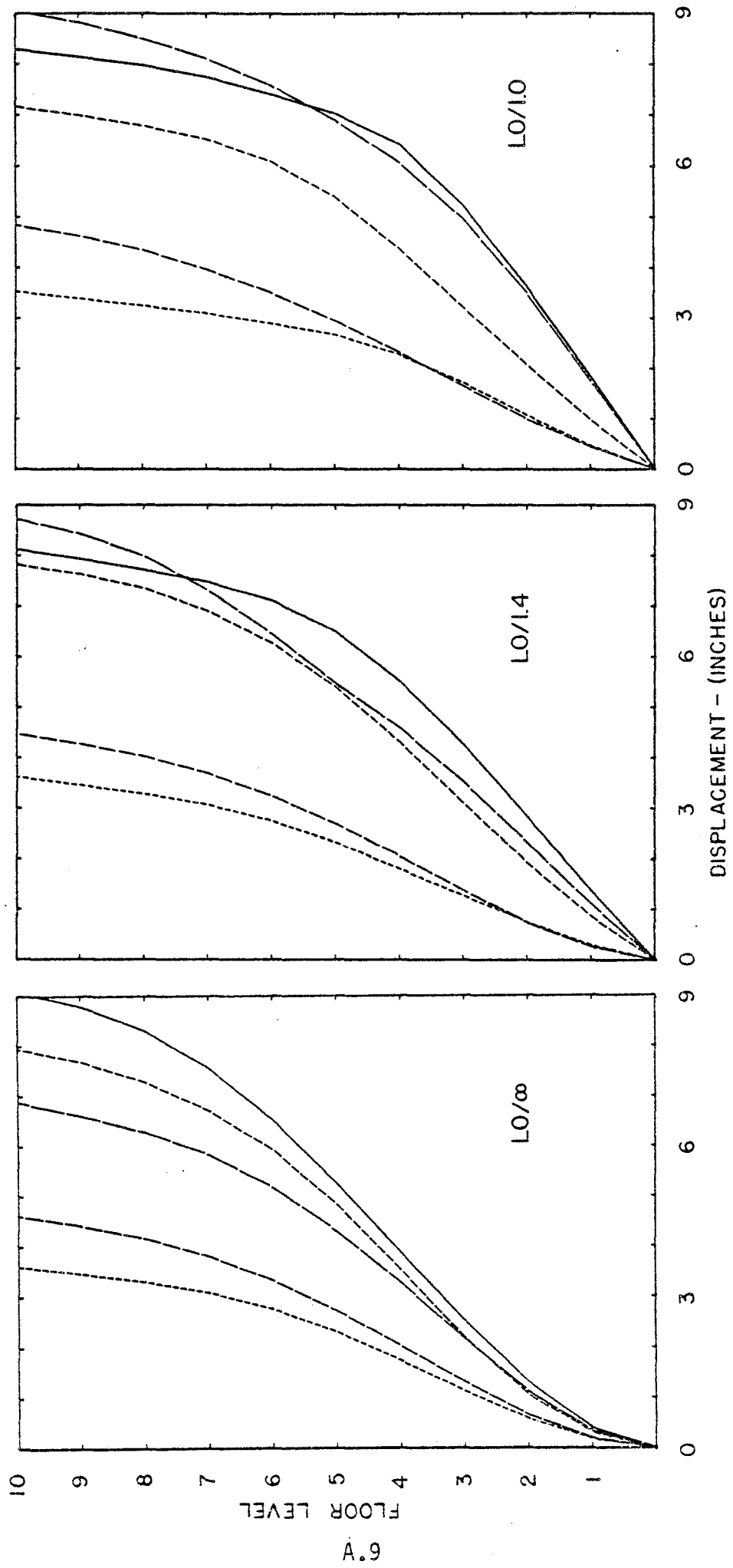


FIG. A-9 LATERAL DISPLACEMENT ENVELOPES
TYPICAL FRAME

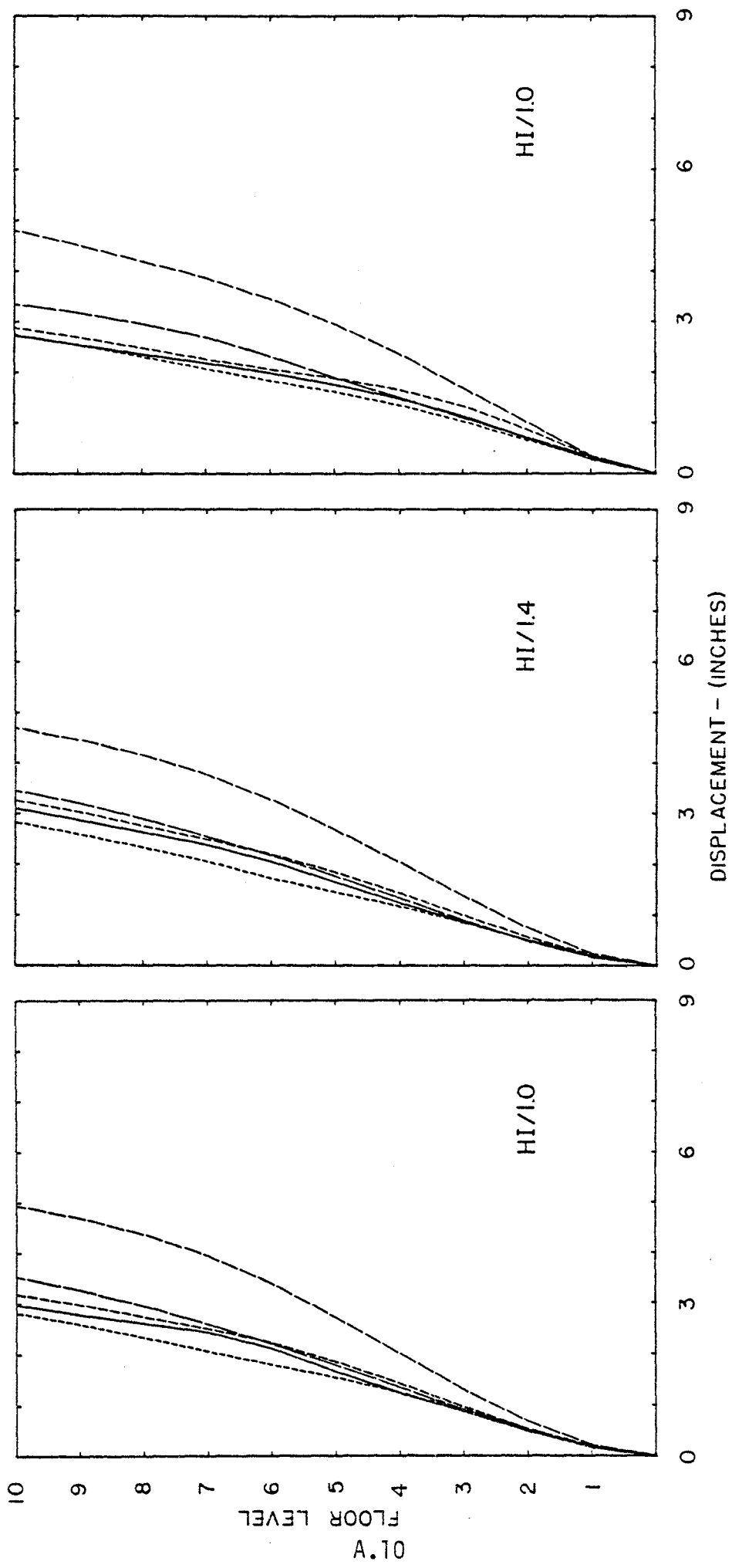


FIG. A-10 LATERAL DISPLACEMENT ENVELOPES
STIFF BEAM FRAME

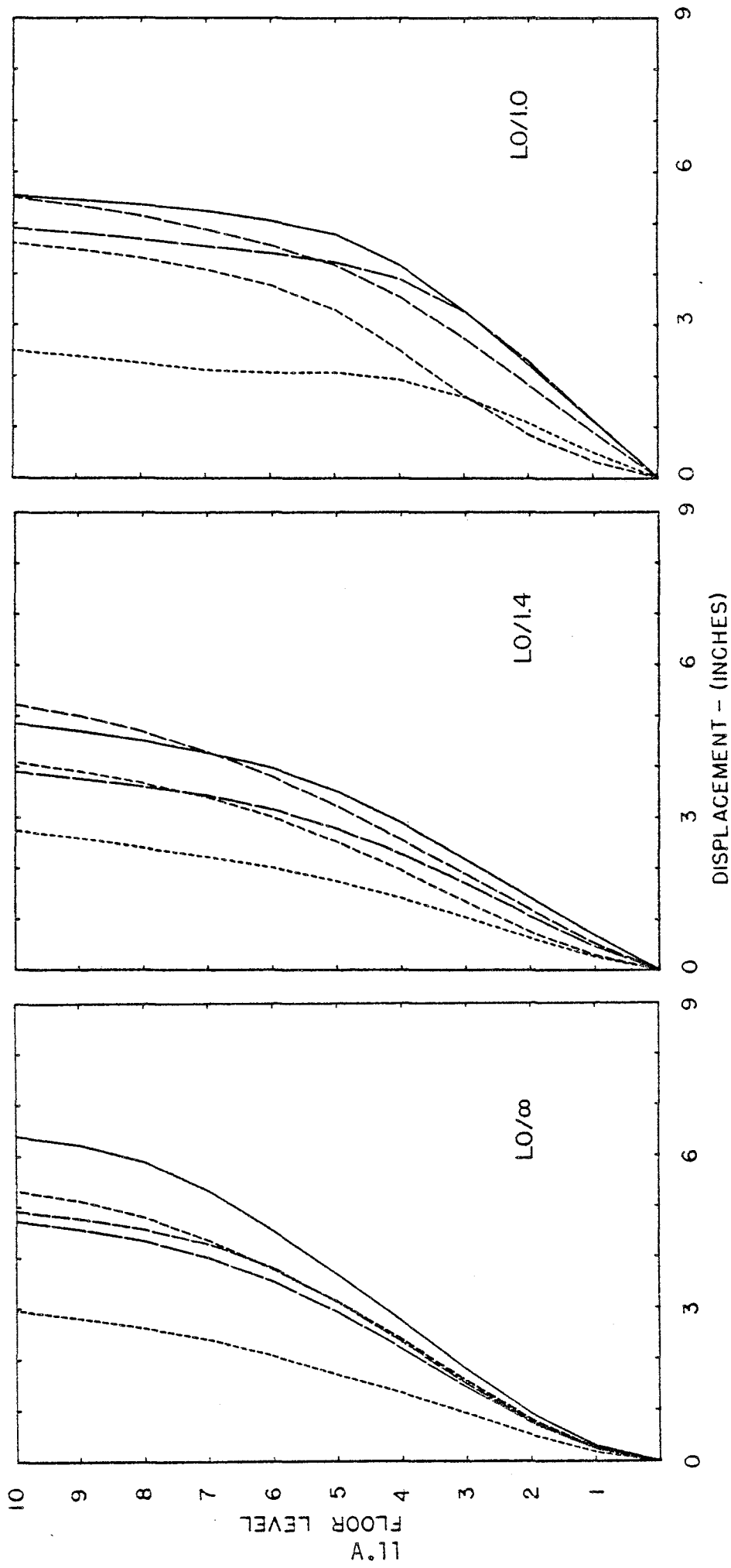


FIG. A-II LATERAL DISPLACEMENT ENVELOPES
STIFF BEAM FRAME

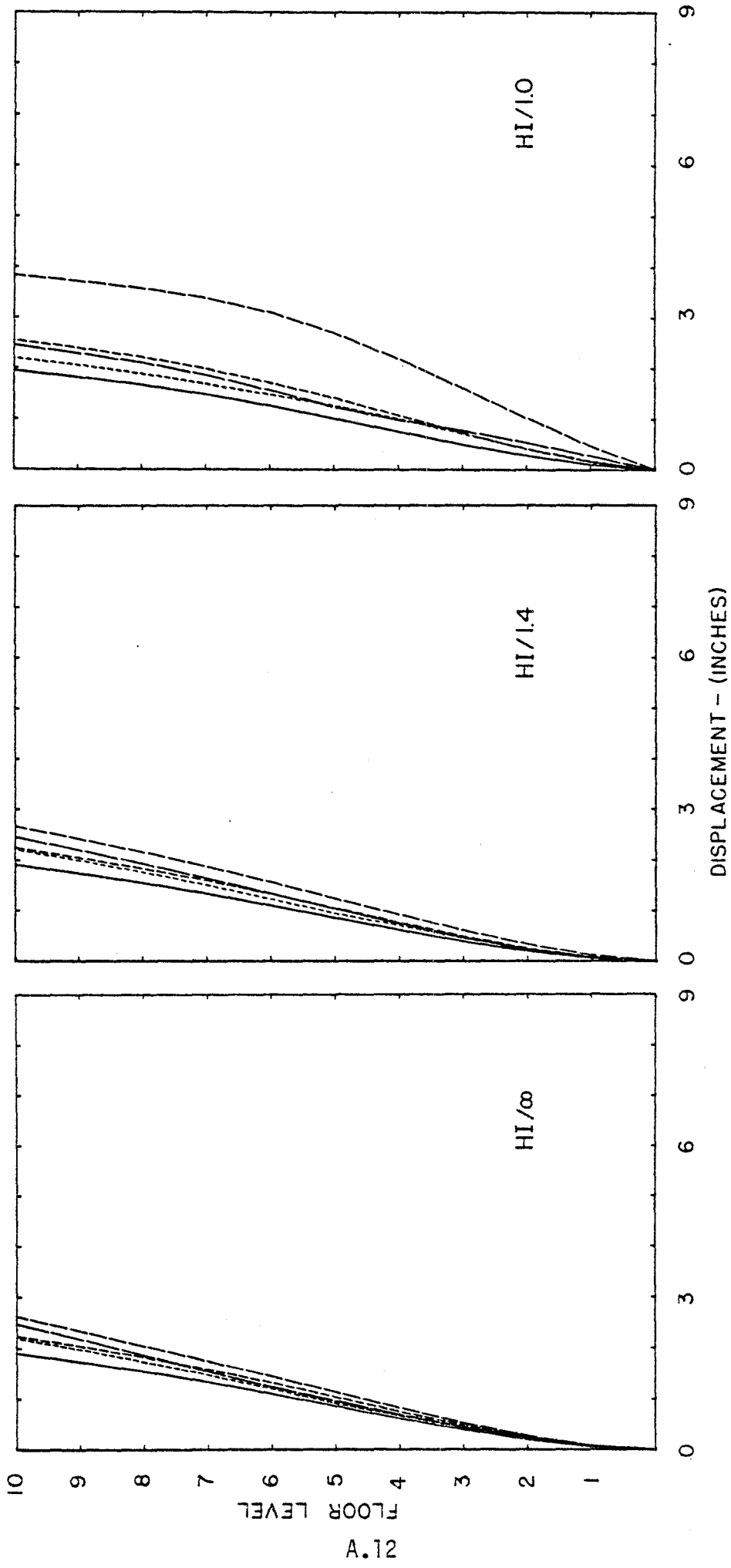


FIG. A-12 LATERAL DISPLACEMENT ENVELOPES
COUPLED WALLS

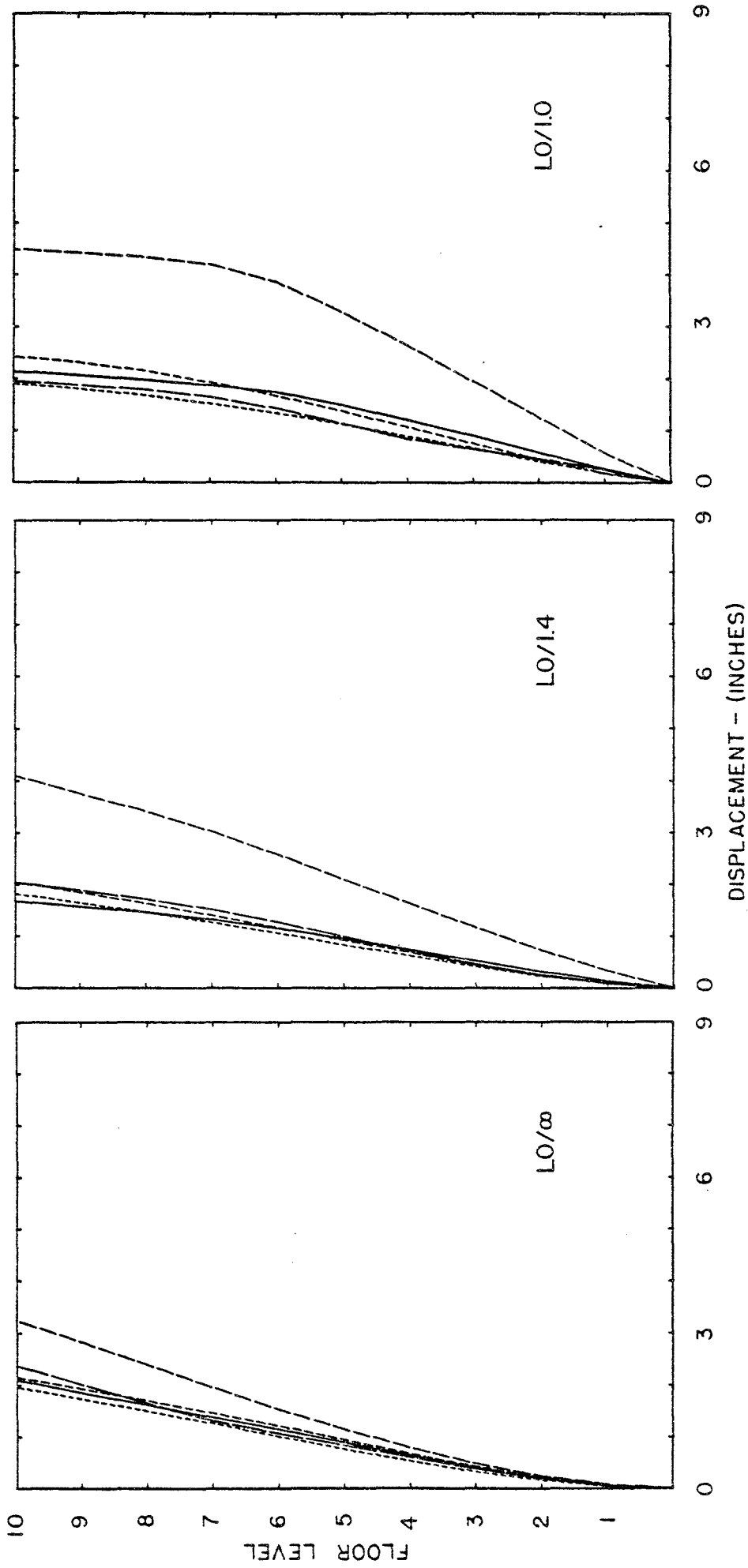
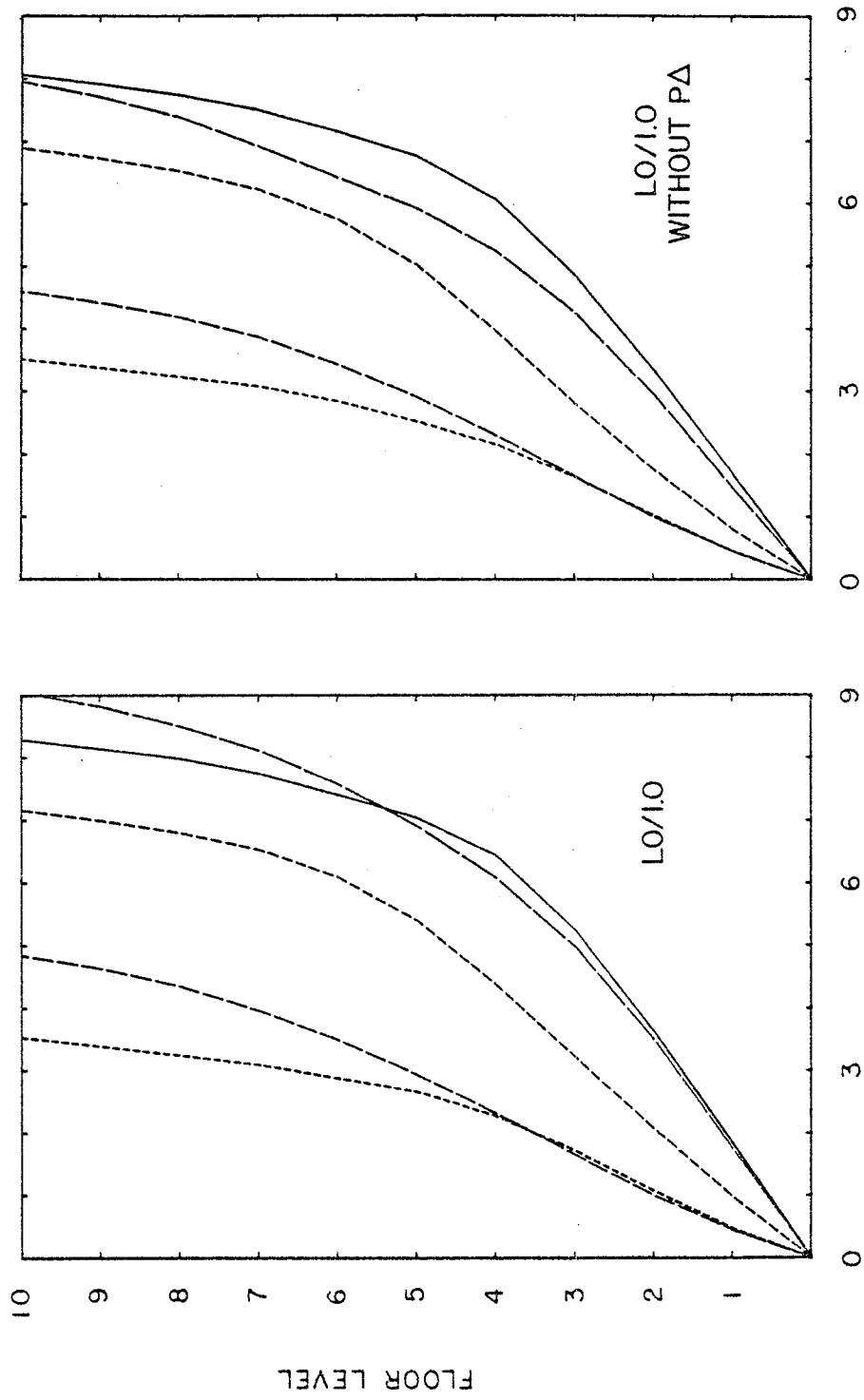


FIG. A-13 LATERAL DISPLACEMENT ENVELOPES
COUPLED WALLS



DISPLACEMENT - (INCHES)

FIG. A-14 LATERAL DISPLACEMENT ENVELOPES
TYPICAL FRAME

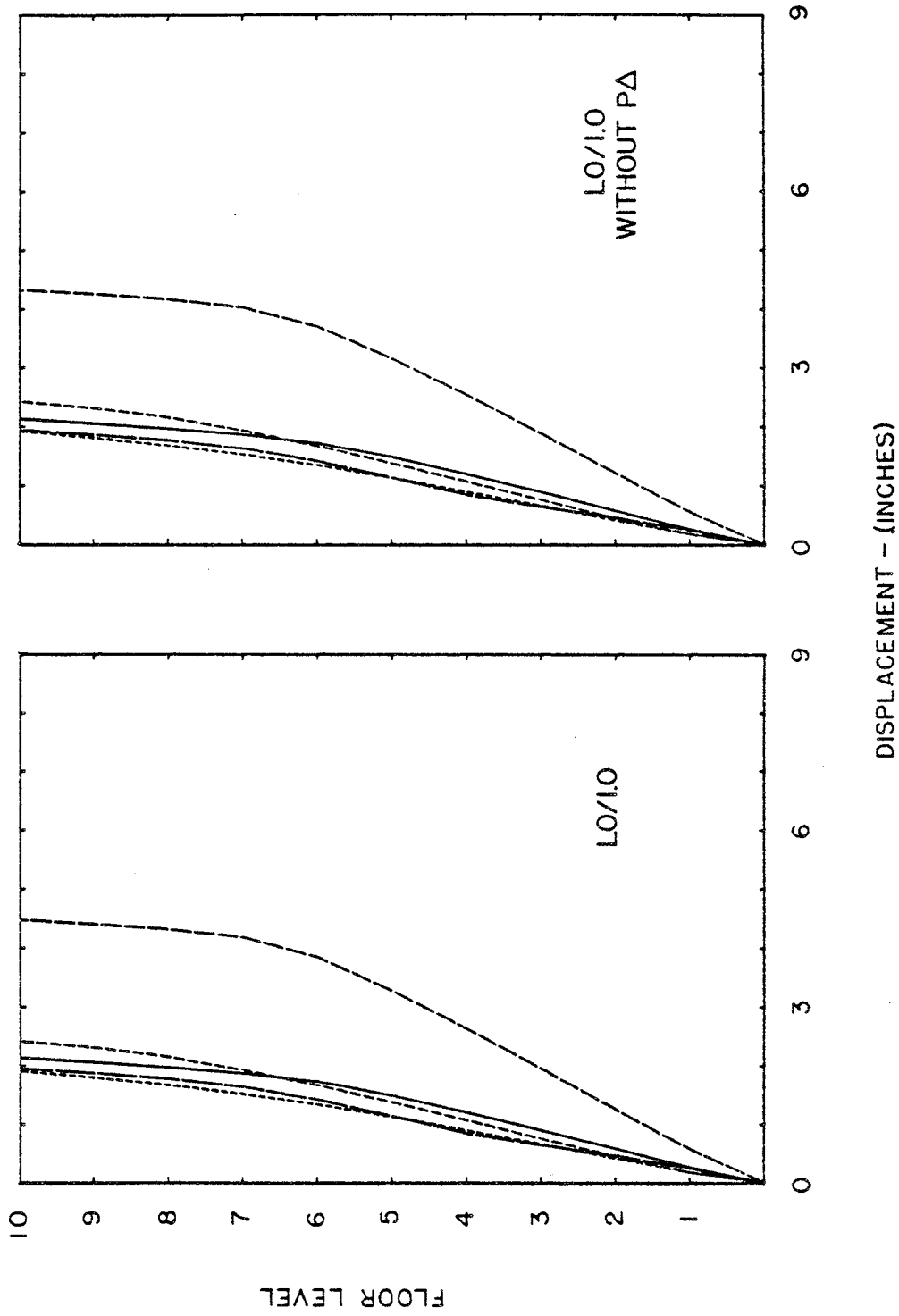


FIG. A-15 LATERAL DISPLACEMENT ENVELOPES
COUPLED WALLS

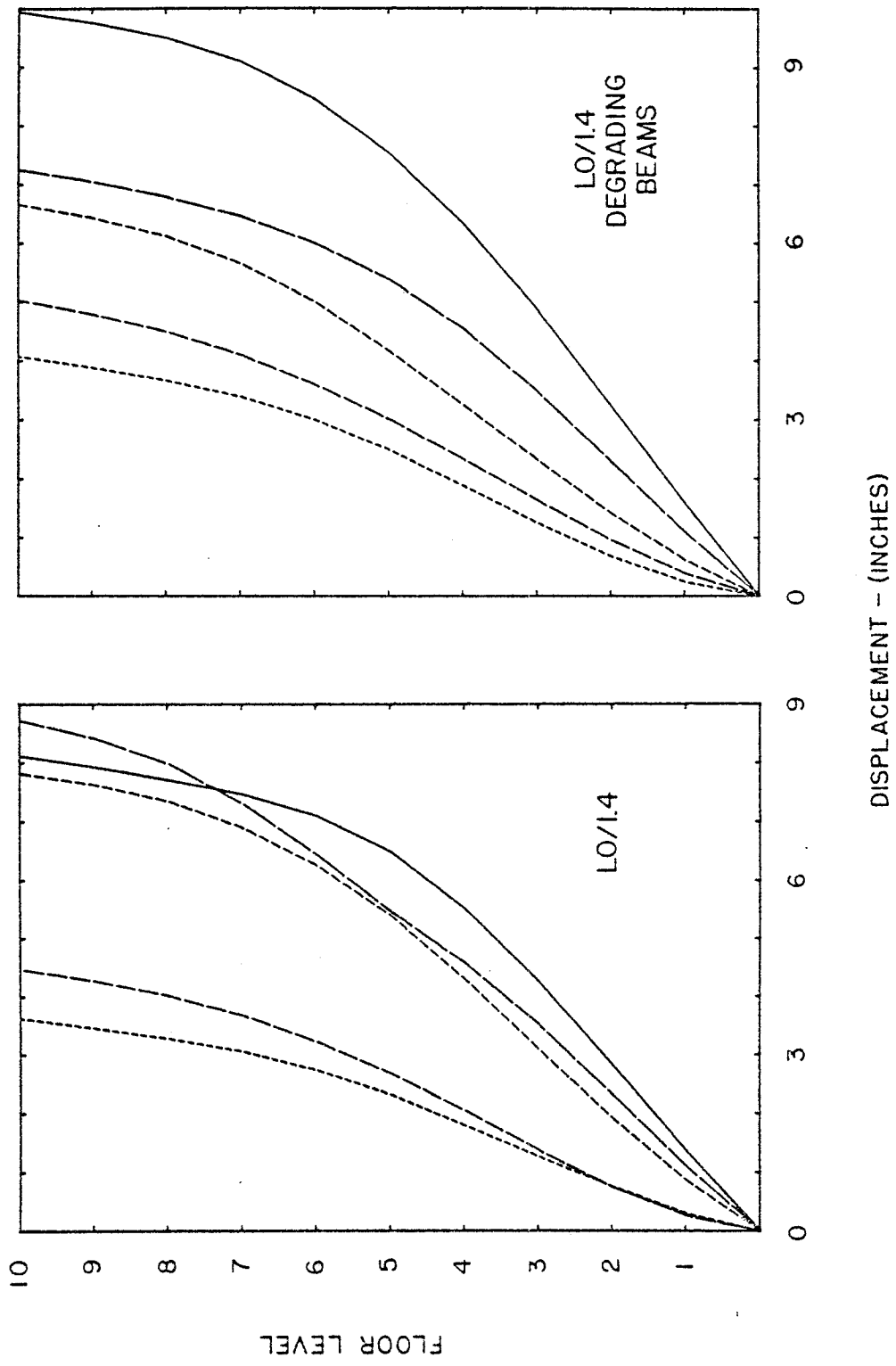


FIG. A-16 LATERAL DISPLACEMENT ENVELOPES
TYPICAL FRAME

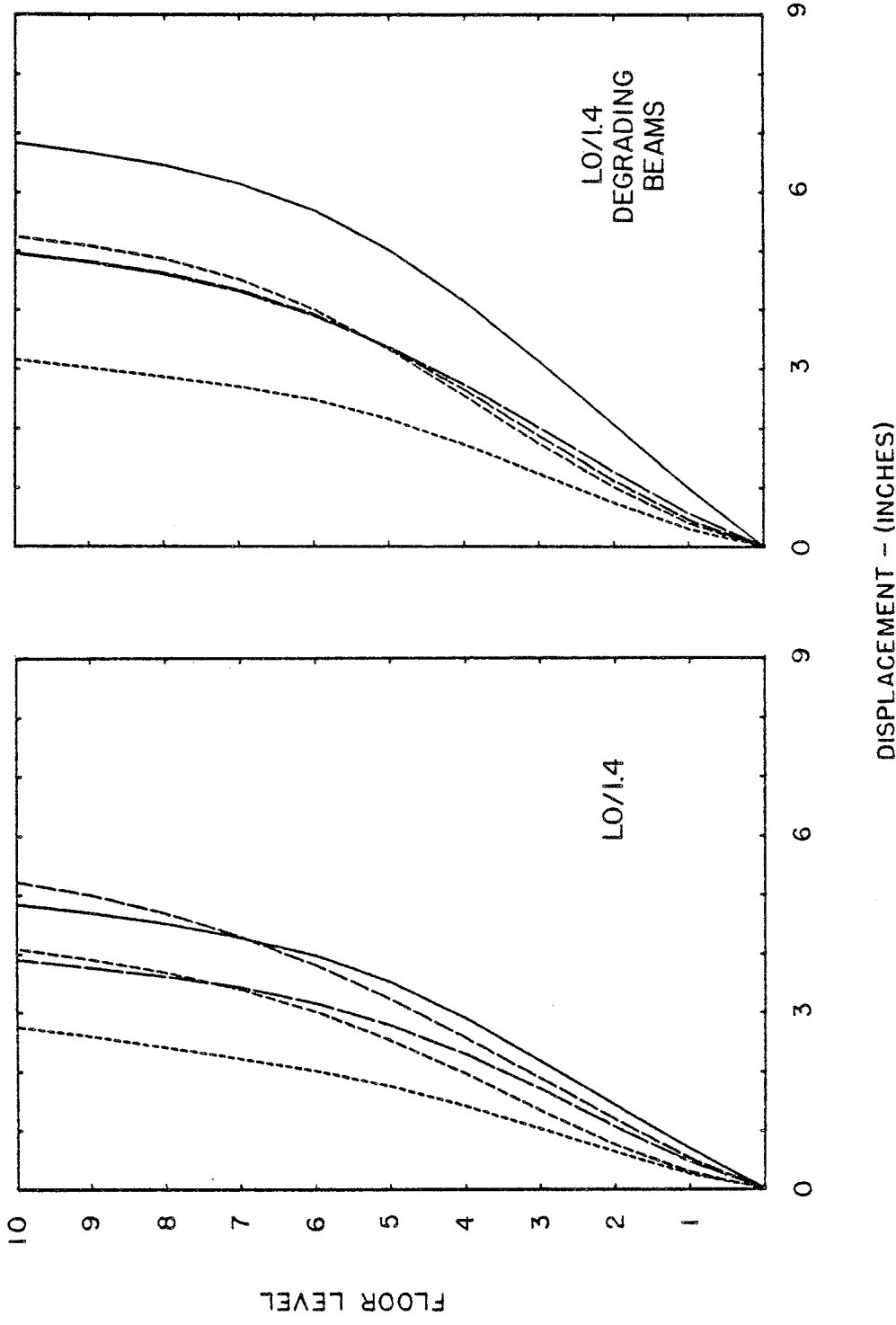


FIG. A-17 LATERAL DISPLACEMENT ENVELOPES
STIFF BEAM FRAME

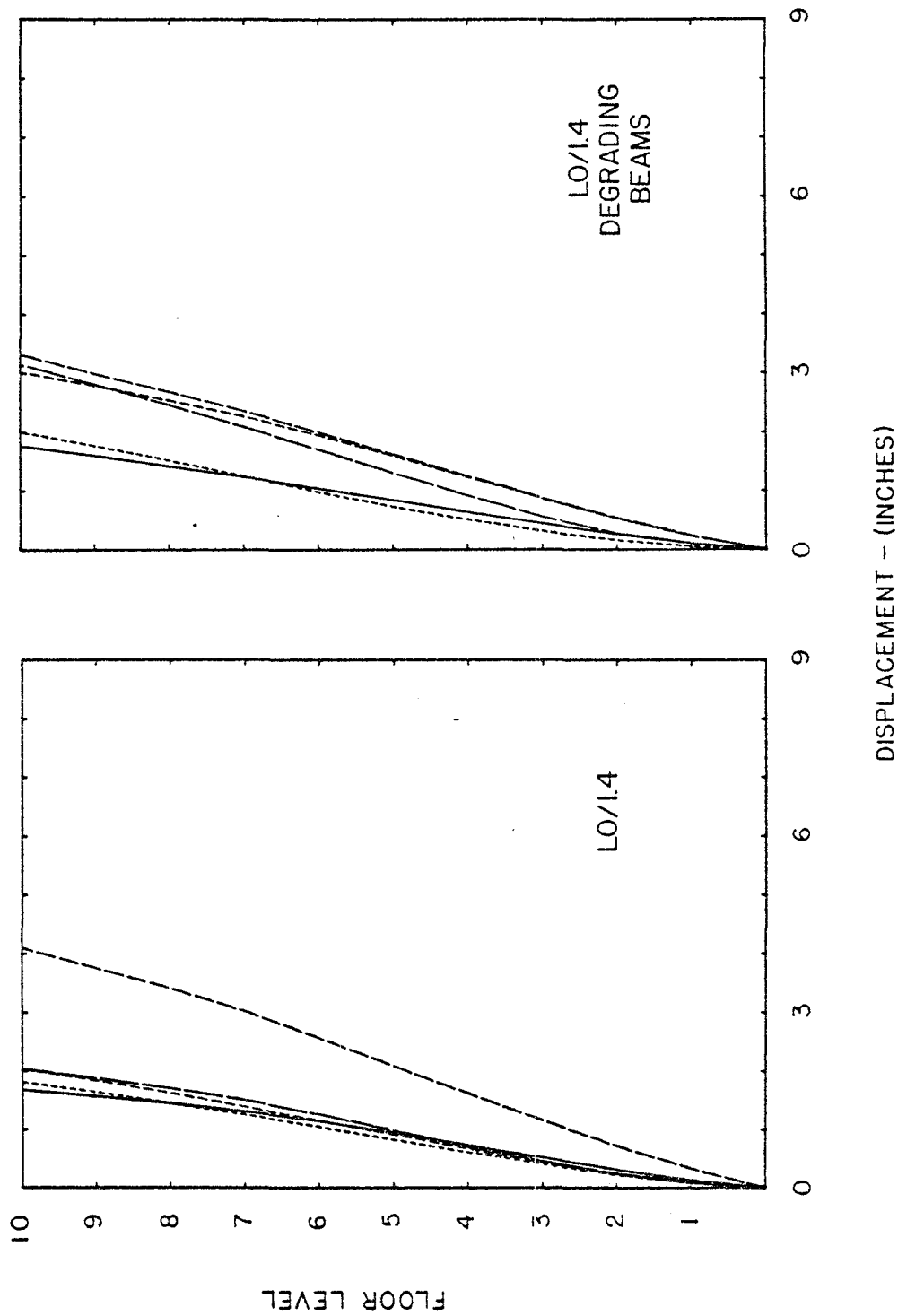


FIG. A-18 LATERAL DISPLACEMENT ENVELOPES
COUPLED WALLS

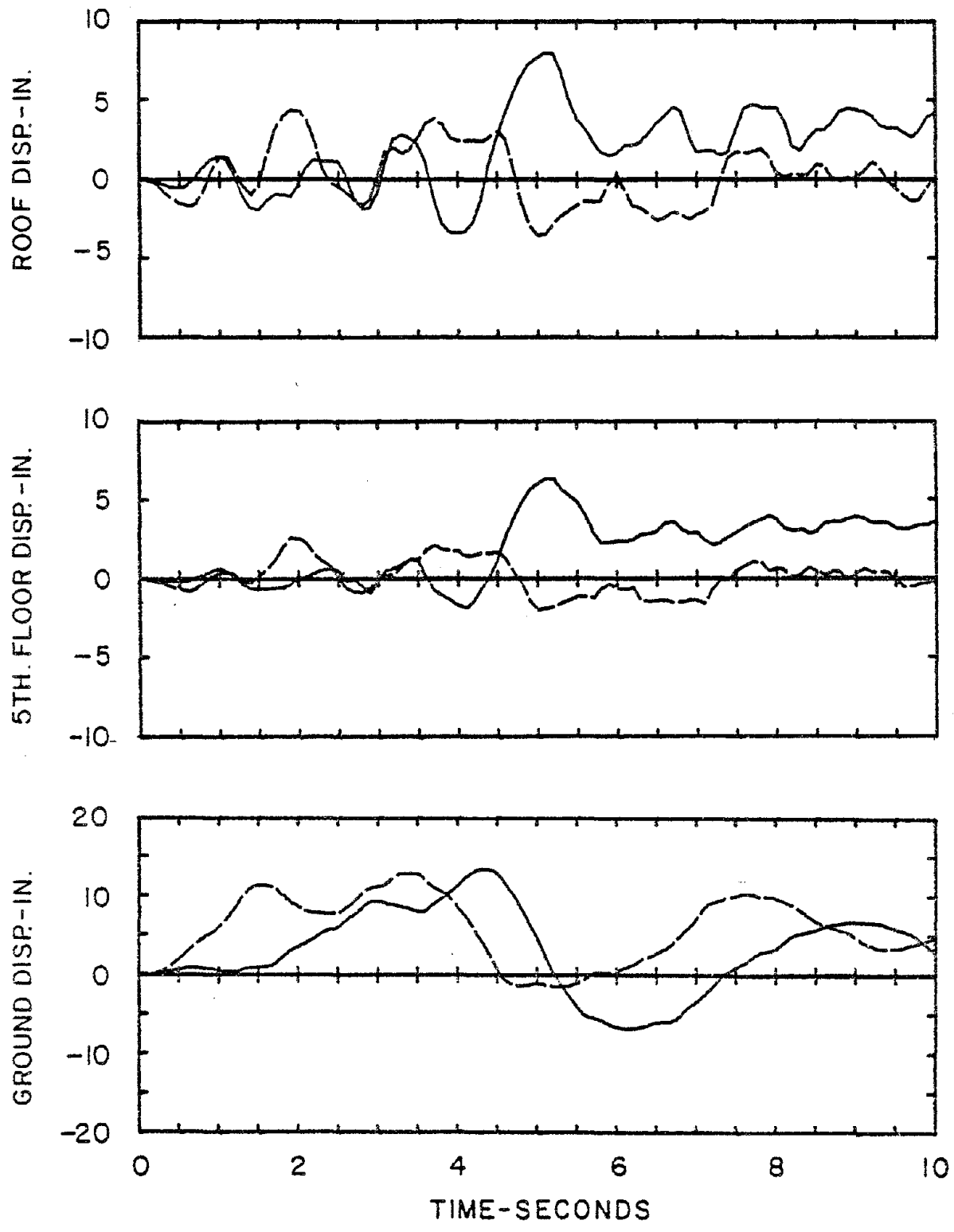


FIG. A-19 ROOF AND 5TH. FLOOR DISPLACEMENT HISTORIES FOR GROUND MOTIONS 1 & 3. TYPICAL FRAME - LO/1.4

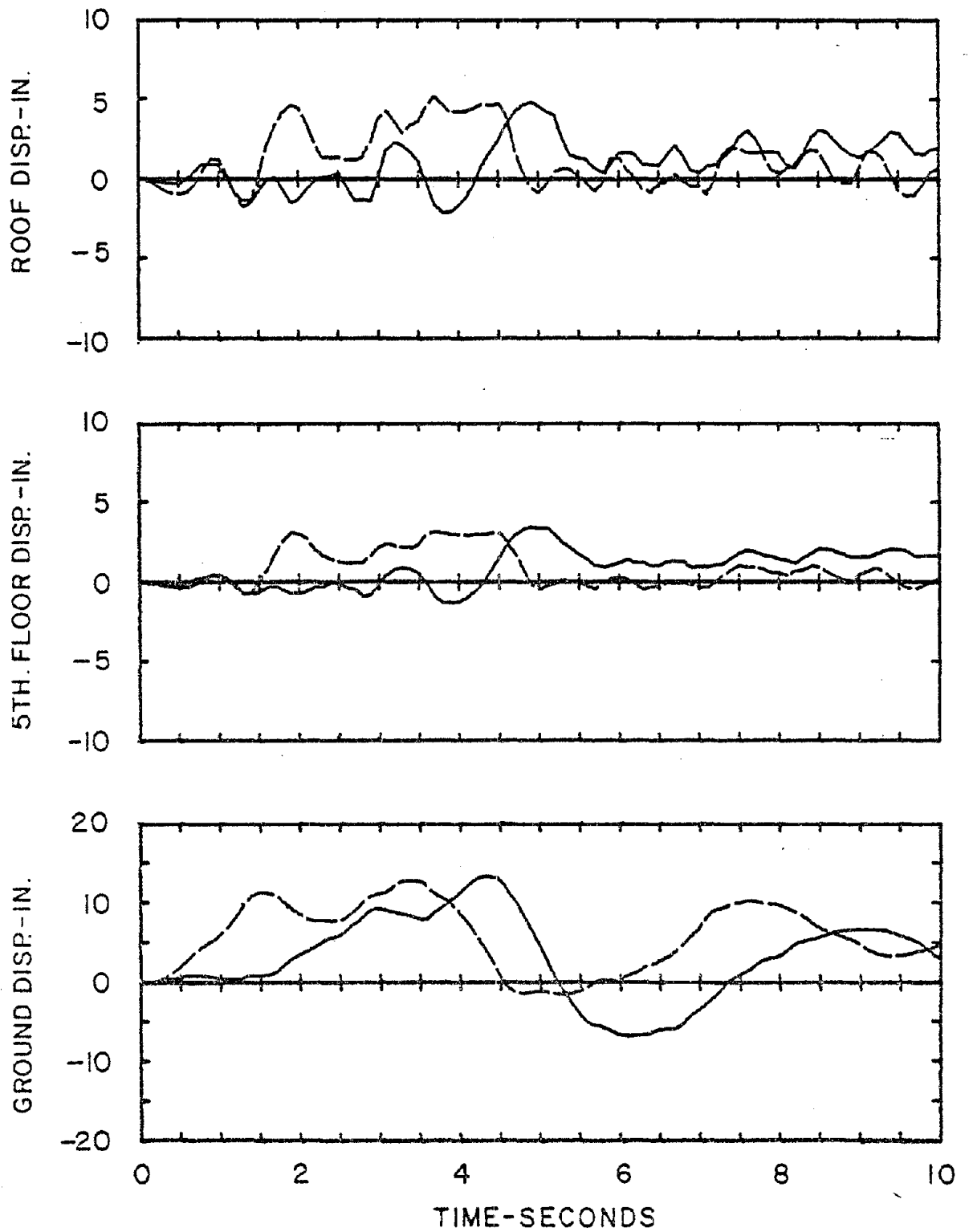


FIG. A-20 ROOF AND 5TH. FLOOR DISPLACEMENT HISTORIES FOR GROUND MOTIONS 1 & 3. STIFF BEAM FRAME -LO/1.4

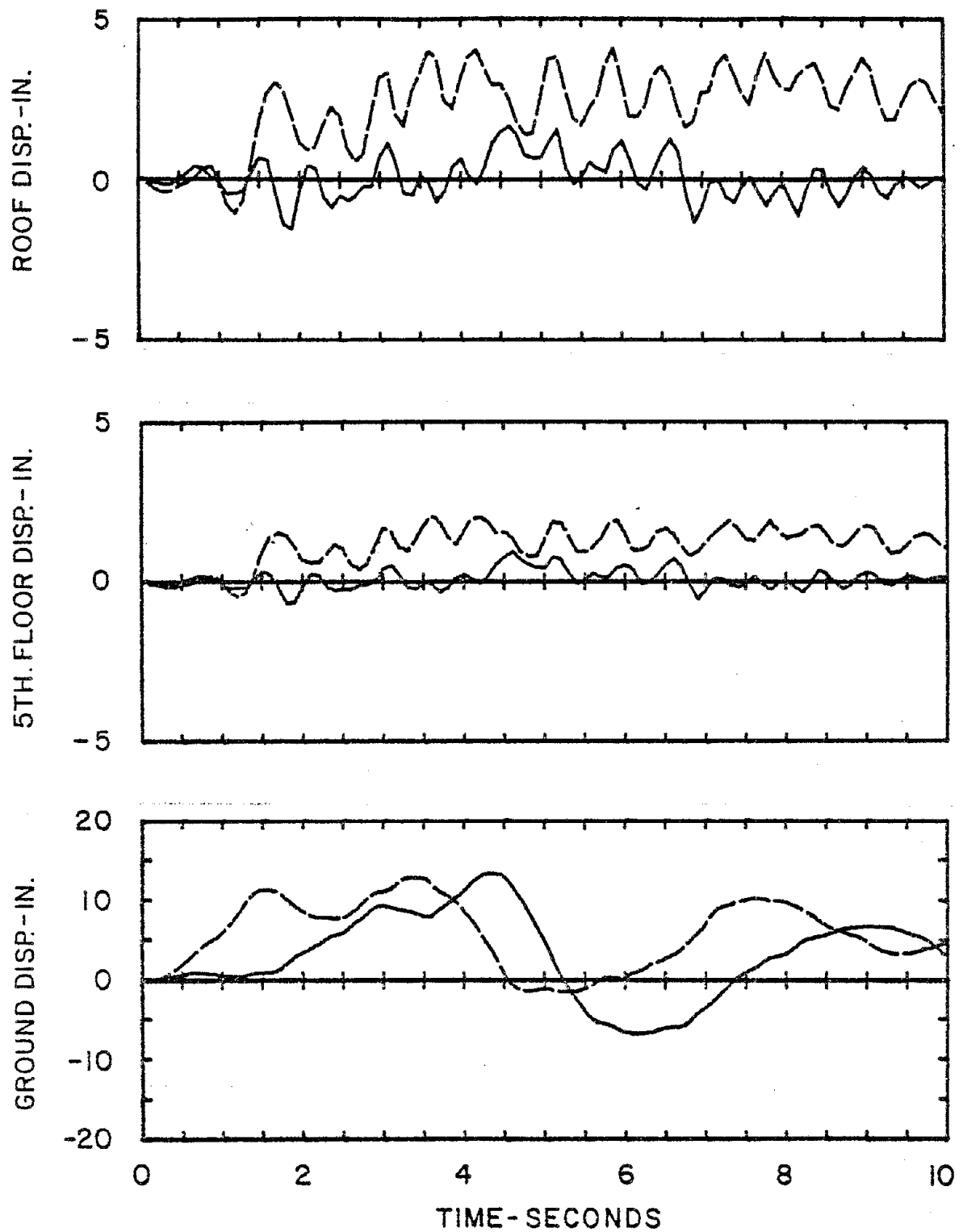


FIG. A.21 ROOF AND 5TH. FLOOR DISPLACEMENT HISTORIES FOR GROUND MOTIONS 1 & 3. COUPLED WALLS - LO/1.4

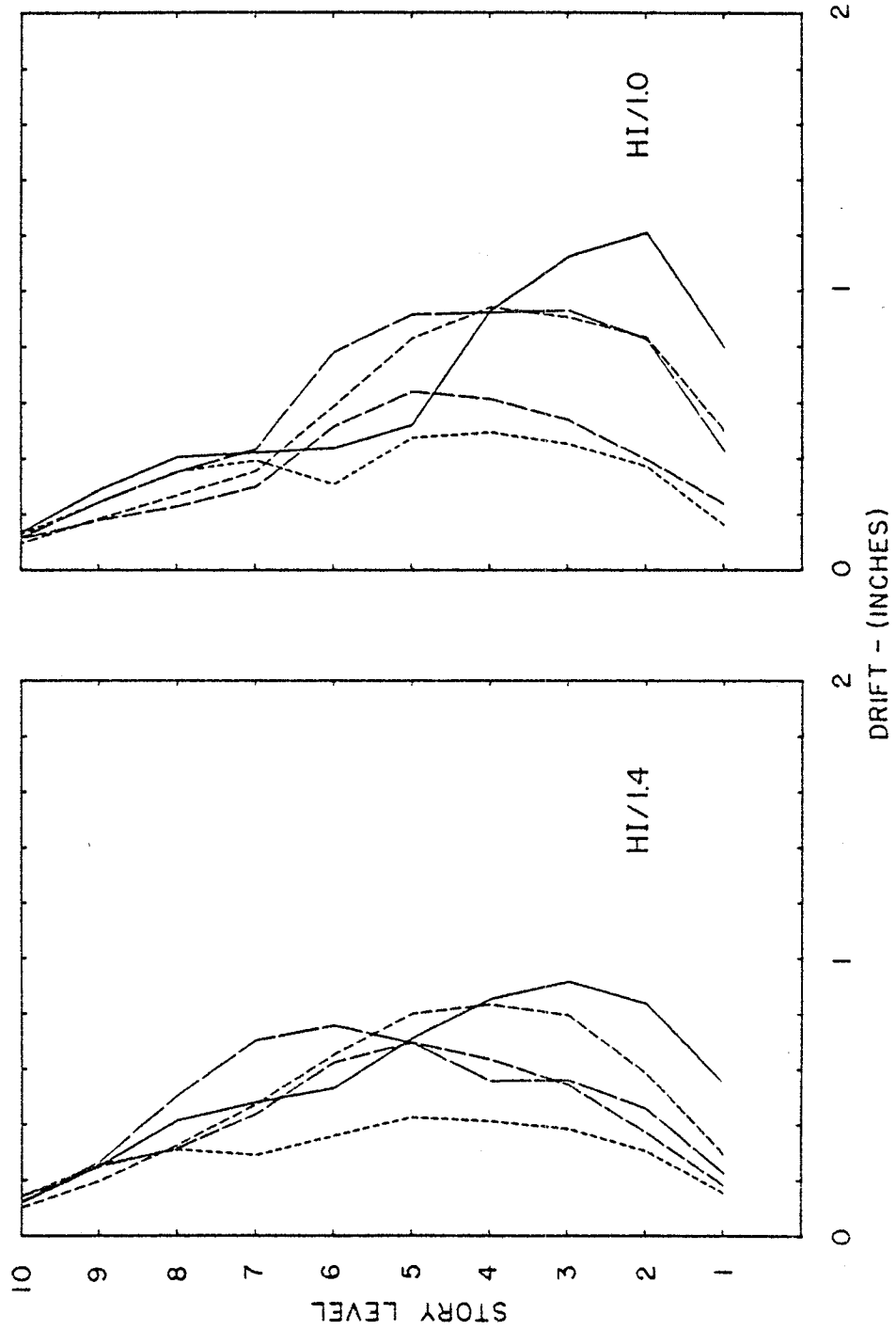


FIG. A-22 INTERSTORY DRIFT ENVELOPES
TYPICAL FRAME

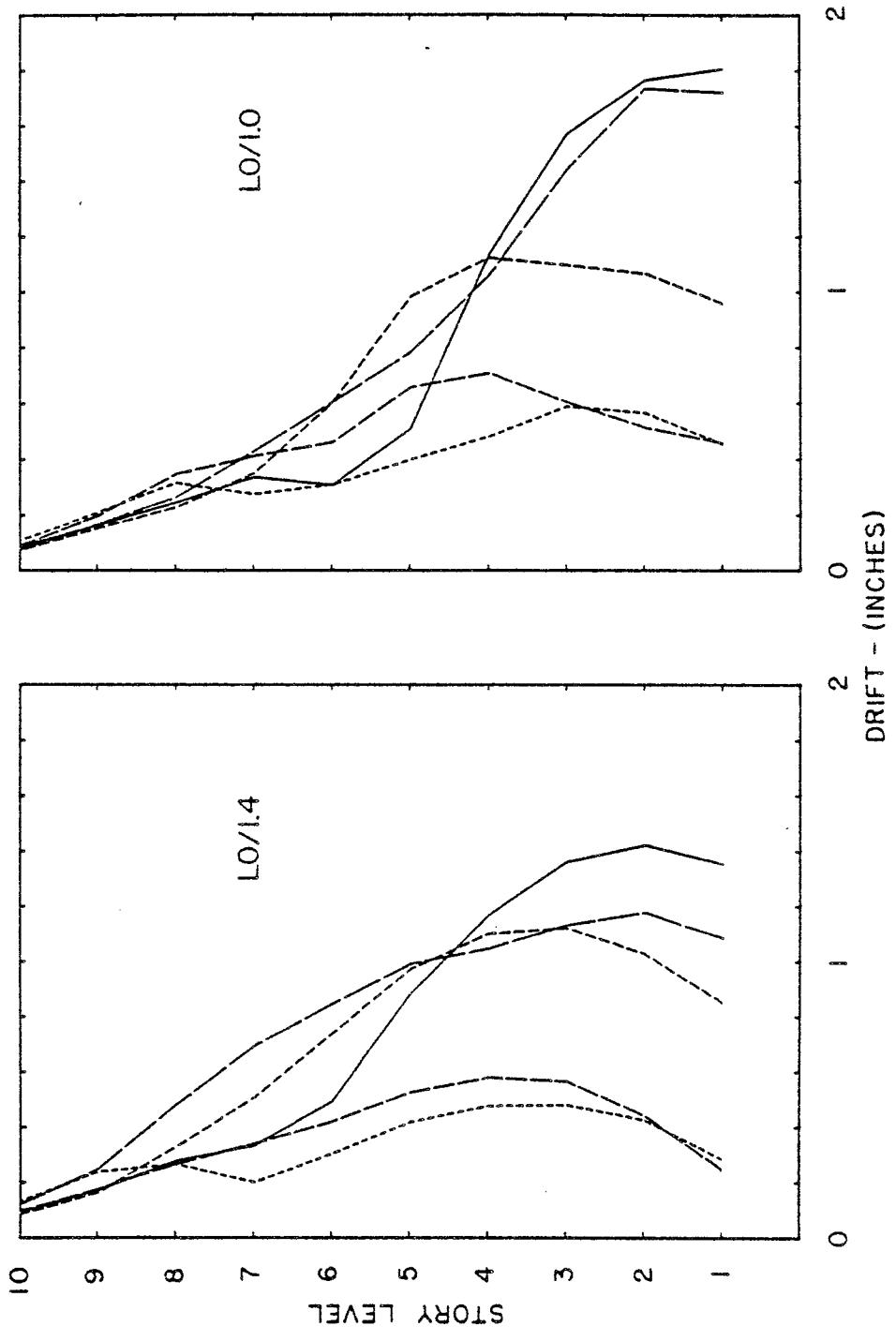


FIG. A-23 INTERSTORY DRIFT ENVELOPES
TYPICAL FRAME

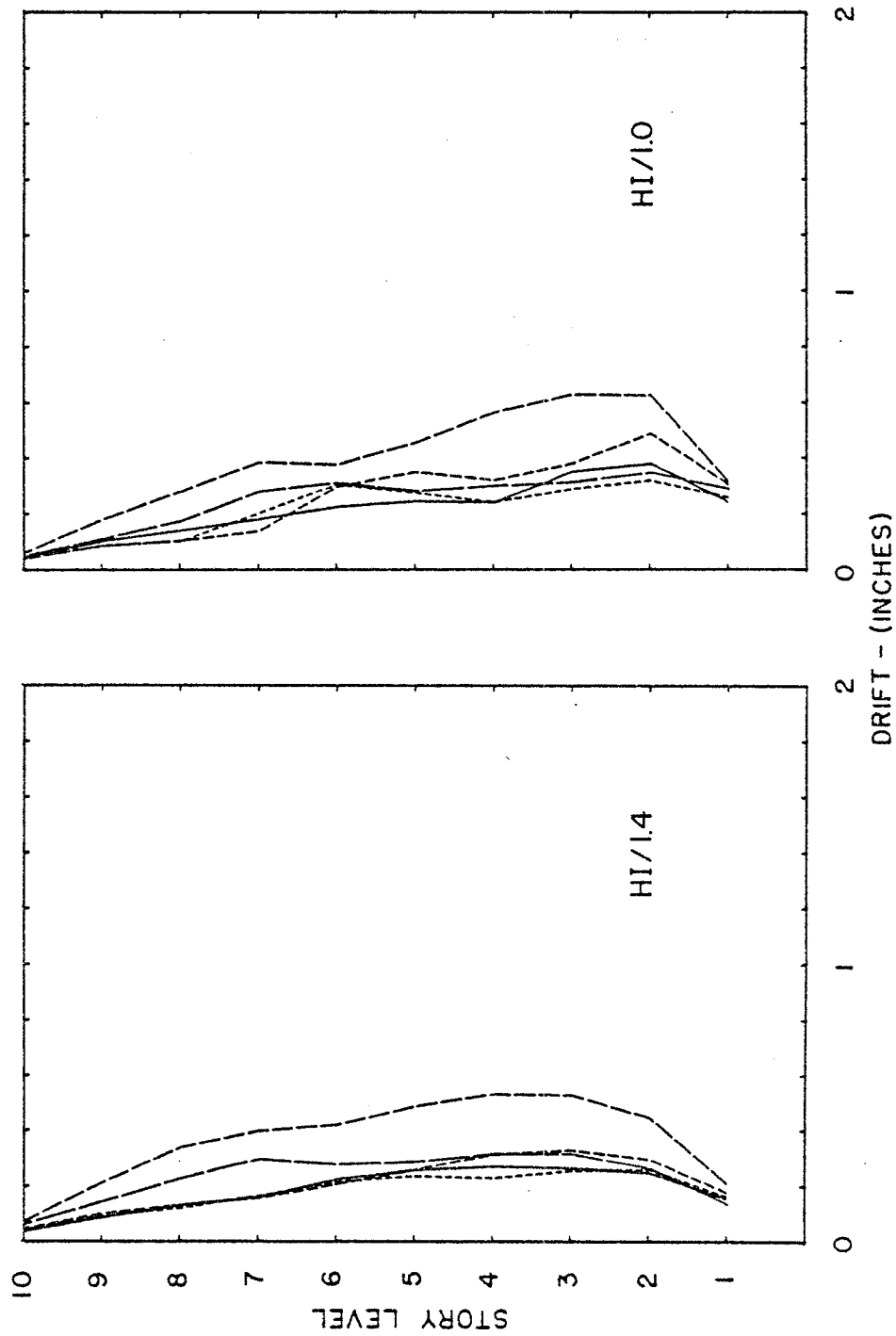


FIG. A-24 INTERSTORY DRIFT ENVELOPES
STIFF BEAM FRAME

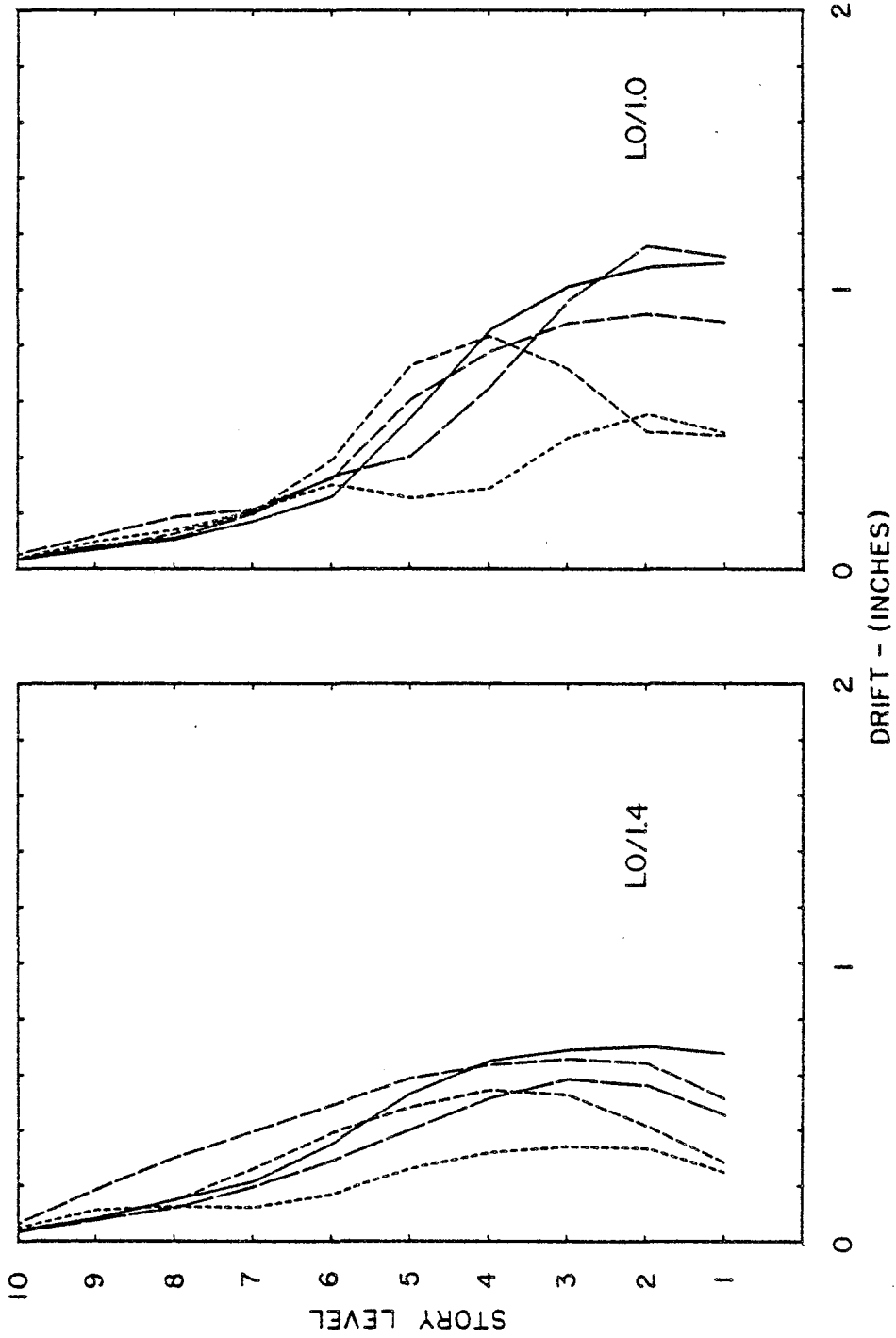


FIG. A-25 INTERSTORY DRIFT ENVELOPES
STIFF BEAM FRAME

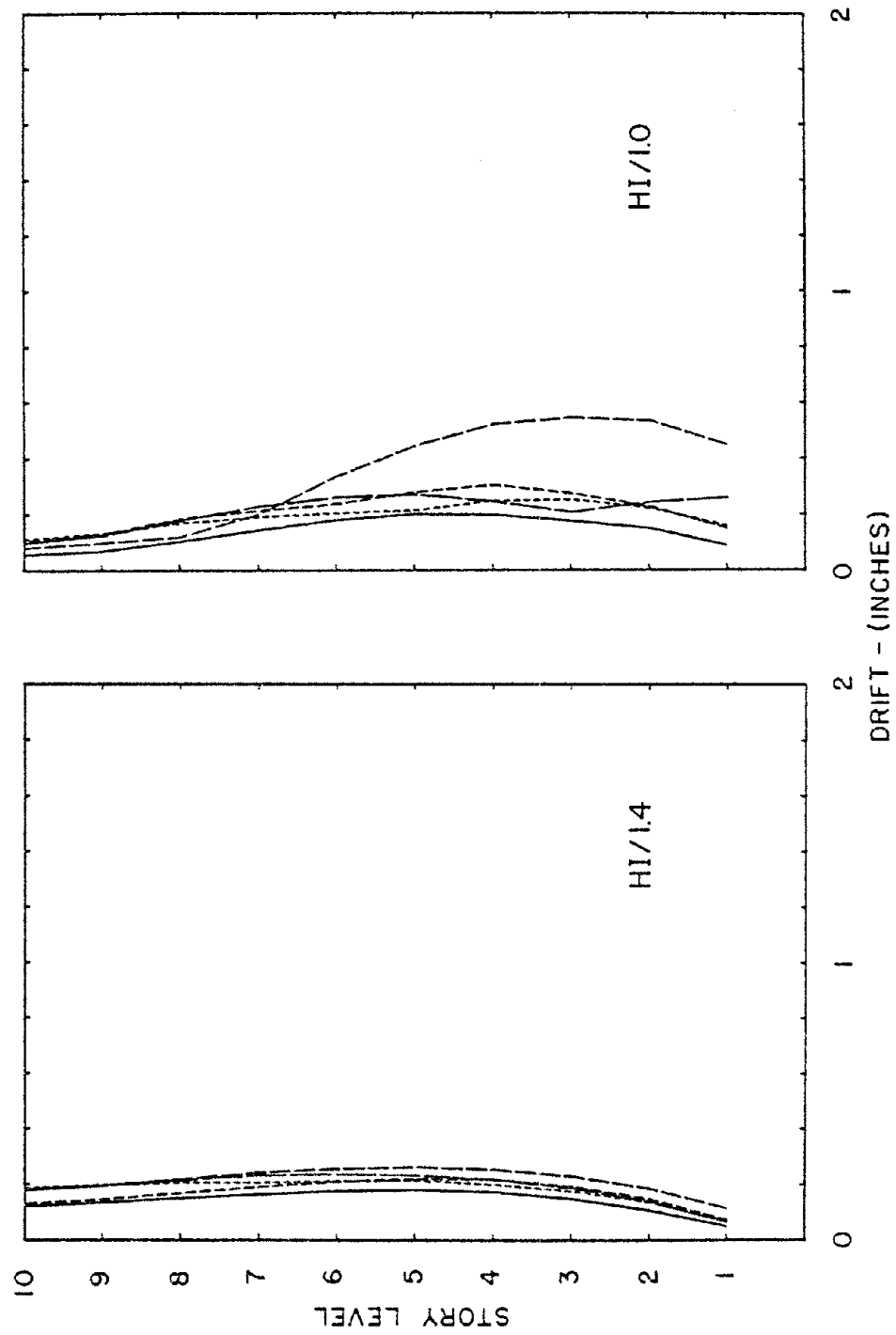


FIG. A-26 INTERSTORY DRIFT ENVELOPES
COUPLED WALLS

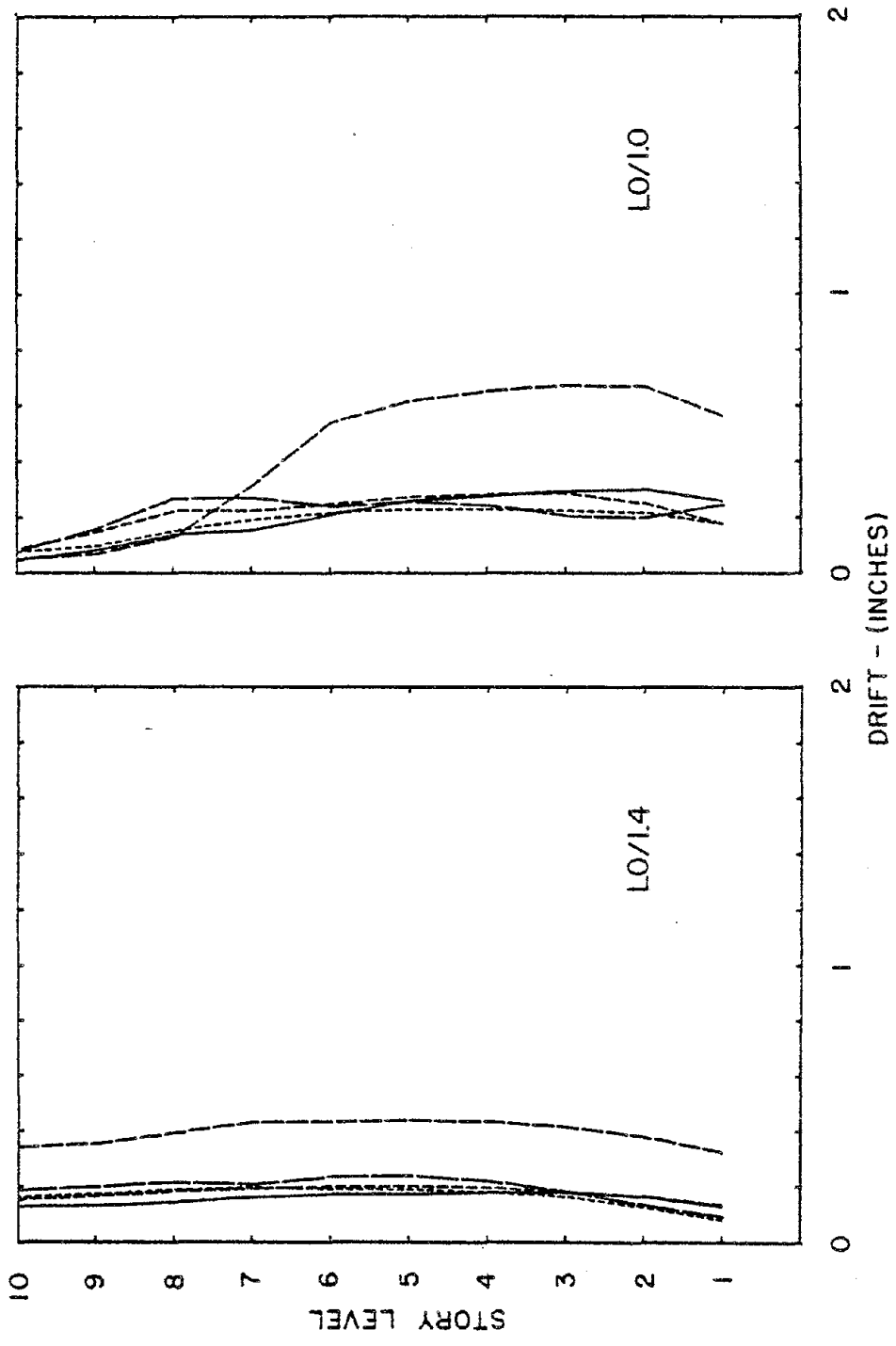


FIG. A-27 INTERSTORY DRIFT ENVELOPES
COUPLED WALLS

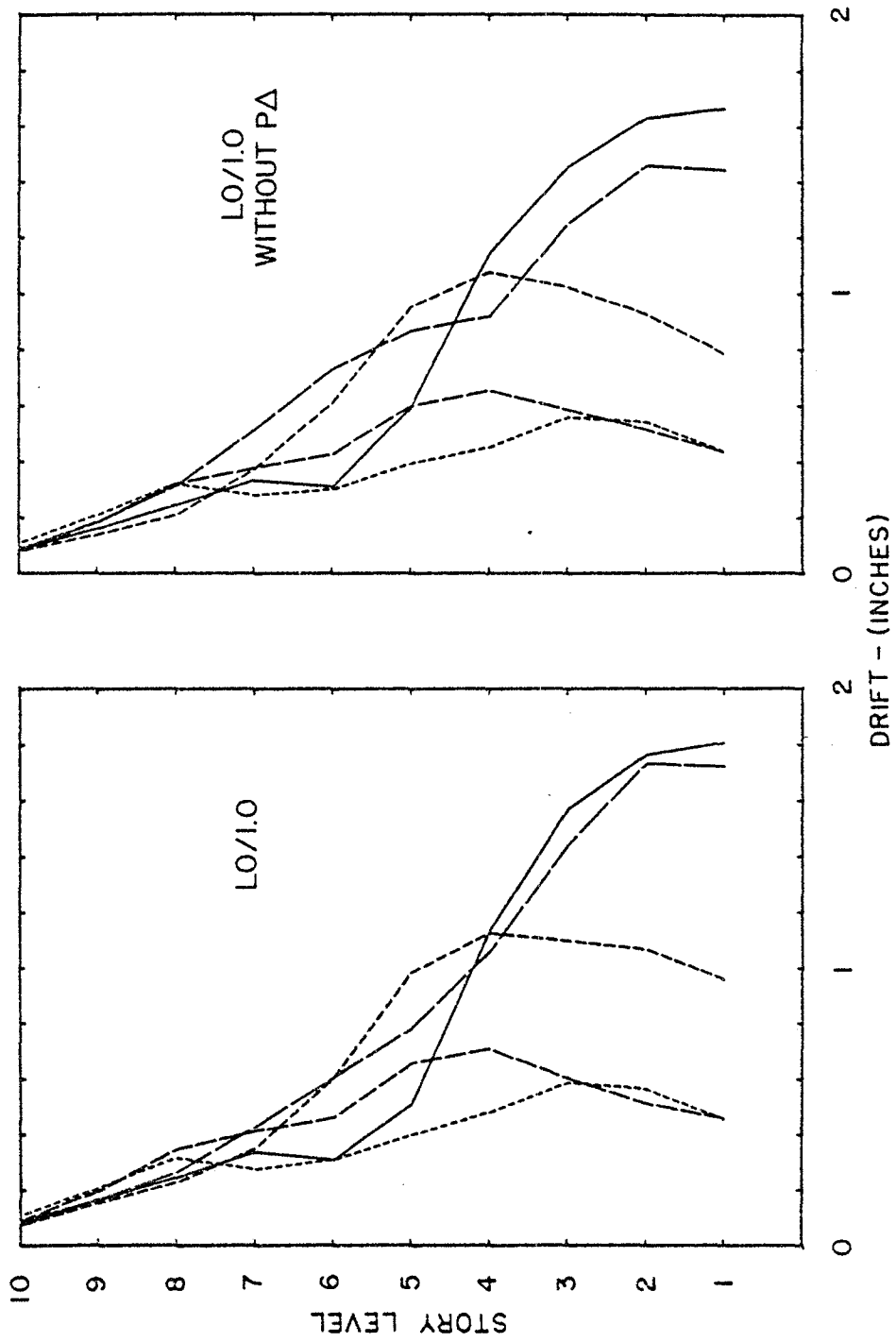


FIG. A-28 INTERSTORY DRIFT ENVELOPES
TYPICAL FRAME

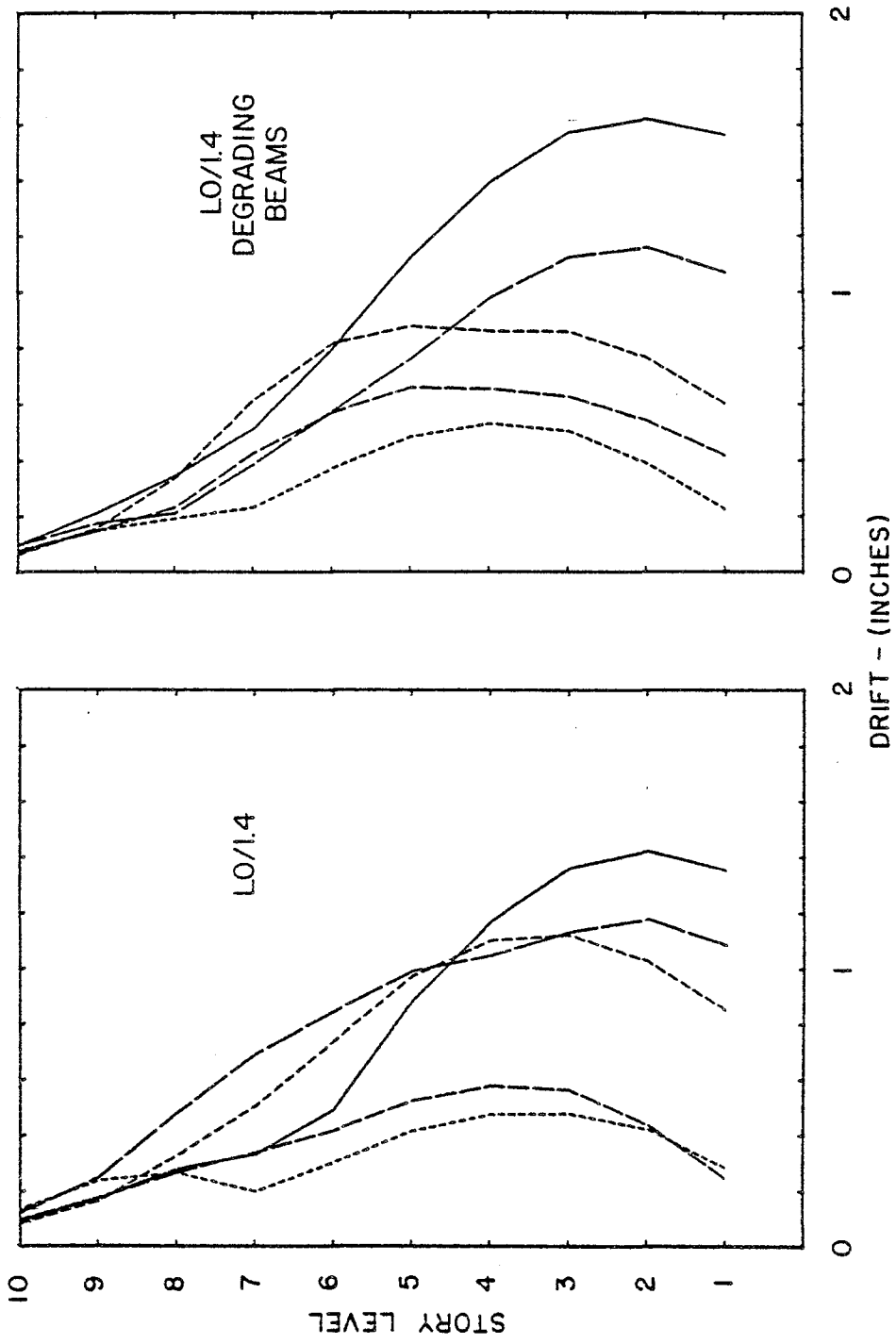


FIG. A-29 INTERSTORY DRIFT ENVELOPES
TYPICAL FRAME

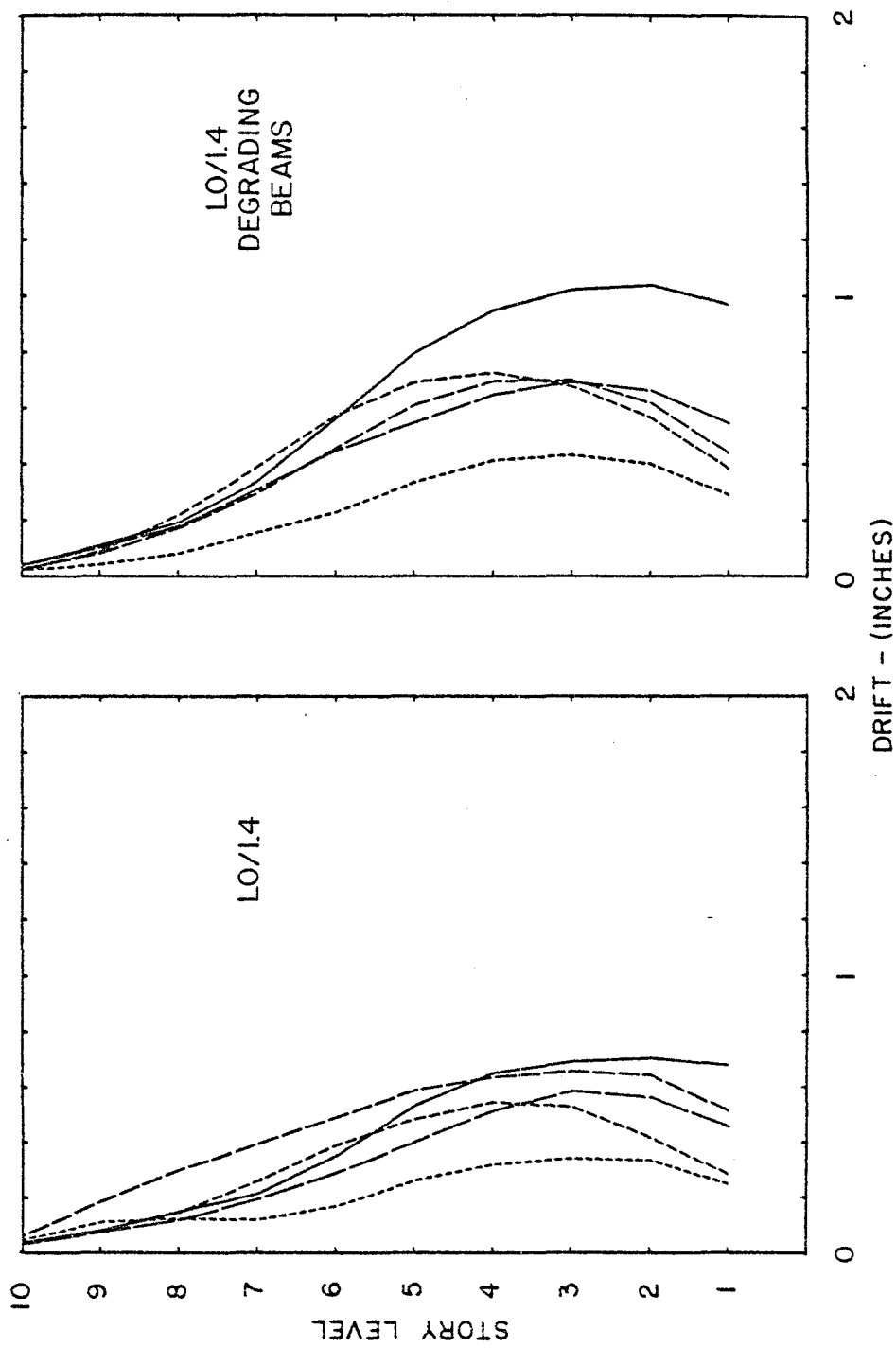


FIG. A-30 INTERSTORY DRIFT ENVELOPES
STIFF BEAM FRAME

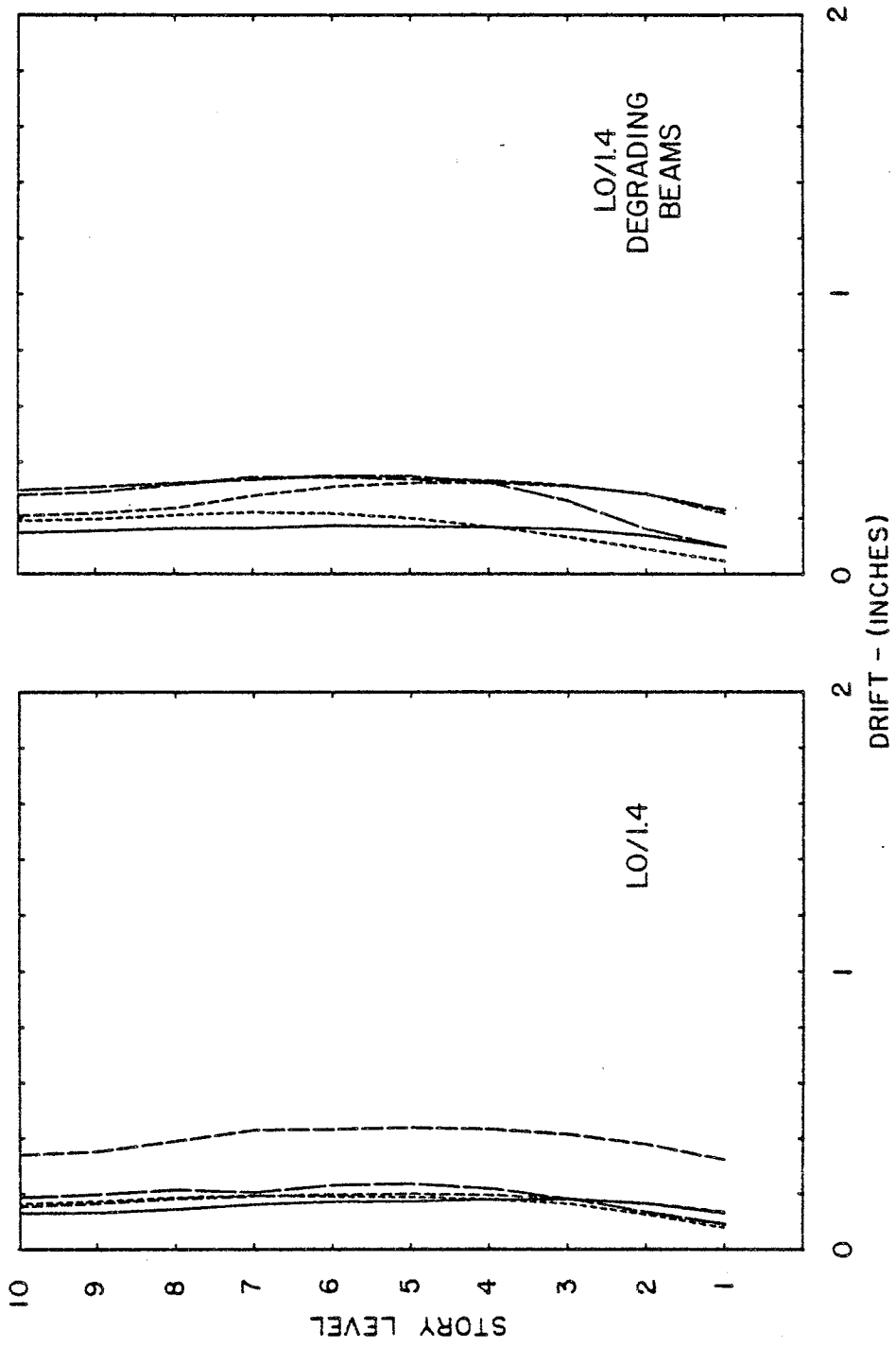


FIG. A-31 INTERSTORY DRIFT ENVELOPES
COUPLED WALLS

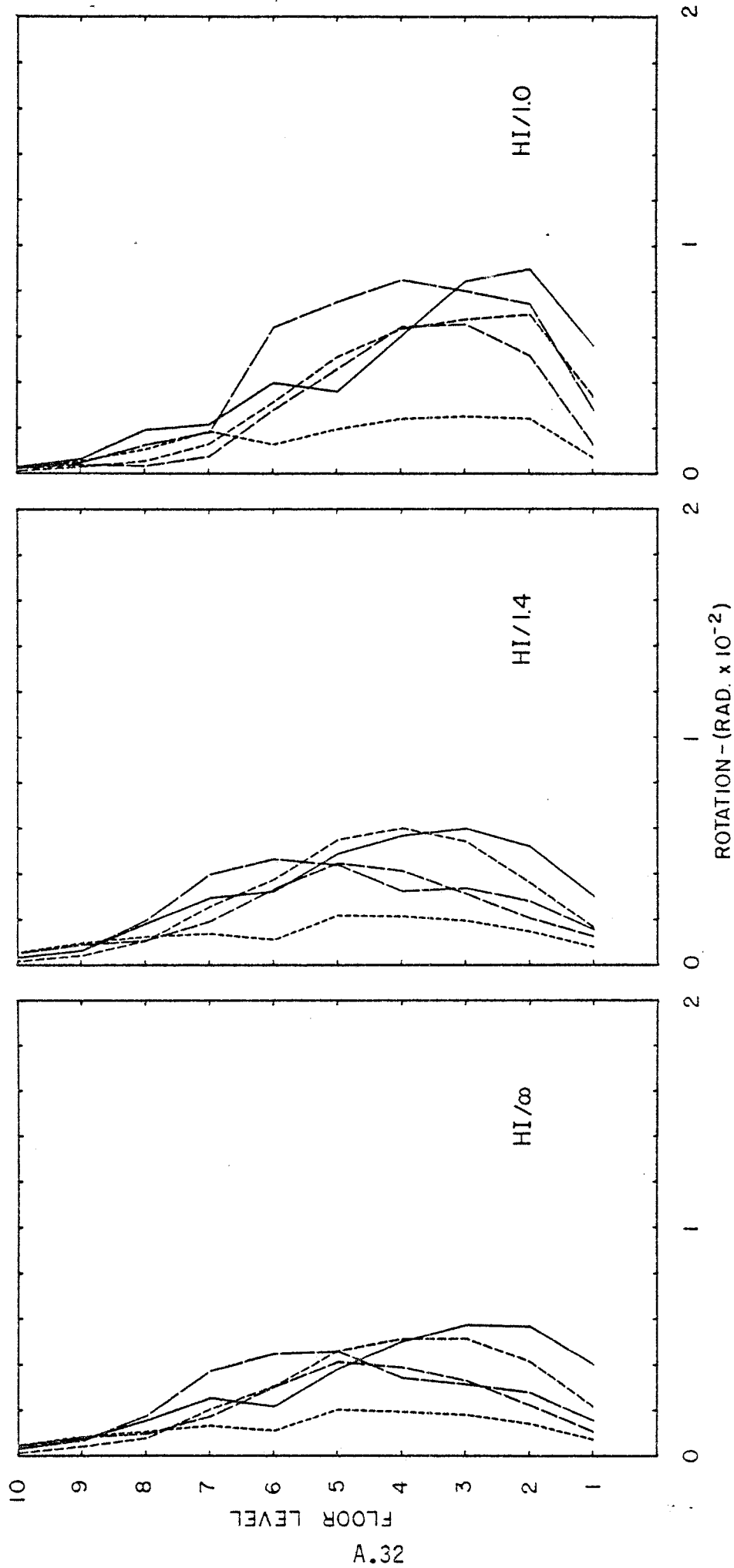


FIG. A-32 MAXIMUM BEAM PLASTIC HINGE ROTATIONS
TYPICAL FRAME

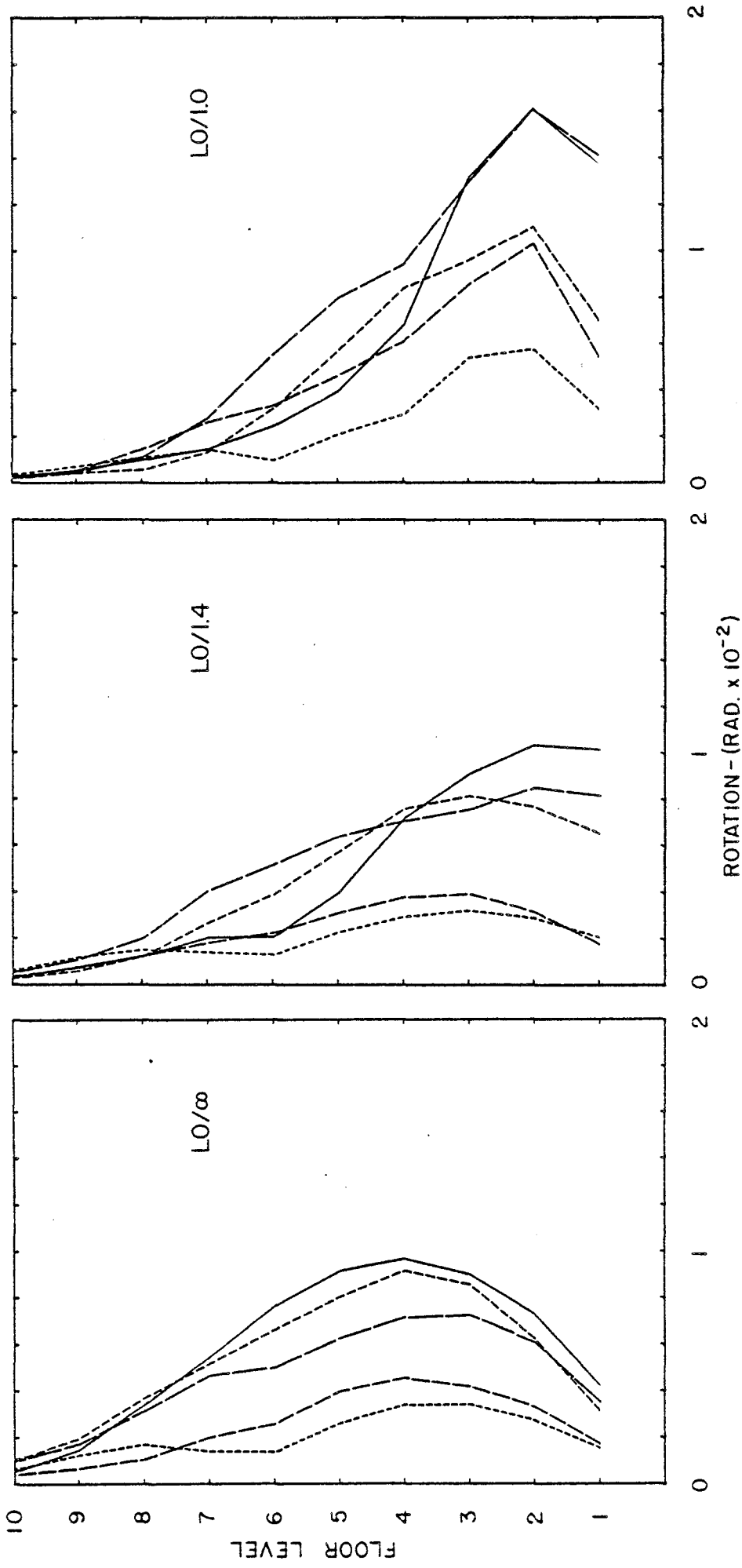


FIG. A-33 MAXIMUM BEAM PLASTIC HINGE ROTATIONS
TYPICAL FRAME

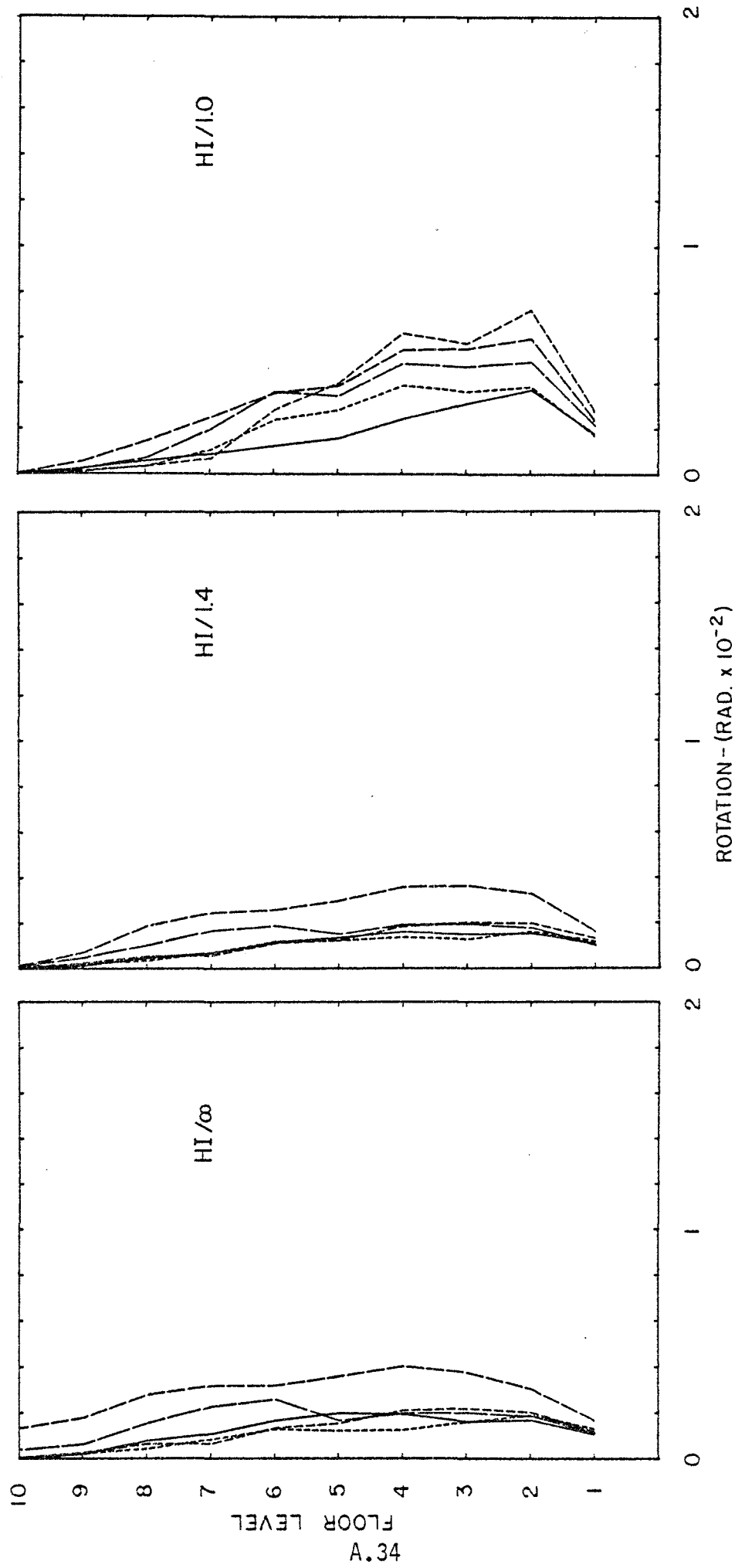


FIG. A-34 MAXIMUM BEAM PLASTIC HINGE ROTATIONS
STIFF BEAM FRAME

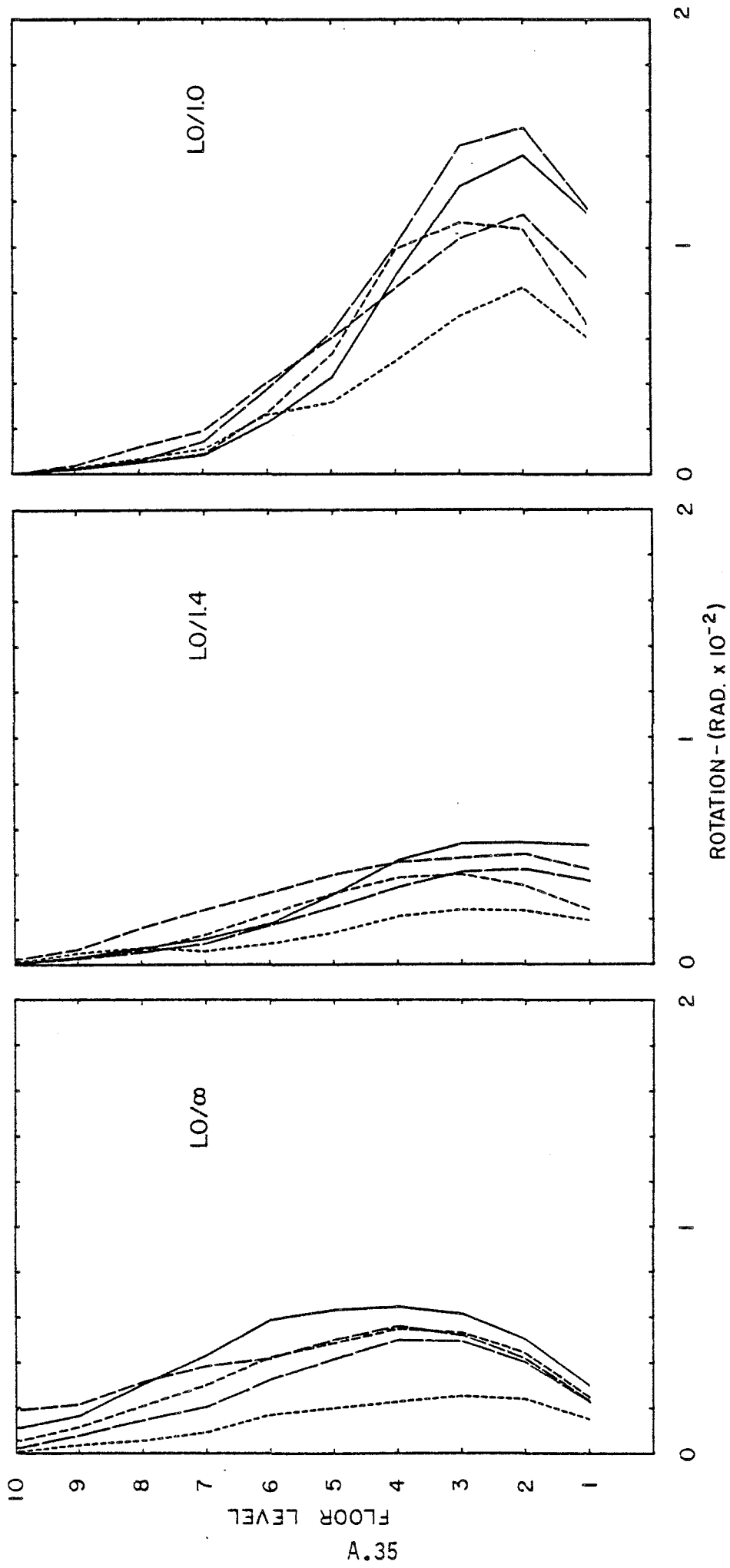


FIG. A-35 MAXIMUM BEAM PLASTIC HINGE ROTATIONS
STIFF BEAM FRAME

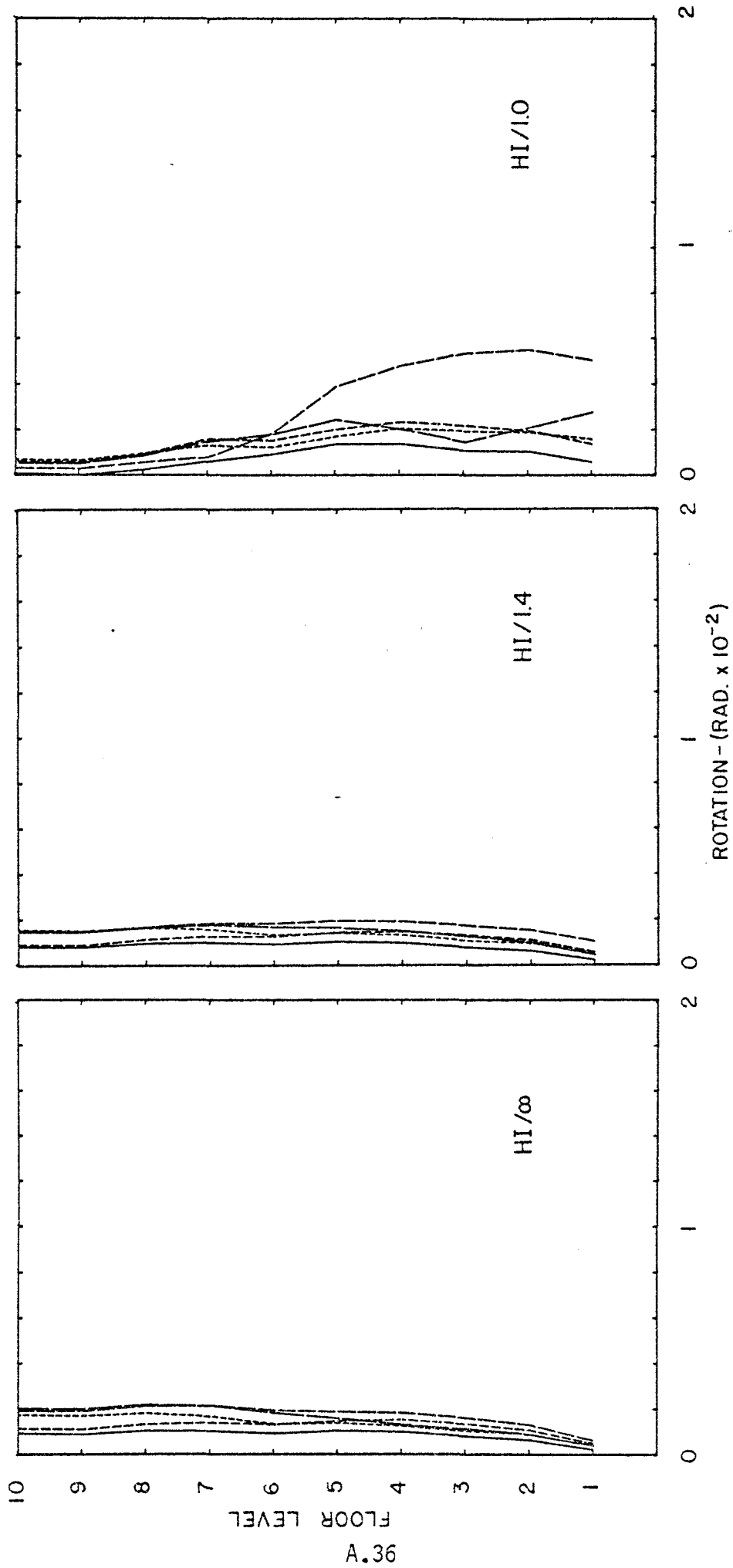


FIG. A-36 MAXIMUM BEAM PLASTIC HINGE ROTATIONS
COUPLED WALLS

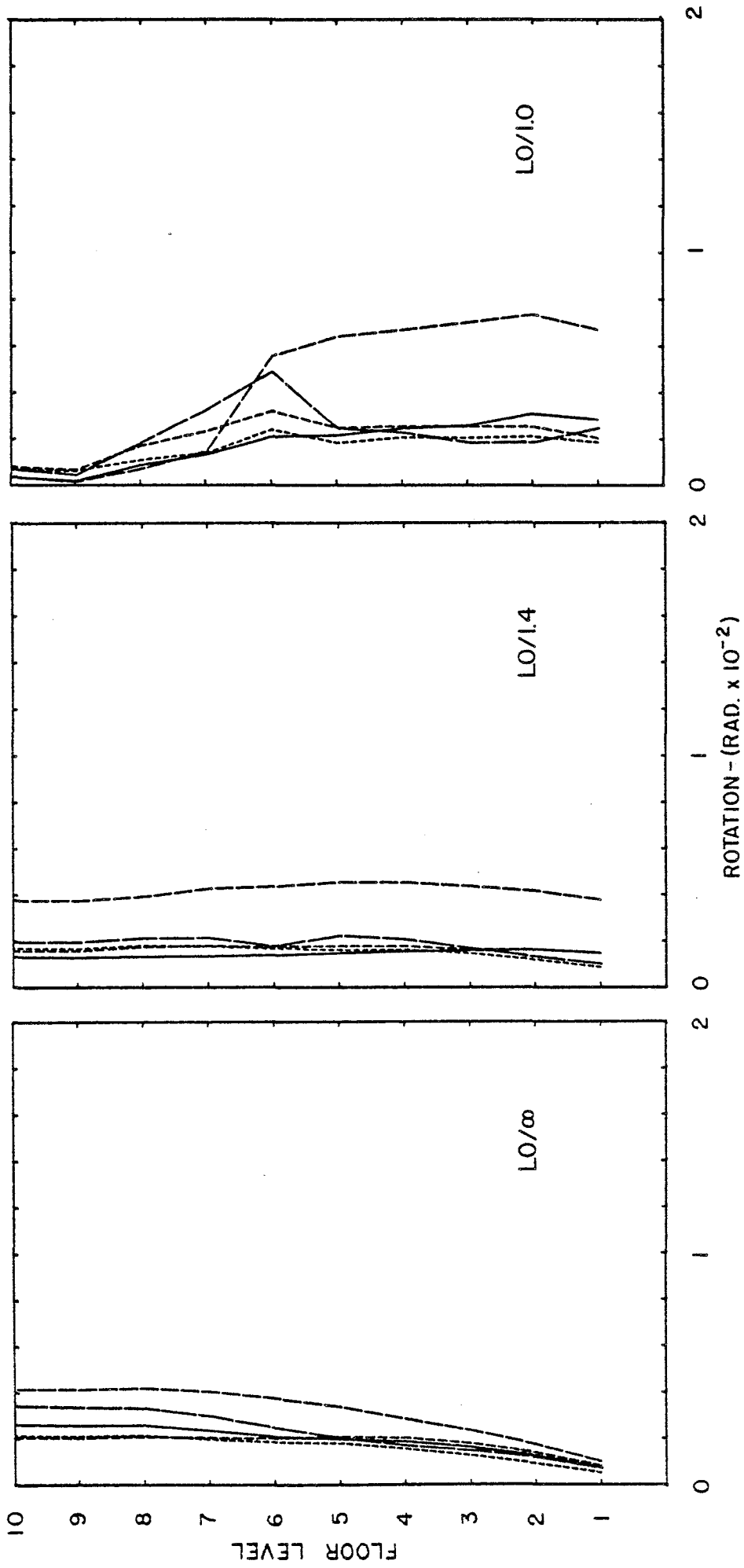


FIG. A-37 MAXIMUM BEAM PLASTIC HINGE ROTATIONS
COUPLED WALLS

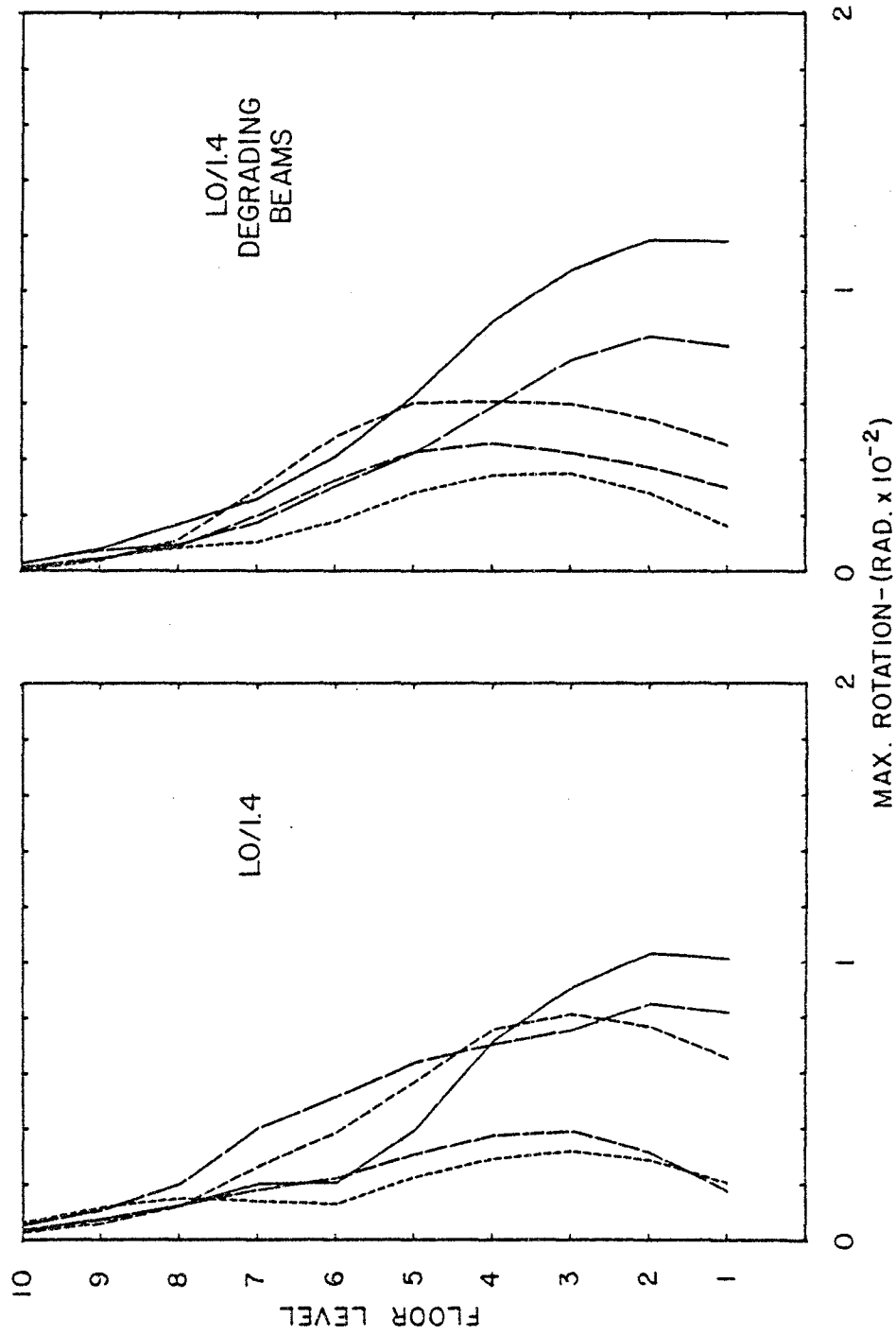


FIG. A-38 MAXIMUM BEAM PLASTIC HINGE ROTATIONS
TYPICAL FRAME

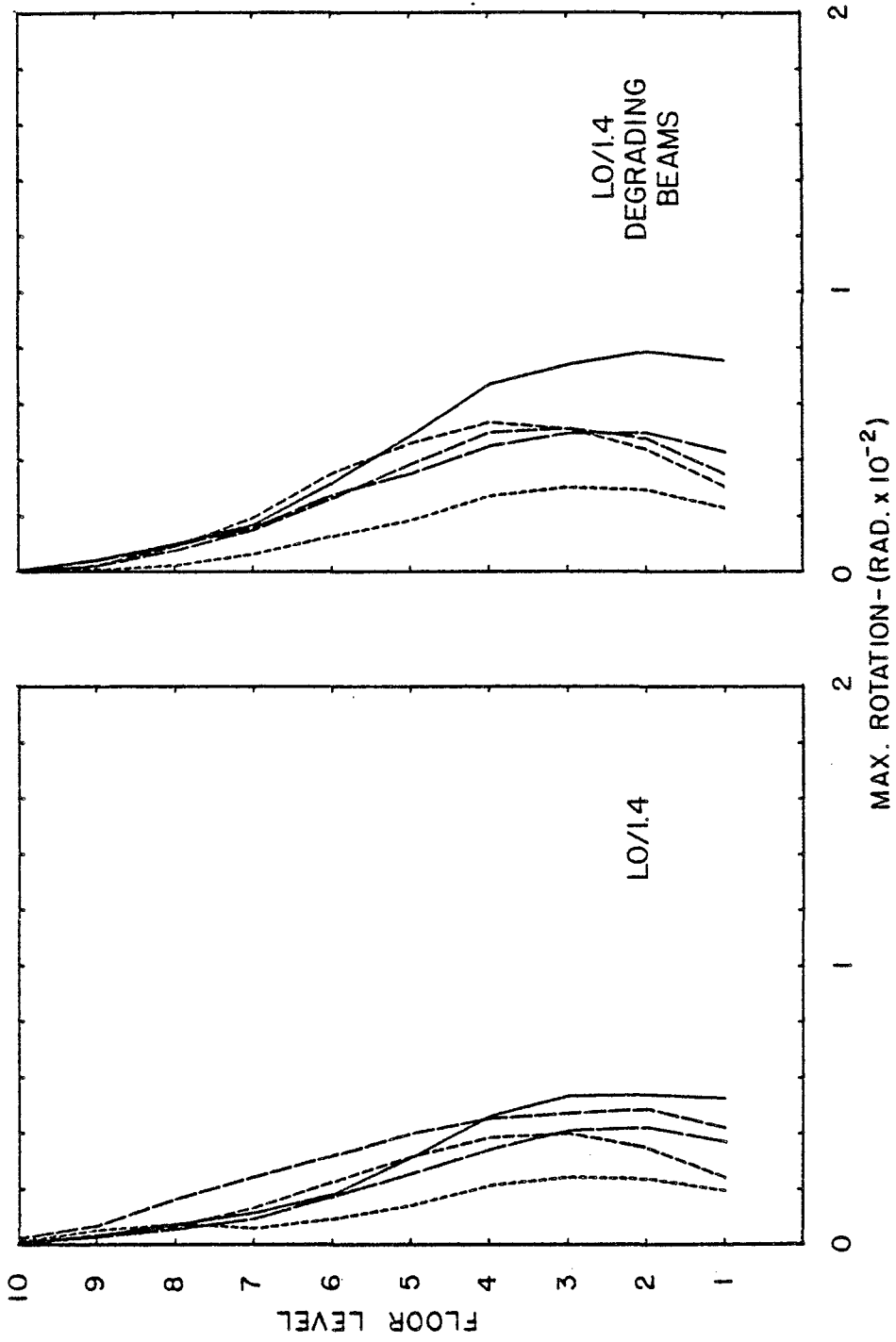


FIG. A-39 MAXIMUM BEAM PLASTIC HINGE ROTATIONS
STIFF BEAM FRAME

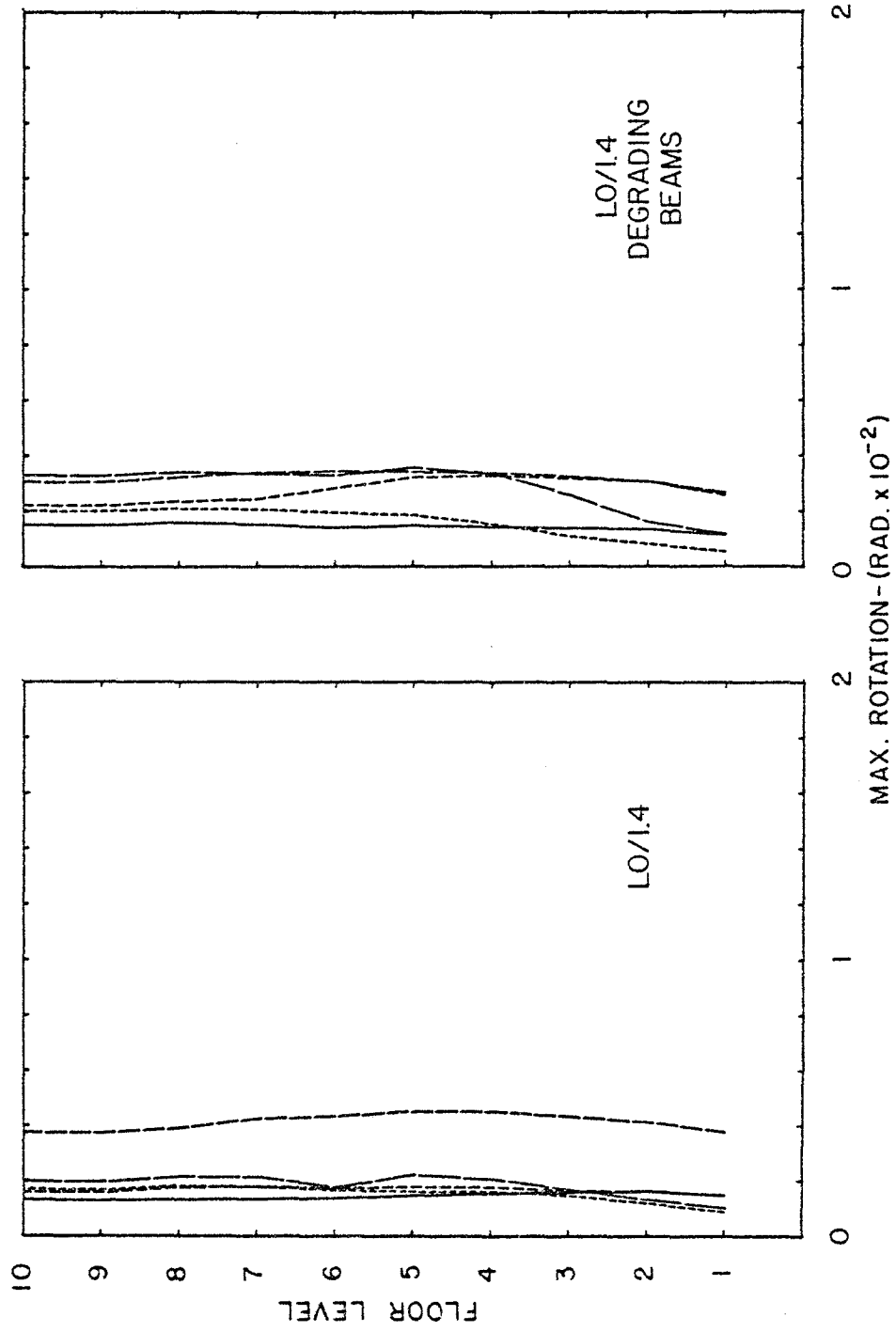


FIG. A-40 MAXIMUM BEAM PLASTIC HINGE ROTATIONS
COUPLED WALLS

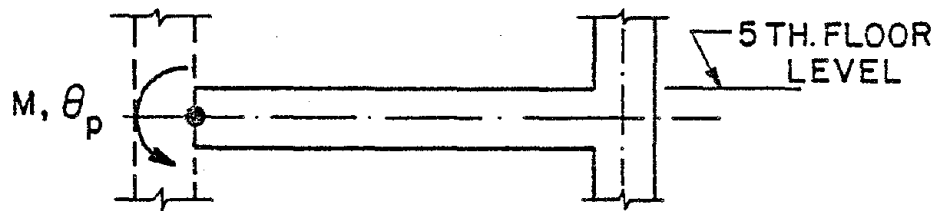
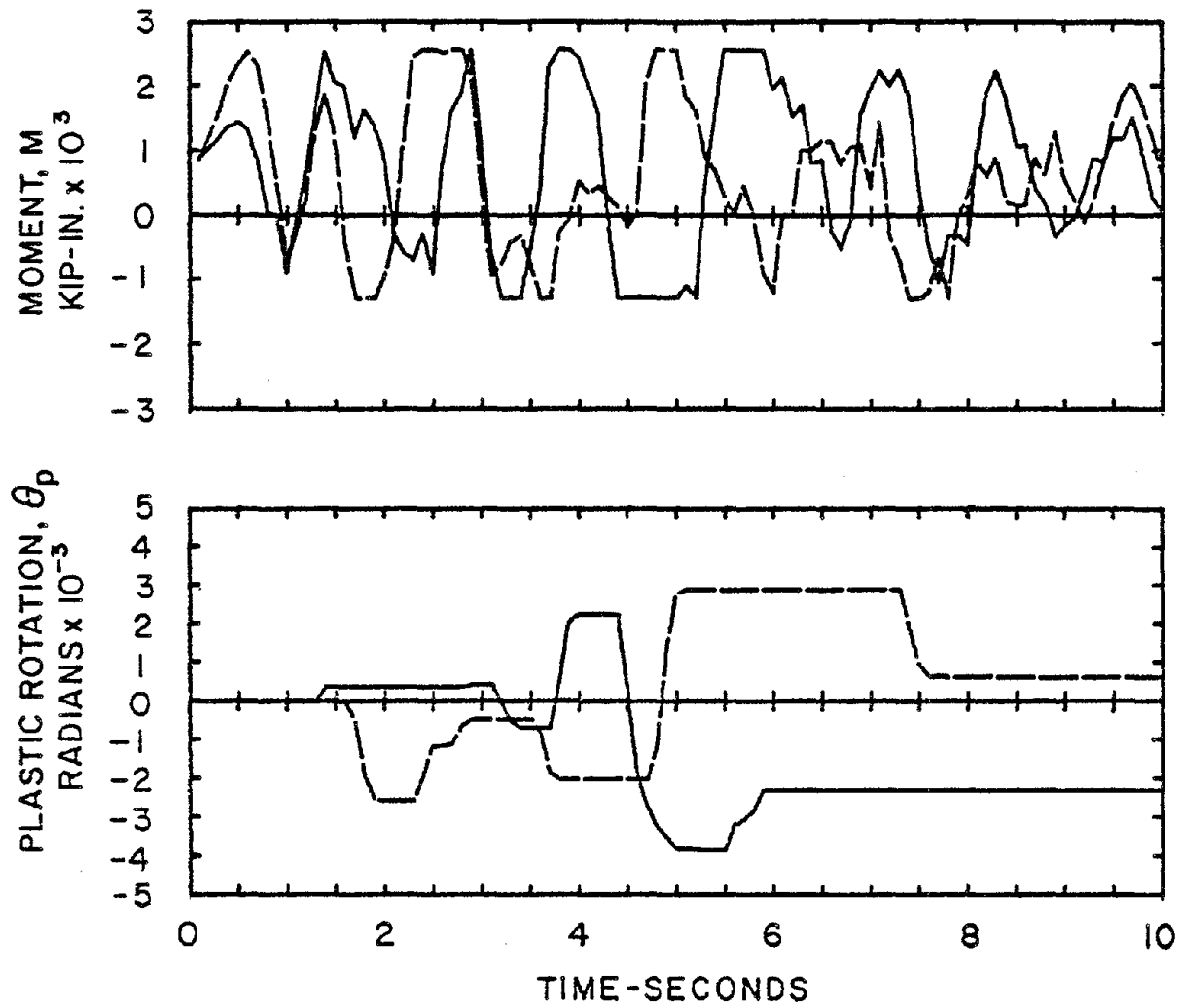


FIG. A-41 5TH. FLOOR BEAM MOMENT AND PLASTIC ROTATION HISTORIES FOR GROUND MOTIONS 1 & 3. TYPICAL FRAME - LO/1.4

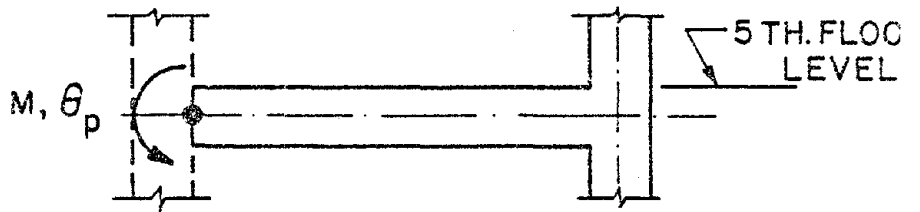
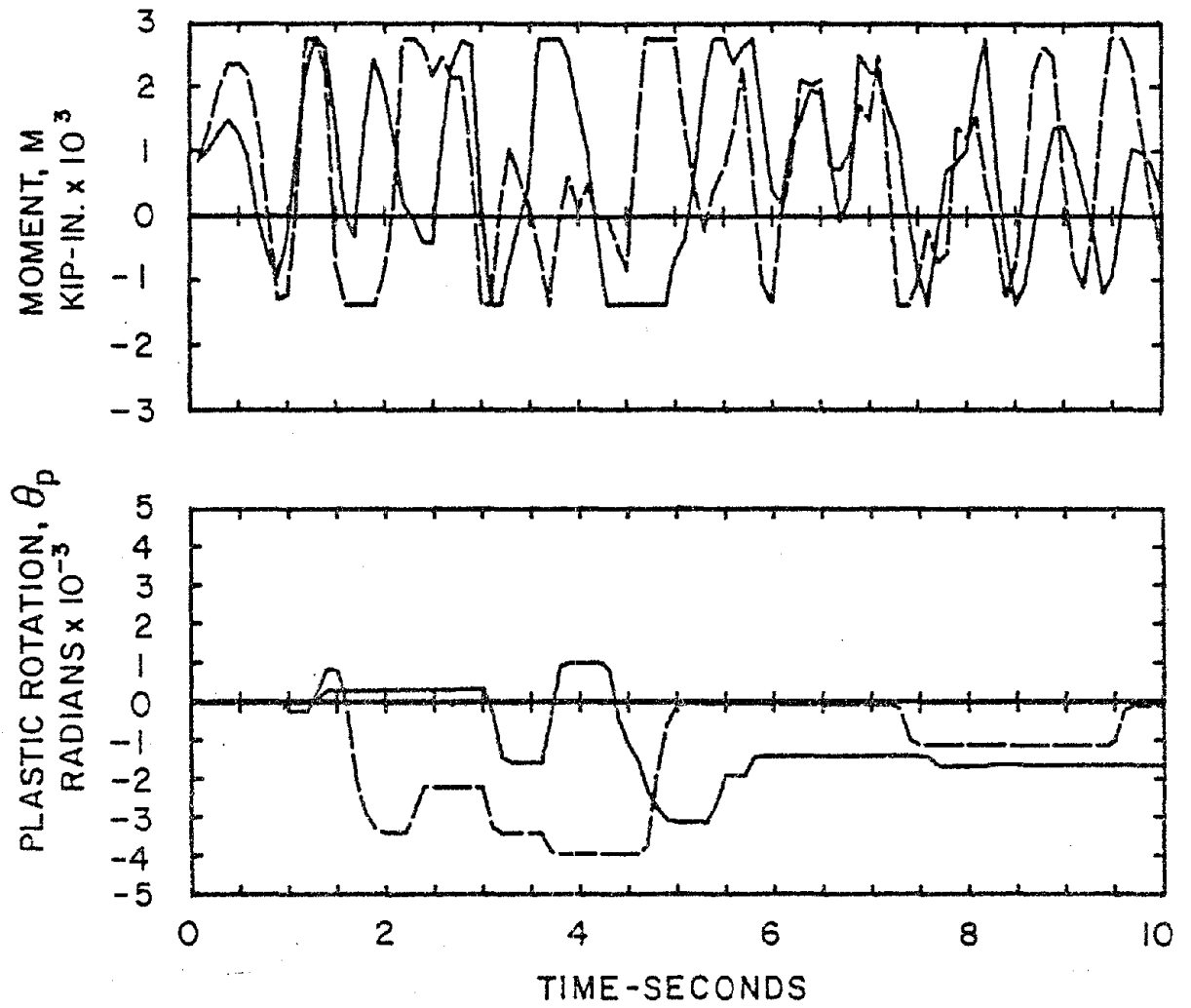


FIG. A-42 5 TH. FLOOR BEAM MOMENT AND PLASTIC ROTATION HISTORIES FOR GROUND MOTIONS 1 & 3. STIFF BEAM FRAME - LO/1.4

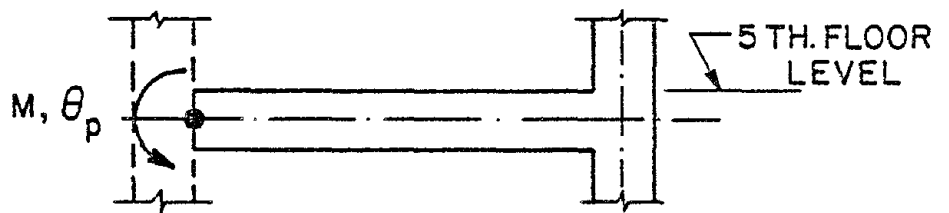
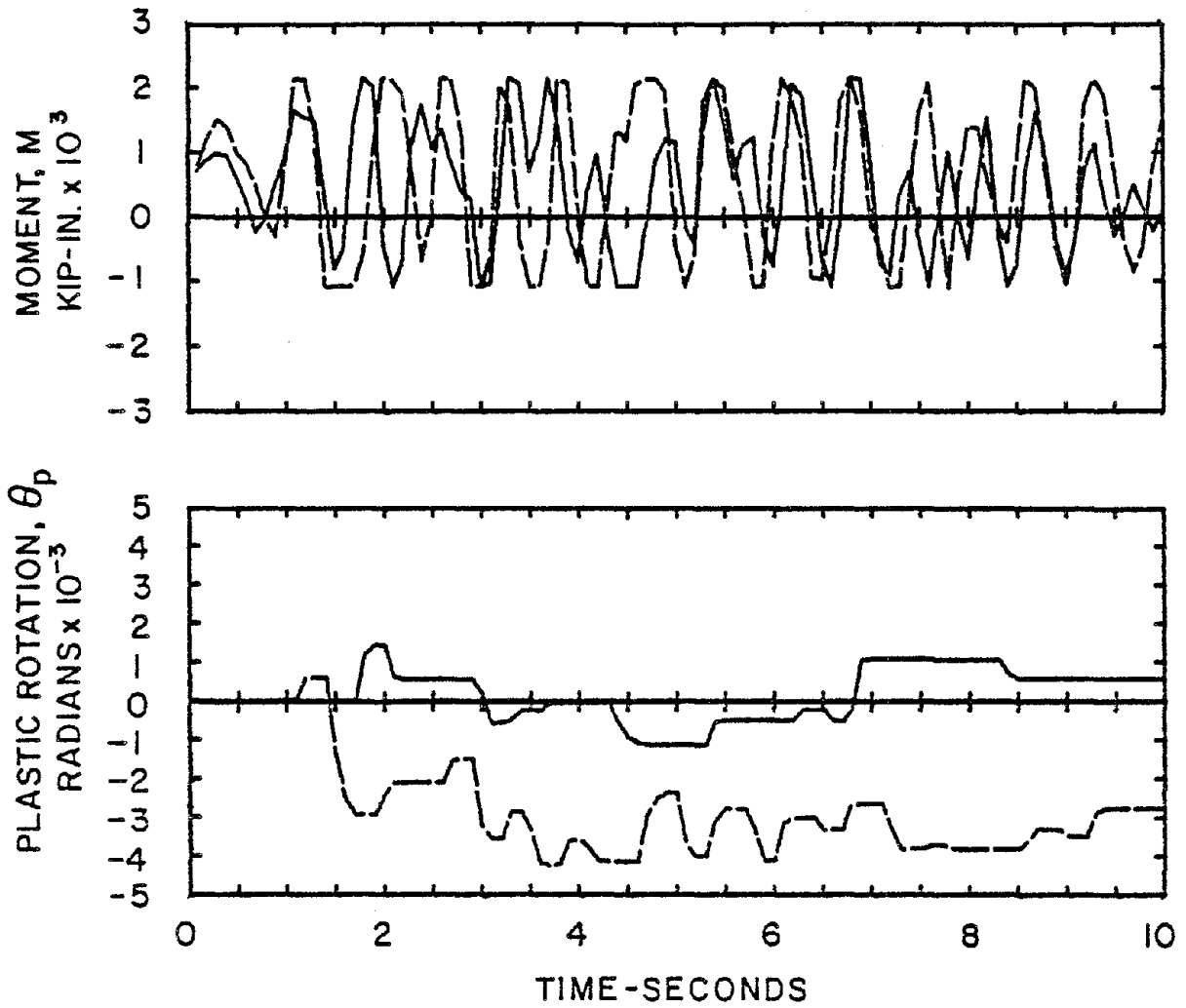


FIG. A-43 5 TH. FLOOR BEAM MOMENT AND PLASTIC ROTATION HISTORIES FOR GROUND MOTIONS 1 & 3. COUPLED WALLS -LO/1.4

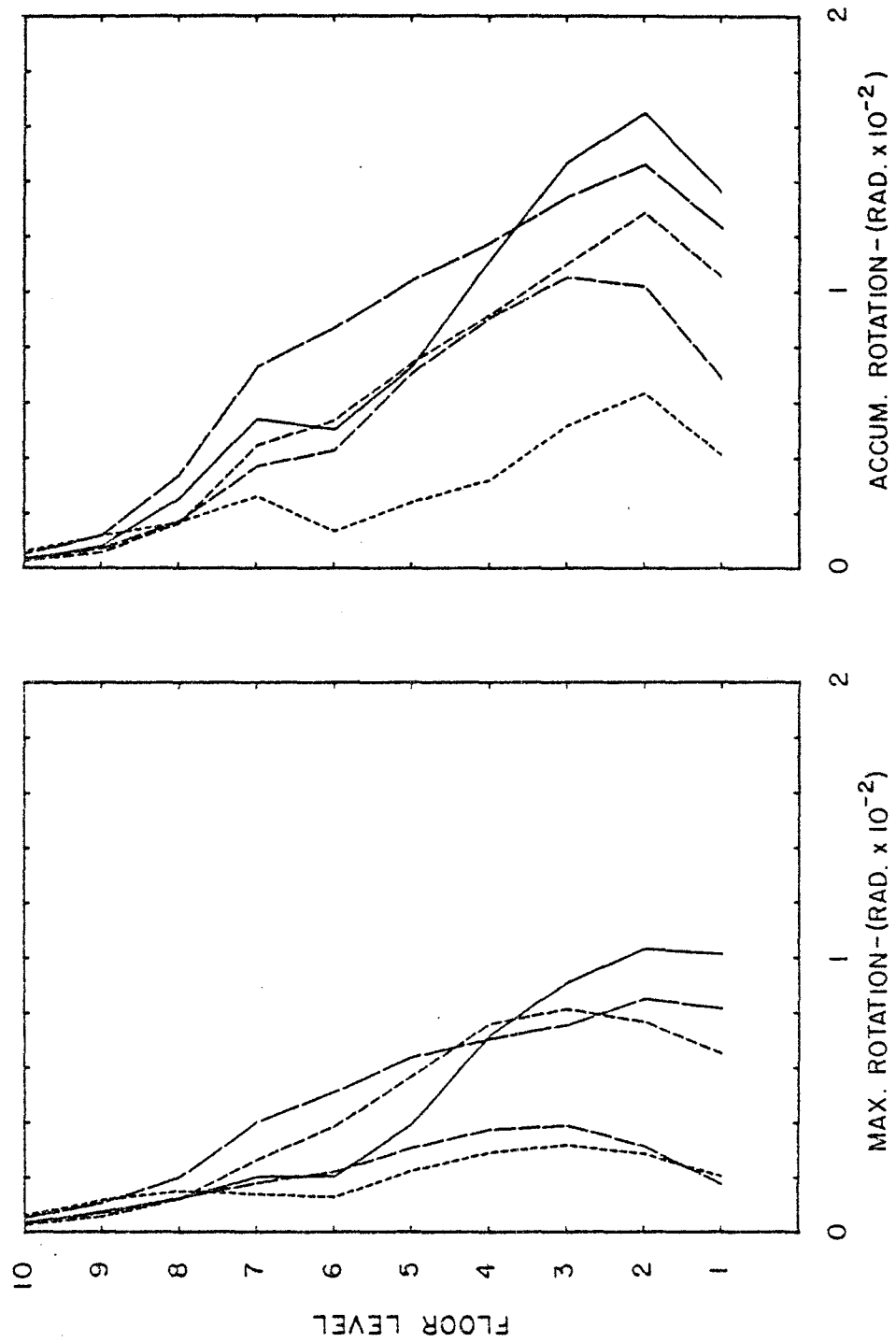


FIG. A-44 MAXIMUM AND ACCUMULATED BEAM PLASTIC HINGE ROTATIONS
TYPICAL FRAME - LO/1.4 DESIGN

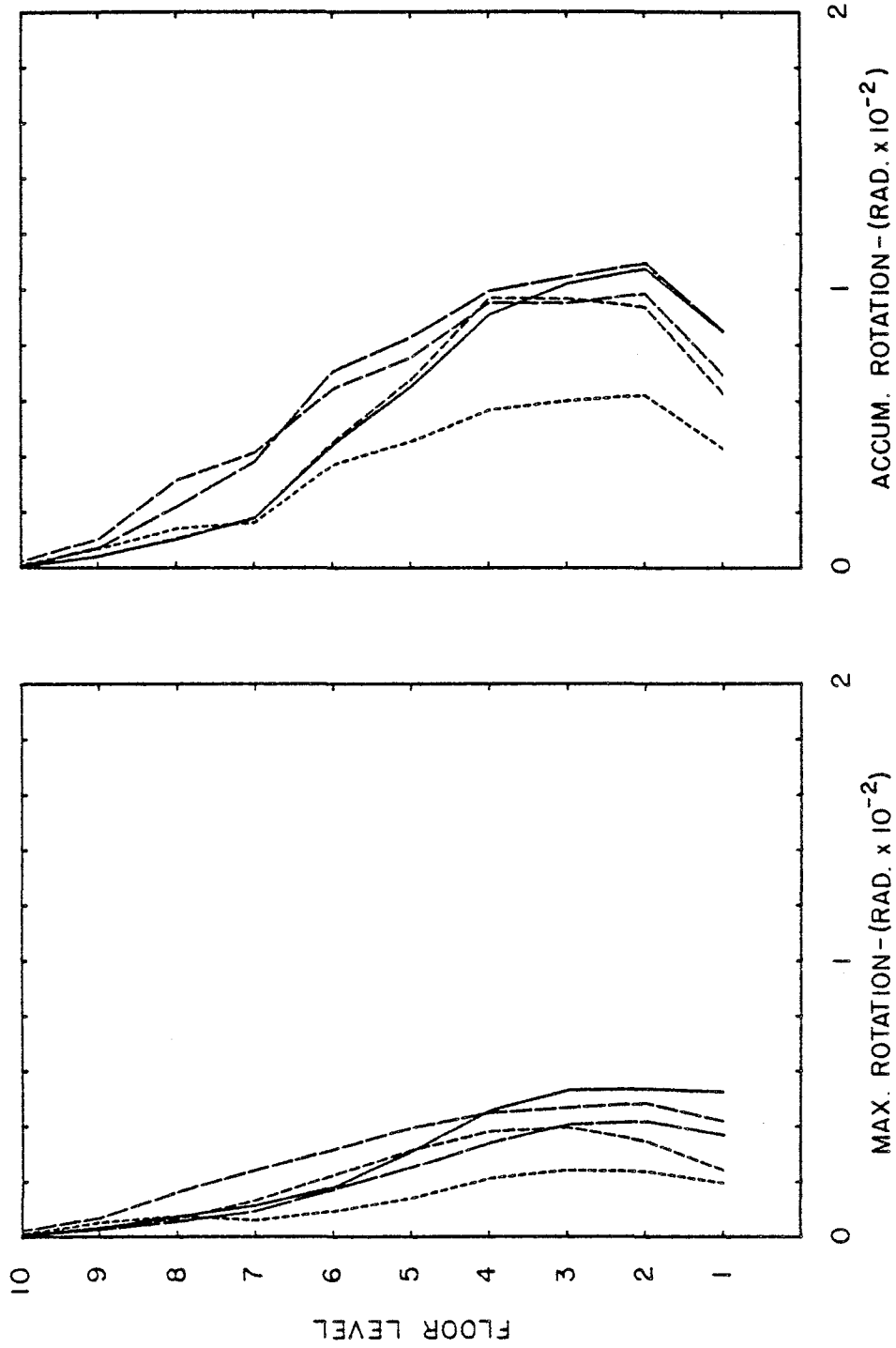


FIG. A-45 MAXIMUM AND ACCUMULATED BEAM PLASTIC HINGE ROTATIONS
STIFF BEAM FRAME - LO/1.4 DESIGN

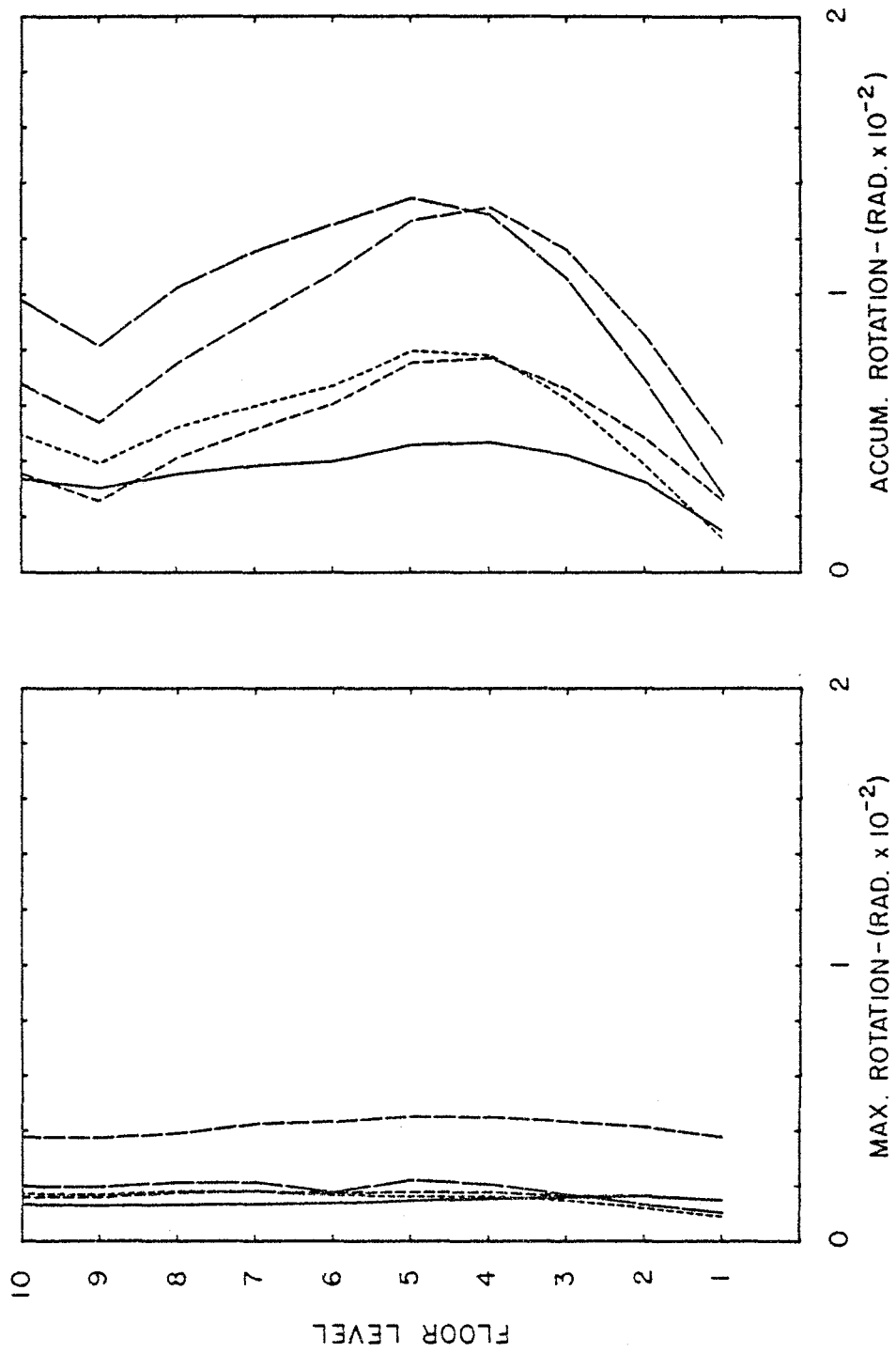


FIG. A-46 MAXIMUM AND ACCUMULATED BEAM PLASTIC HINGE ROTATIONS
COUPLED WALLS - LO/I.4 DESIGN

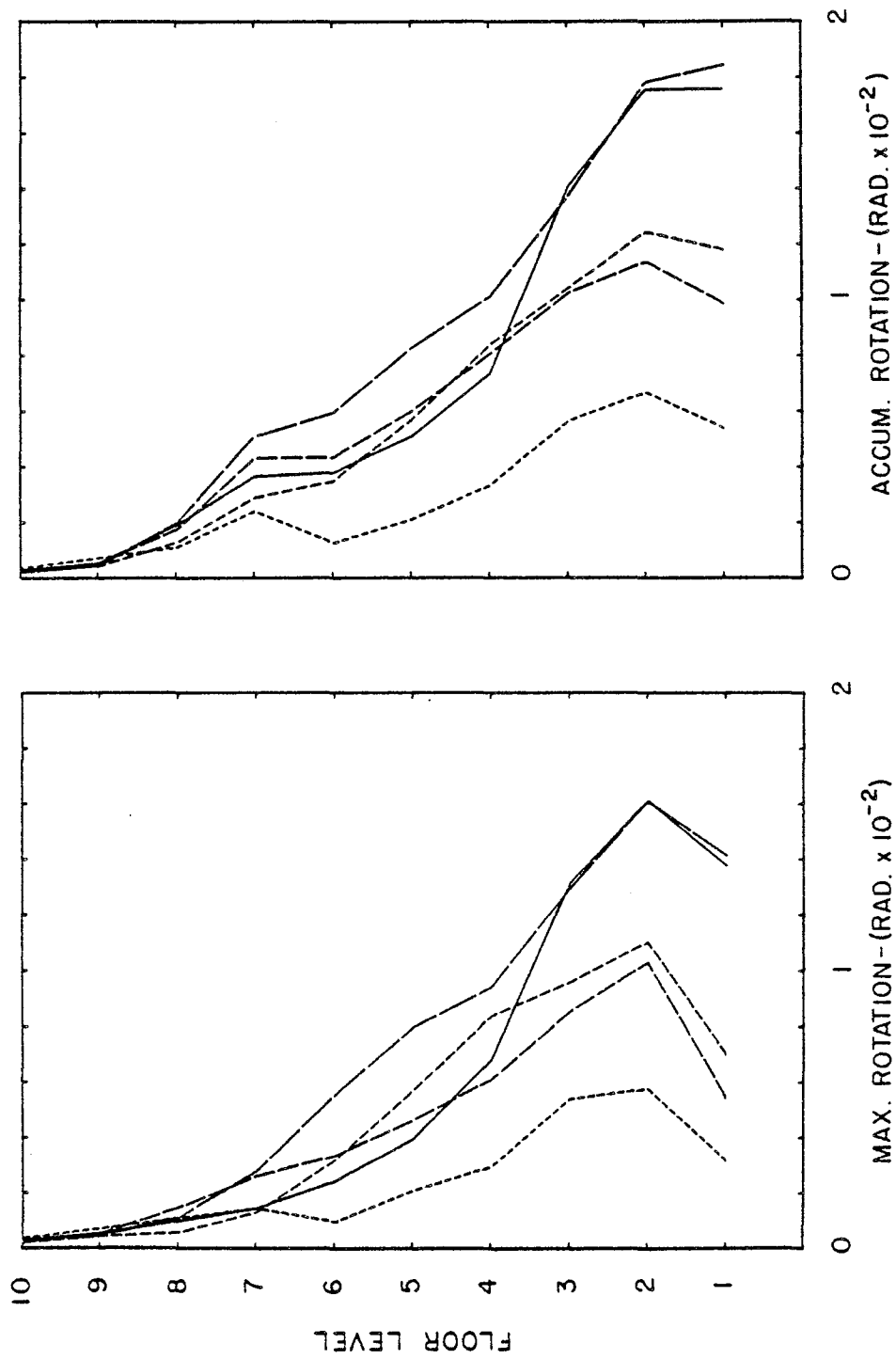


FIG. A-47 MAXIMUM AND ACCUMULATED BEAM PLASTIC HINGE ROTATIONS
TYPICAL FRAME - LO/1.0 DESIGN

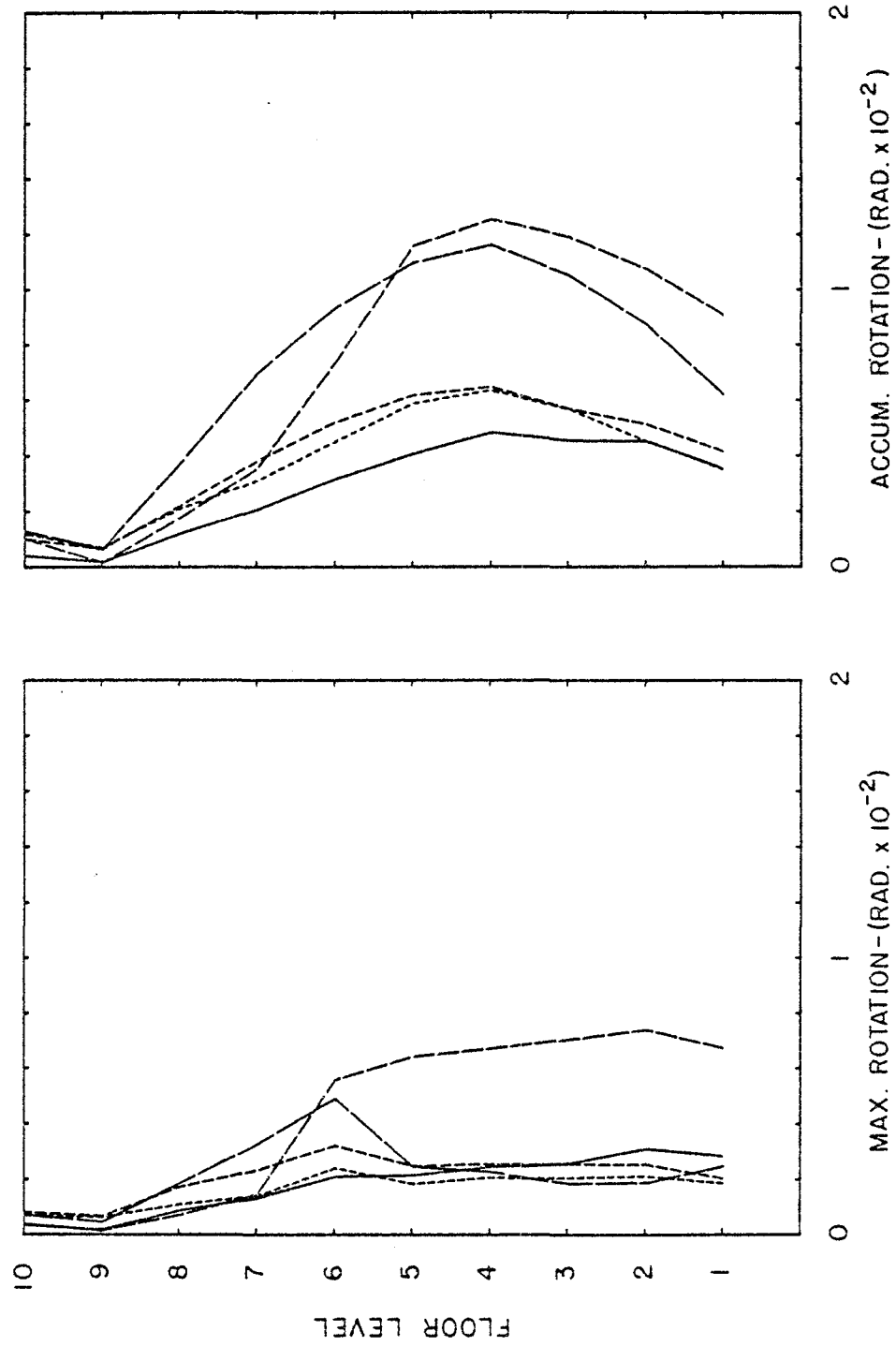


FIG. A-48 MAXIMUM AND ACCUMULATED BEAM PLASTIC HINGE ROTATIONS
COUPLED WALLS - LO/1.0 DESIGN

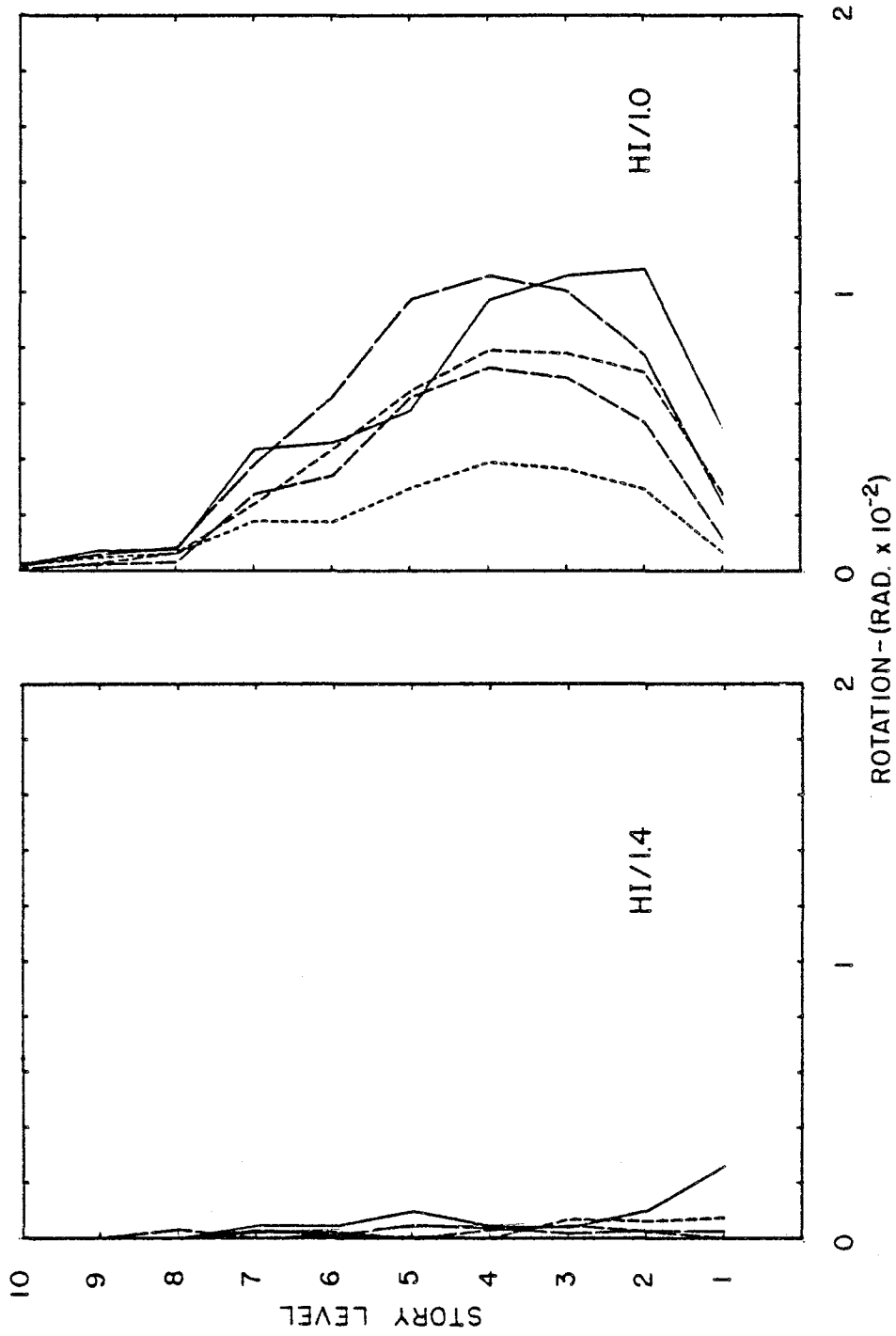


FIG. A-49 MAXIMUM COLUMN PLASTIC HINGE ROTATIONS
TYPICAL FRAME

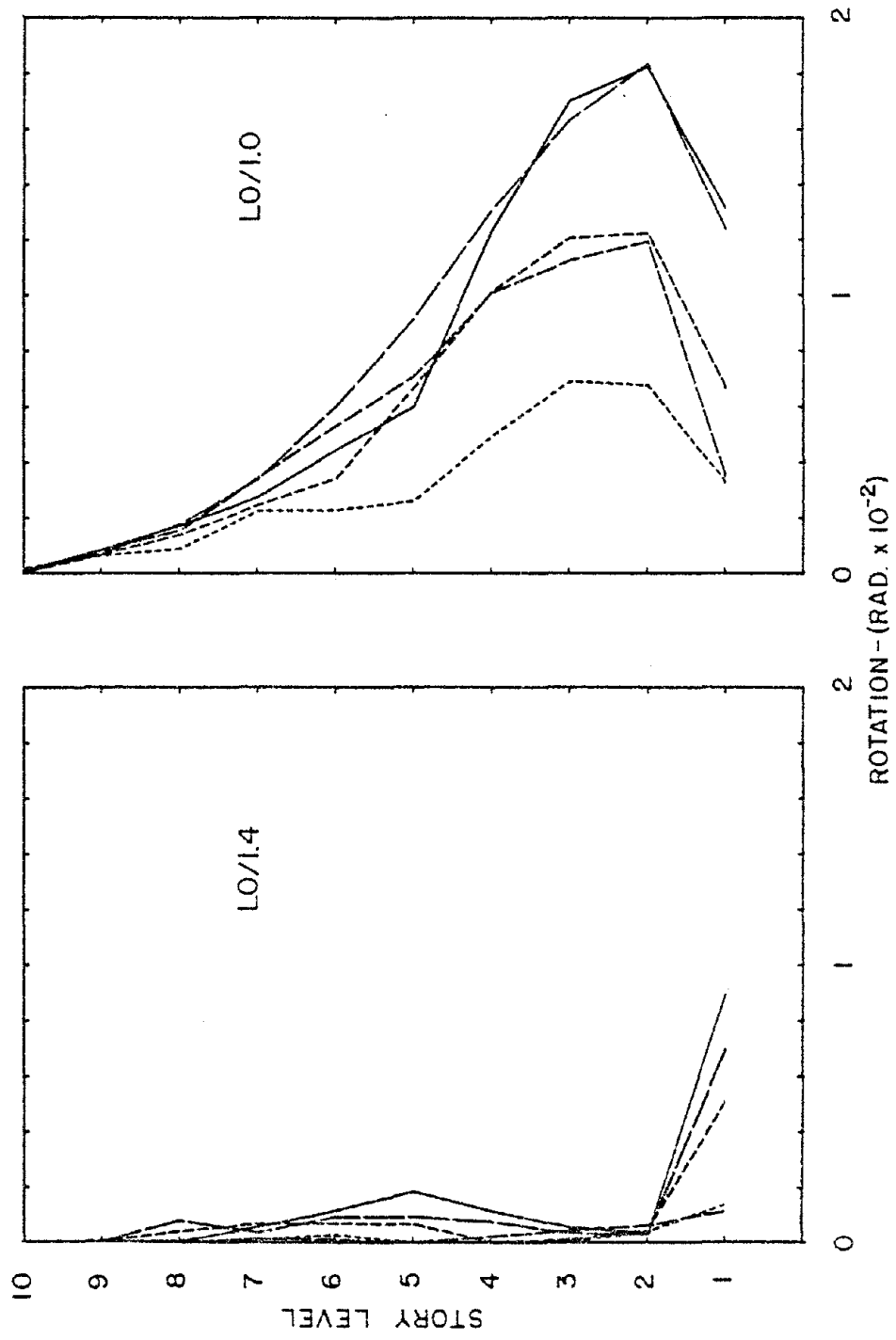


FIG. A-50 MAXIMUM COLUMN PLASTIC HINGE ROTATIONS
TYPICAL FRAME

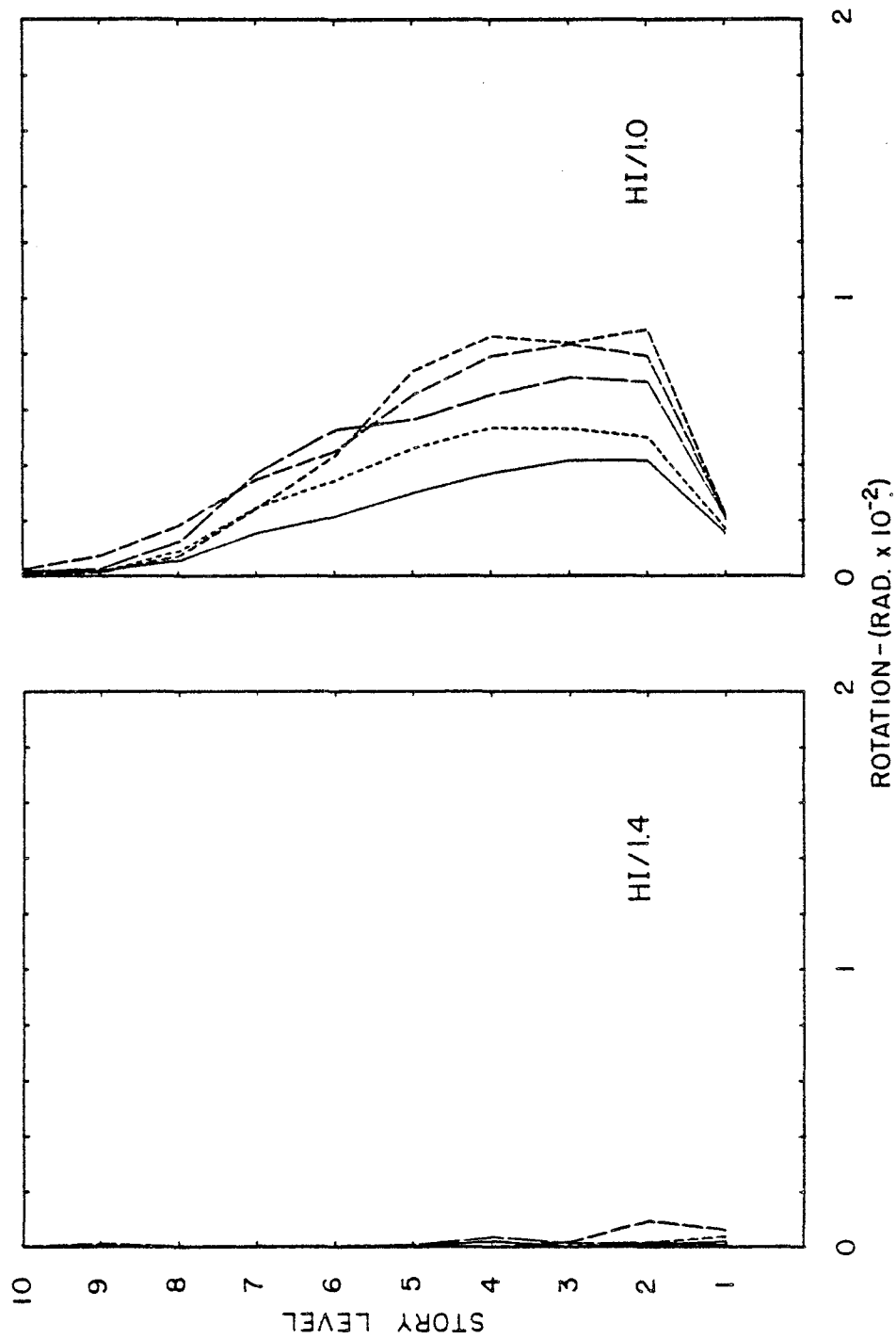


FIG. A-51 MAXIMUM COLUMN PLASTIC HINGE ROTATIONS
STIFF BEAM FRAME

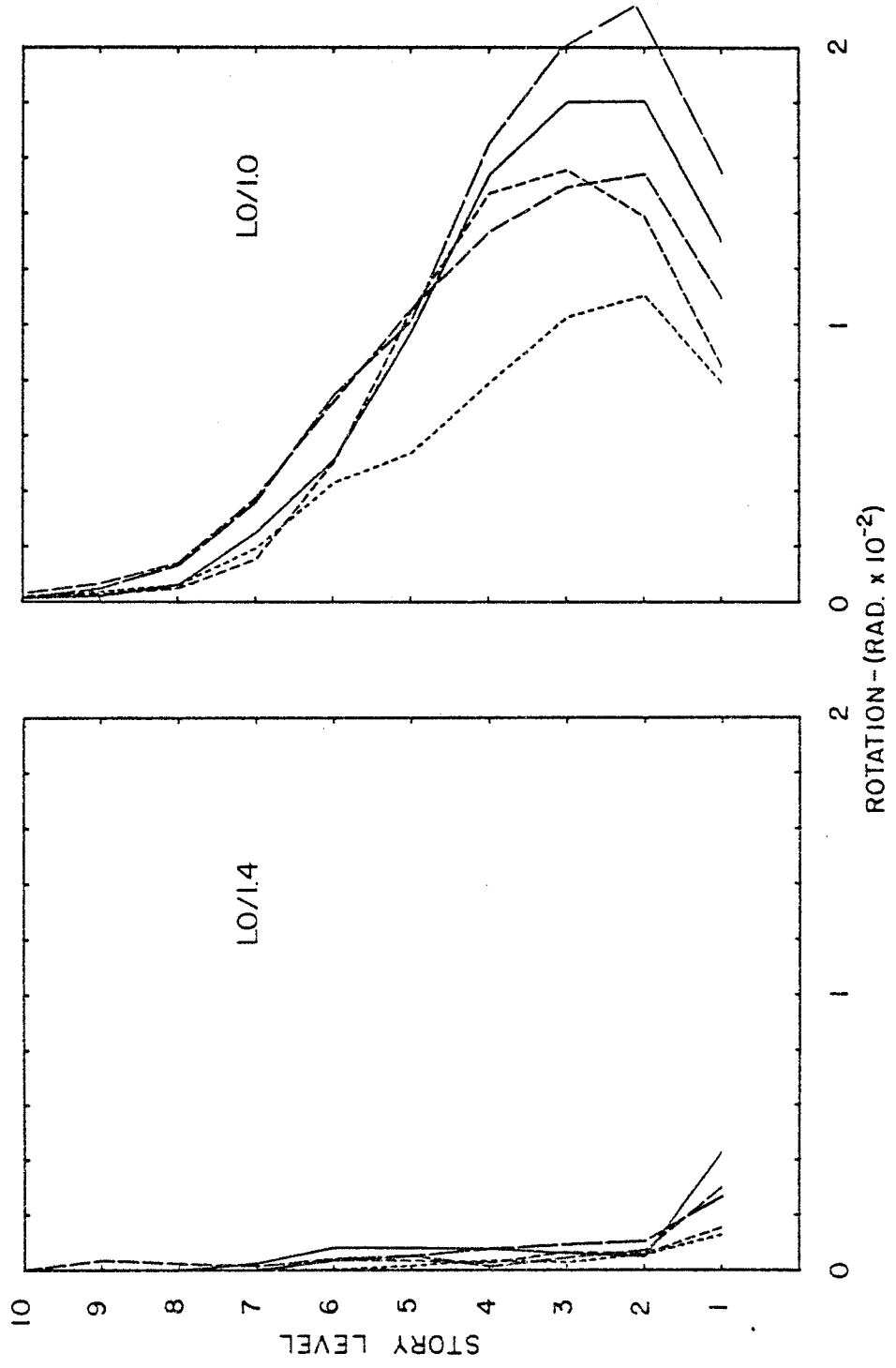


FIG. A-52 MAXIMUM COLUMN PLASTIC HINGE ROTATIONS
STIFF BEAM FRAME

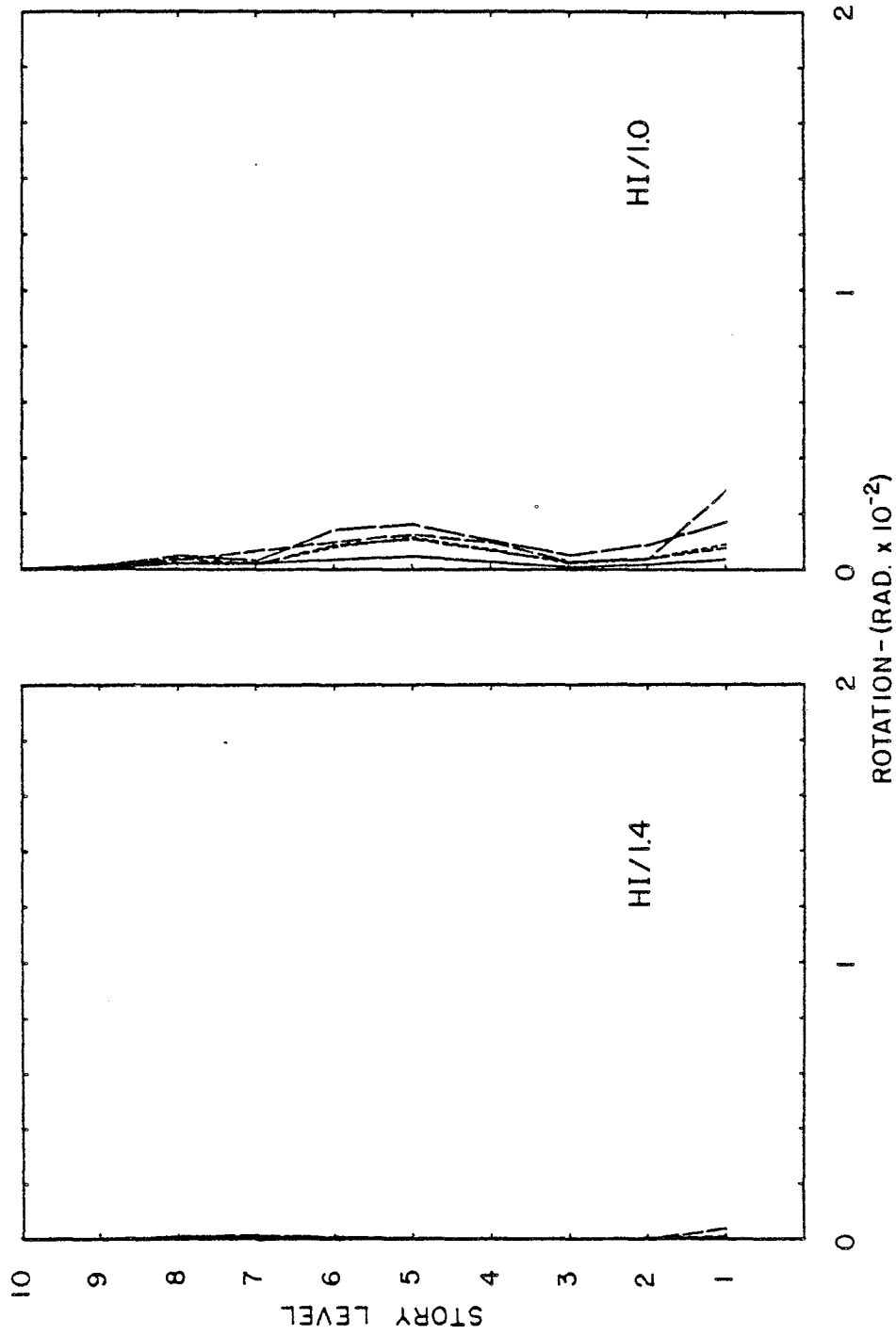


FIG. A-53 MAXIMUM COLUMN PLASTIC HINGE ROTATIONS
COUPLED WALLS

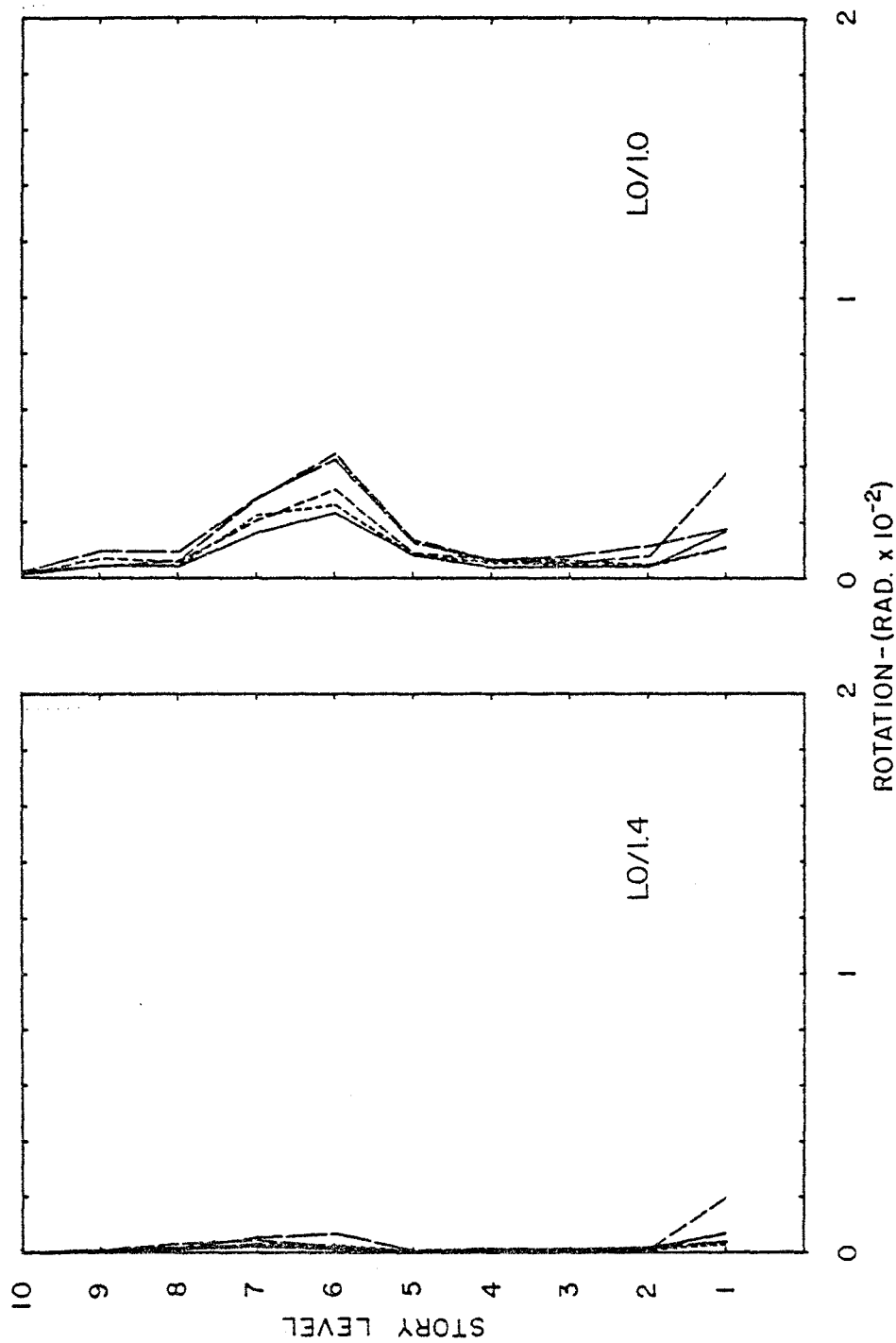


FIG. A-54 MAXIMUM COLUMN PLASTIC HINGE ROTATIONS
COUPLED WALLS

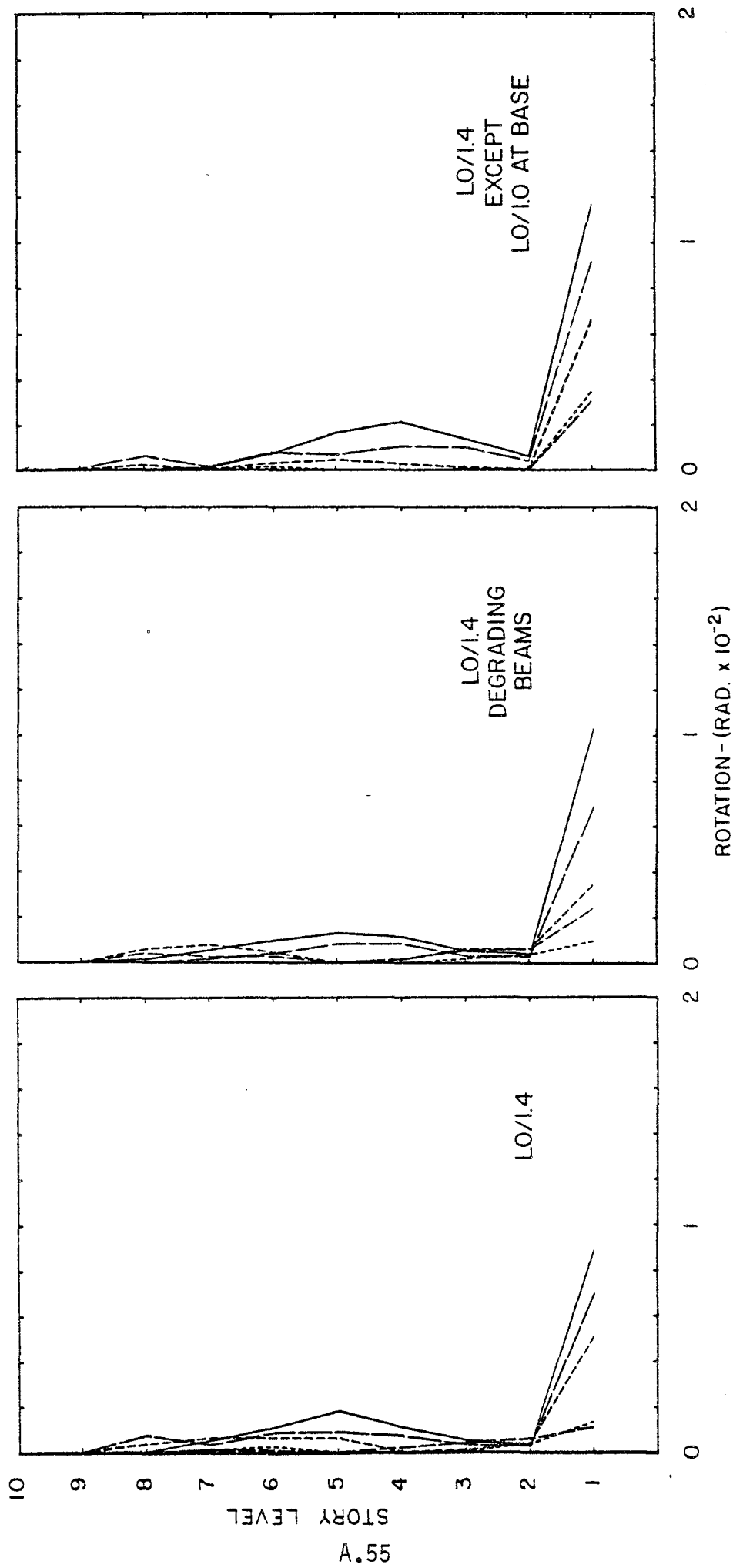


FIG. A-55 MAXIMUM COLUMN PLASTIC HINGE ROTATIONS
TYPICAL FRAME

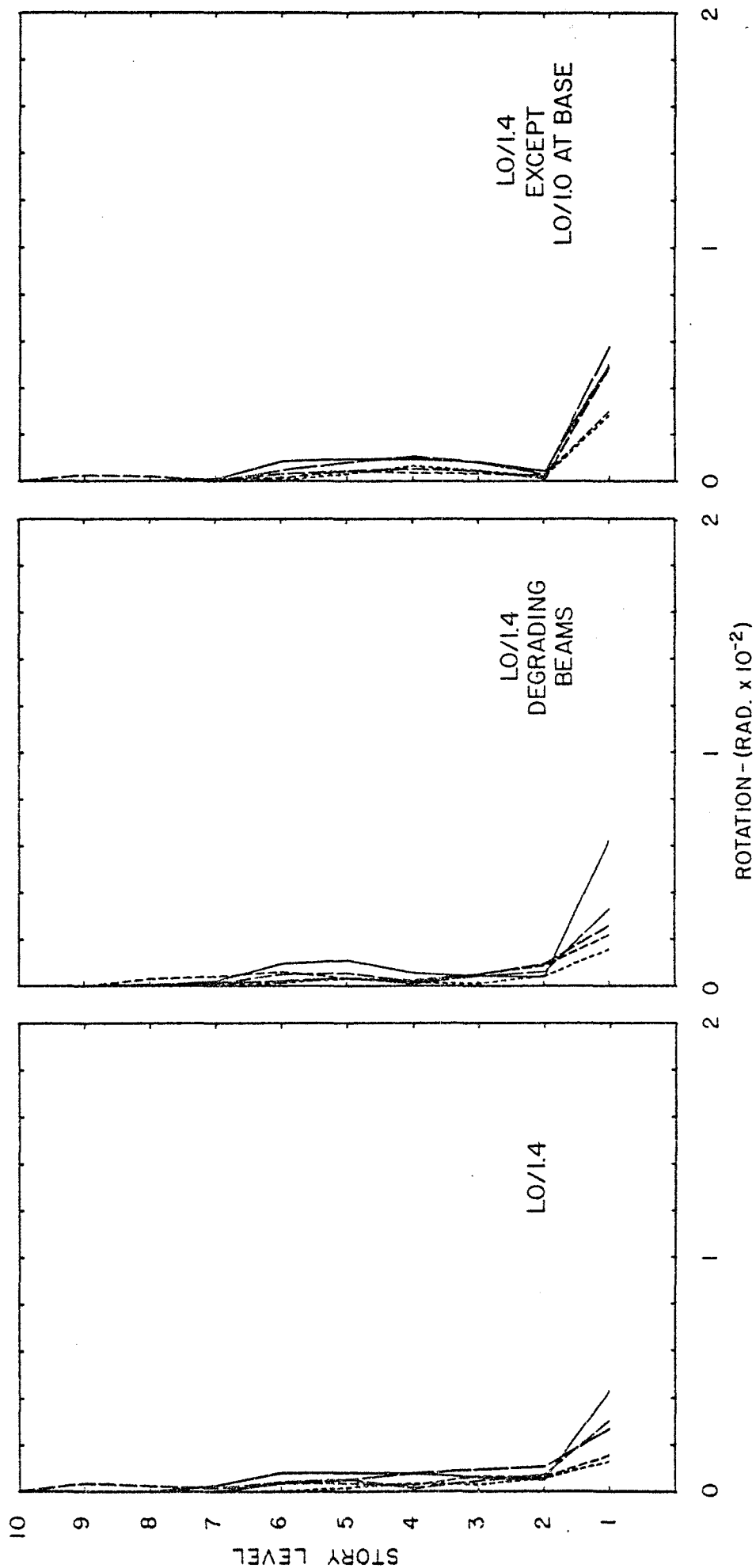


FIG. A-56 MAXIMUM COLUMN PLASTIC HINGE ROTATIONS
STIFF BEAM FRAME

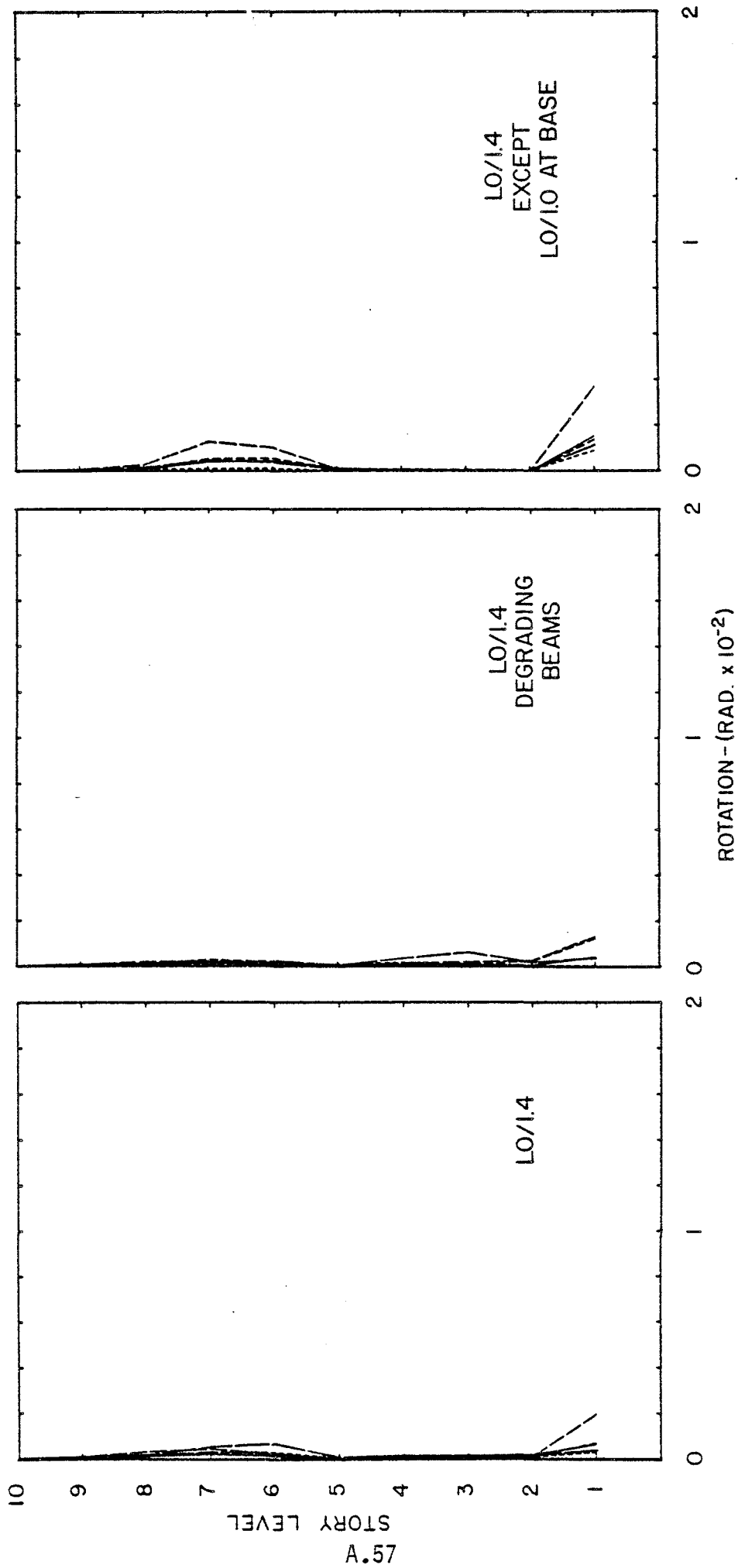


FIG. A-57 MAXIMUM COLUMN PLASTIC HINGE ROTATIONS
COUPLED WALLS

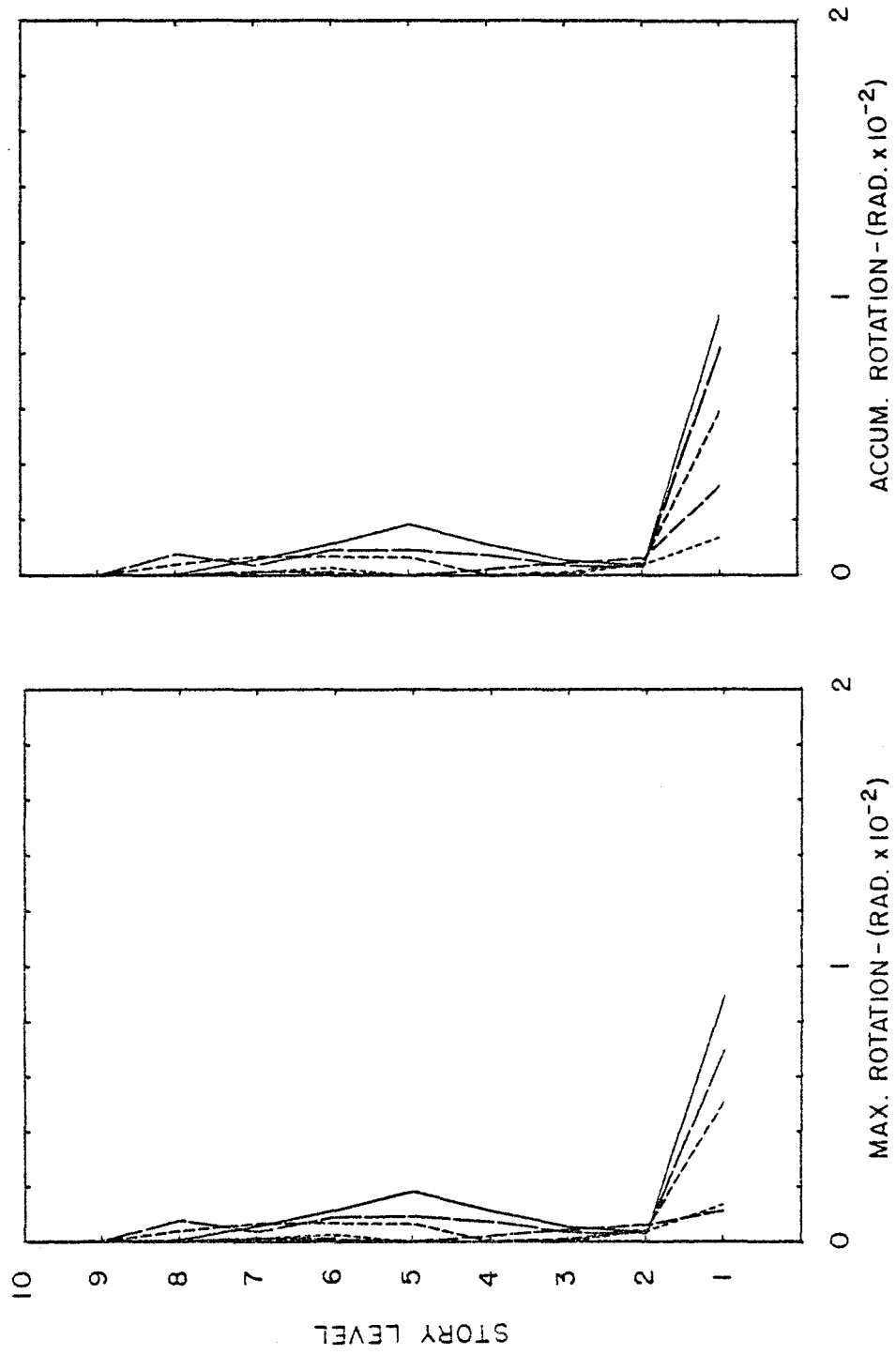


FIG. A-58 MAXIMUM AND ACCUMULATED COLUMN PLASTIC HINGE ROTATIONS
TYPICAL FRAME - LO/1.4 DESIGN

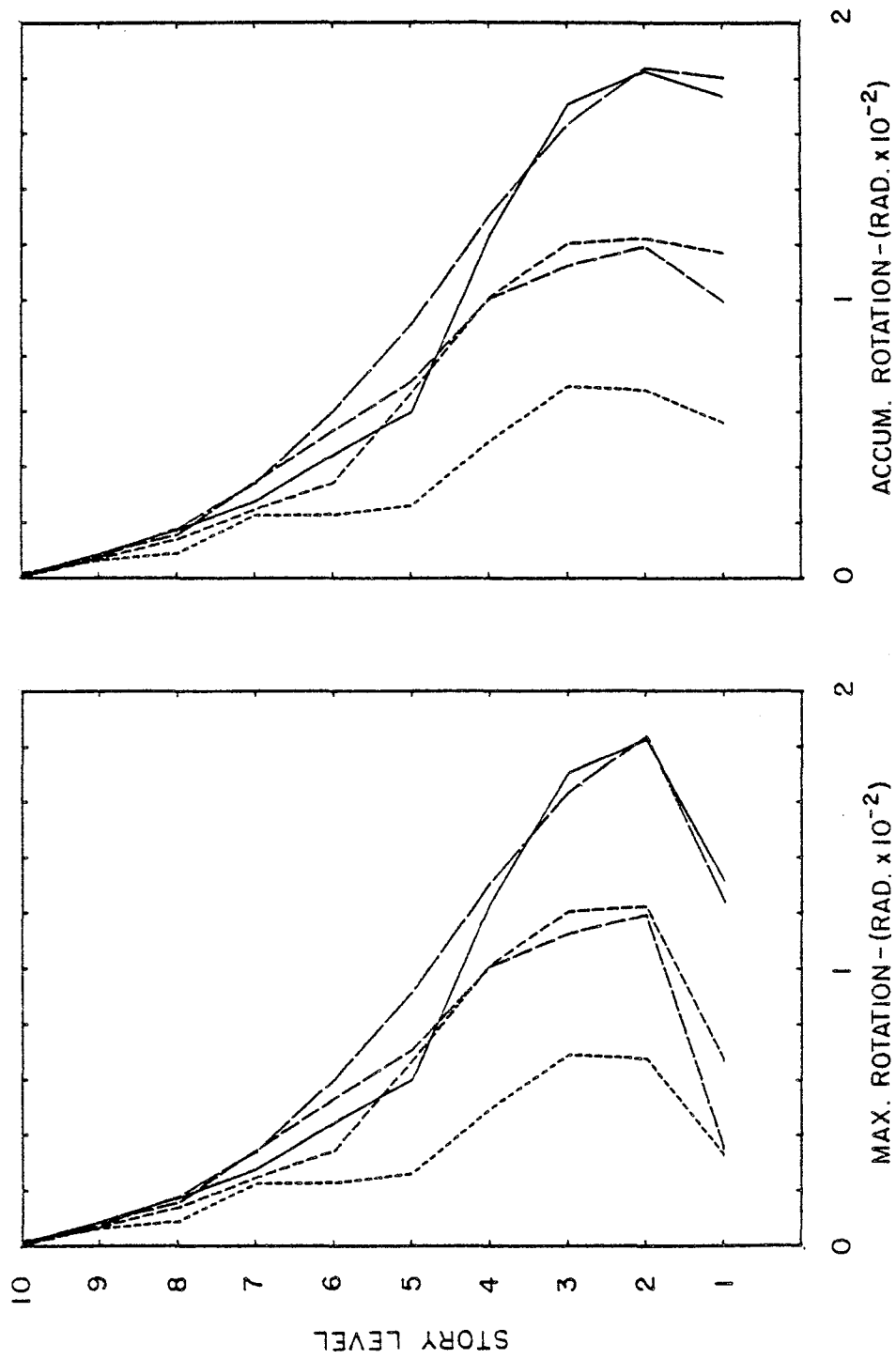


FIG. A-59 MAXIMUM AND ACCUMULATED COLUMN PLASTIC HINGE ROTATIONS
TYPICAL FRAME - LO/1.0 DESIGN

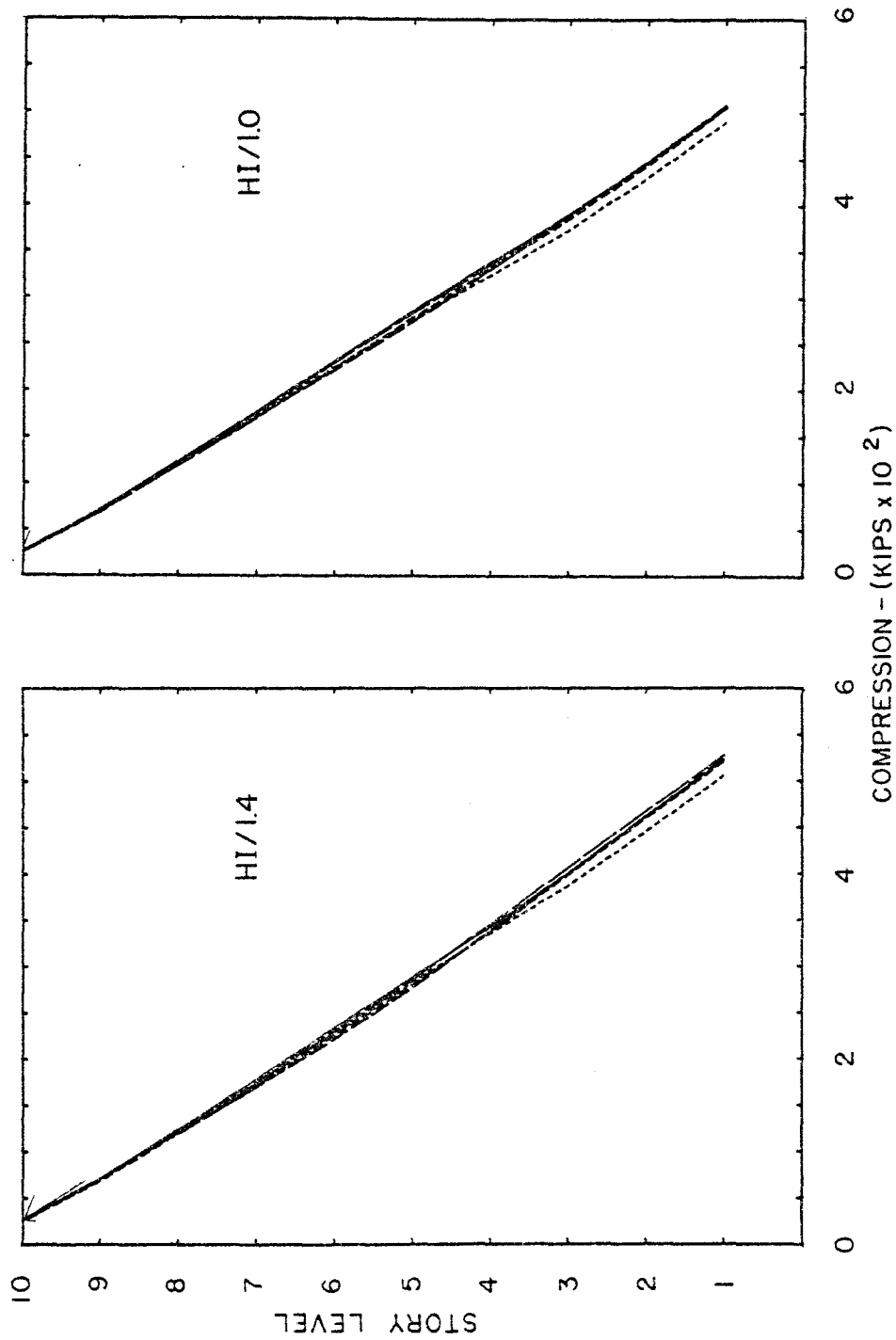


FIG. A-60 MAXIMUM COLUMN AXIAL COMPRESSIONS
TYPICAL FRAME

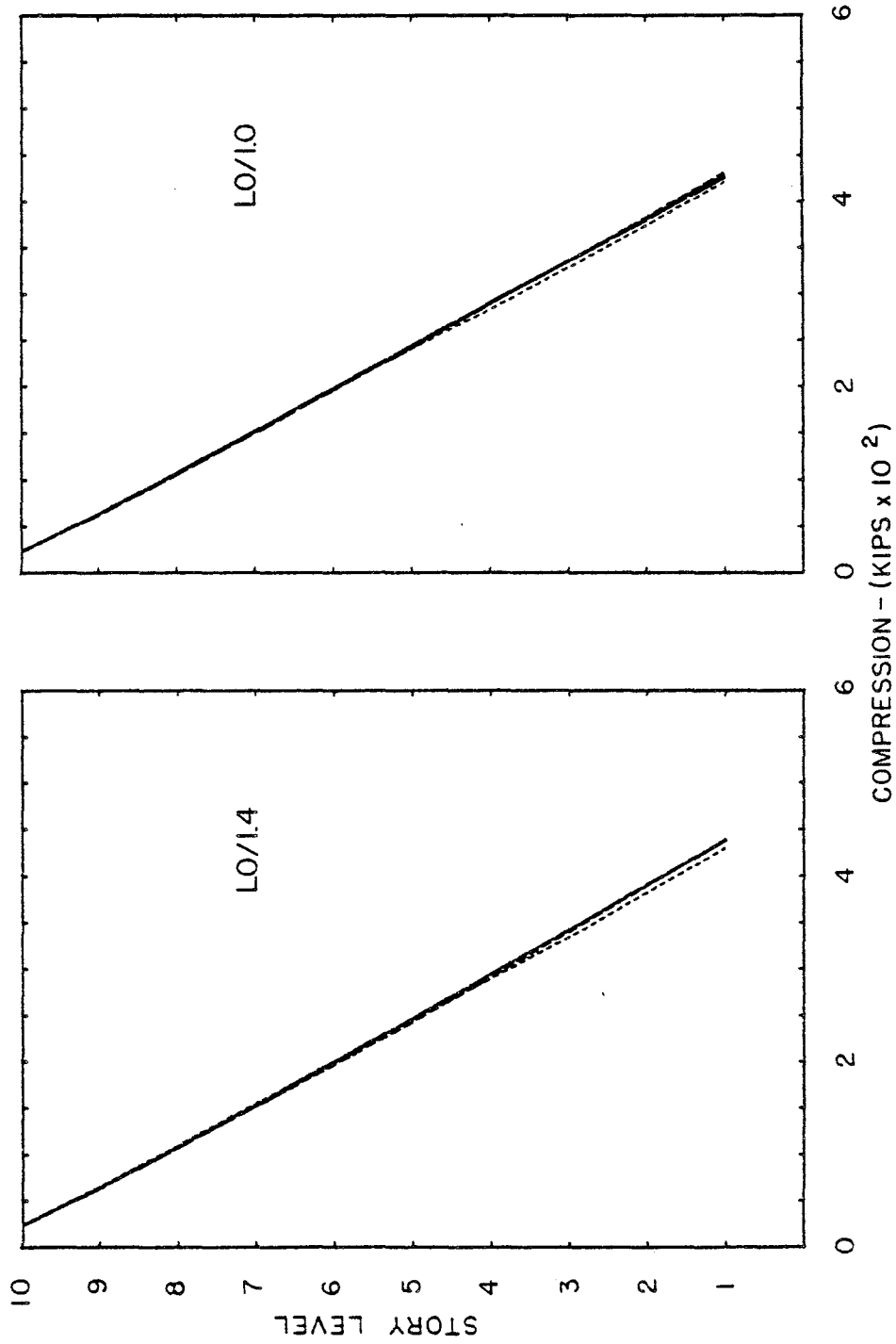


FIG. A-61 MAXIMUM COLUMN AXIAL COMPRESSIONS
TYPICAL FRAME

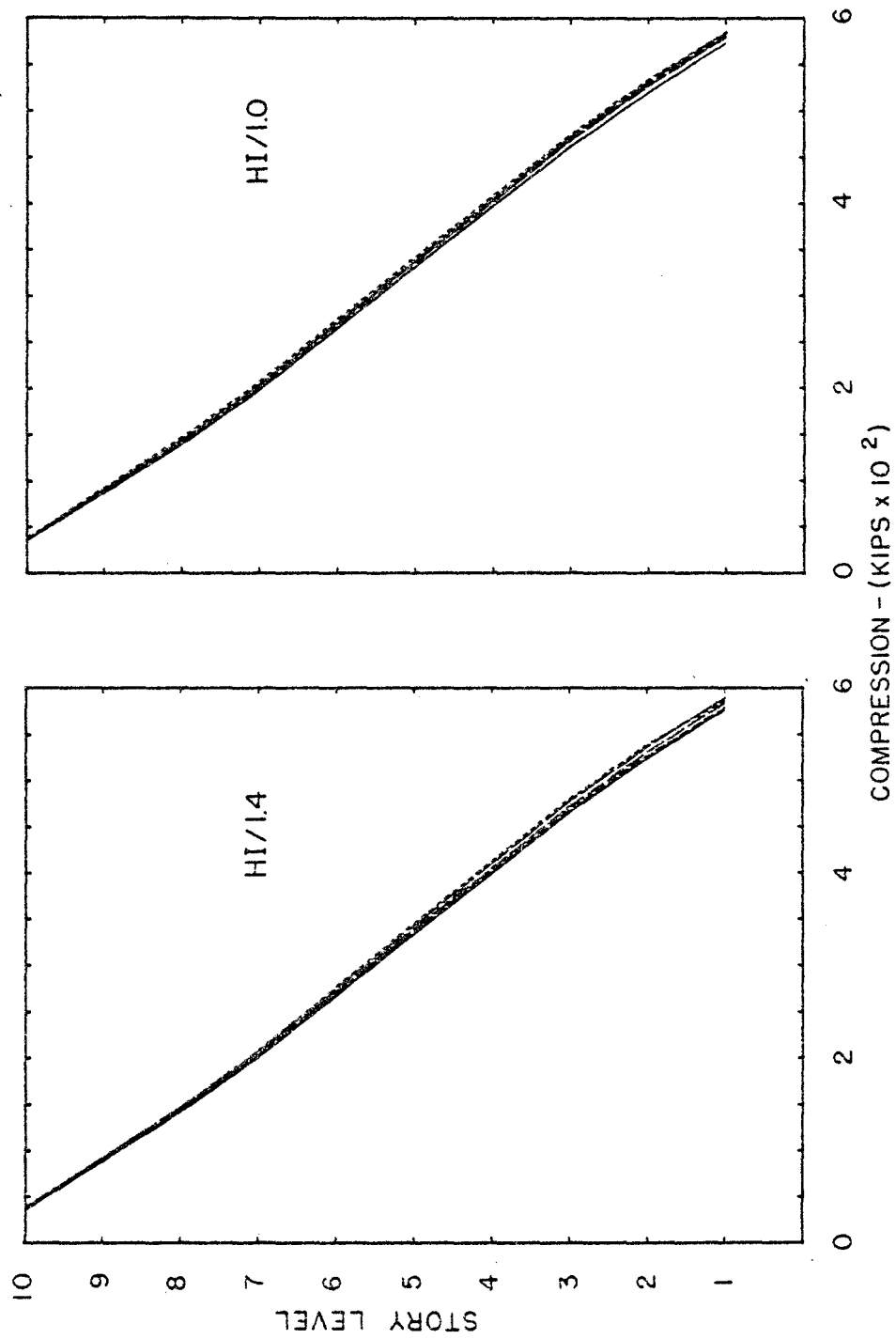


FIG. A-62 MAXIMUM COLUMN AXIAL COMPRESSIONS
COUPLED WALLS